that direct deuterium addition to the 2-phenylethyl carbonium ion was not a major pathway.

In another reaction, molecular hydrogen was replaced with isopentane as a hydrogen donor solvent. Isopentane is a good hydride donor in reactions in superacid media. This reaction resulted in almost the same conversion and product distribution as in the reaction without hydrogen. As before, a significant fraction of the substrate was converted into coke and condensation products. A quantitative amount of isopentane was recovered at the end of the reaction. These results show that isopentane does not directly transfer hydride to the fragments formed from the cracking of bibenzyl with the solid acid catalyst. It also does not reduce the condensation products or indirectly transfer hydrogen to the products.

3.3.1.2.2 Catalytic Hydrotreating of 1-Methylnaphthalene

In continuation with our studies of the relative kinetics of the hydrotreating reactions of polynuclear aromatics with solid acid catalysts (Silica gel-zinc chloride), the effects of hydrogen and hydrogen donor solvent on the hydrotreating of methylnaphthalene were examined during this quarter. The

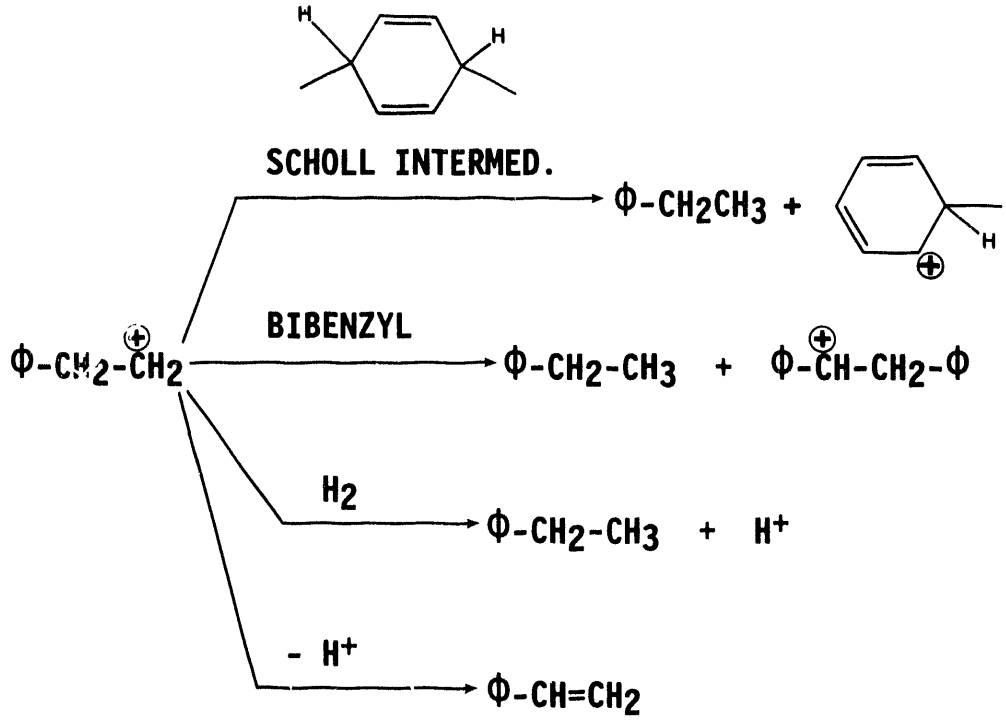

Figure 1. Reactions of phenylethylcarbonium ion.

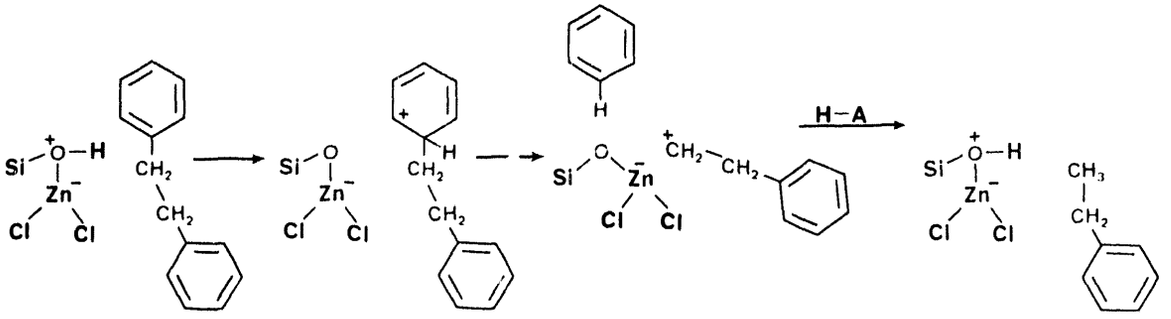

Figure 2. Mechanism of hydrodealkylation of bibenzyl.

reactions of 1-methylnaphthalene with silica gel-zinc chloride catalyst were carried out at 400°C in the absence of hydrogen. This reaction gave products which are indicative of three reactions, namely isomerization (rearrangement), hydrogenation, and demethylation (hydrocracking), occurring during catalytic hydrotreating of 1-methylnaphthalene. The formation of polymethylnaphthalenes is regarded as a major part of the demethylation reaction (transmethylation). The percent conversion, measured as the amount of methylnaphthalenes disappearing during the reaction, was 74.6% (Table 2). Remaining methylnaphthalene was present as a mixture of 1- and 2-methylnaphthalenes in the ratio of 0.41. Products of this reaction were naphthalene and polymethylnaphthalenes, along with benzene, toluene, ethylbenzene as the minor products. Almost 14% of the starting 1-methylnaphthalene was converted into coke. When the same reaction was carried out using isopentane as the hydrogen donor solvent, almost 88% of 1-methylnaphthalene was converted into products. At the end of the reaction a mixture of 1- and 2-methylnaphthalenes in the ratio of 0.44 was obtained. The product distribution was the same as in the previous reaction. A significant fraction of the substrate (30%) was converted into coke.

The data from these two reactions at 400°C indicate that the isomerization reaction is rapid at this temperature. It apparently does not reach an exact equilibrium point, owing to different reactivities of the 1- and 2-methylnaphthalenes in the subsequent reactions (hydrogenation, hydrocracking), which occur at slower rates. This lack of steady state concentrations makes kinetic analysis difficult. We may conclude that the isomerization reaction of 1- and 2-methylnaphthalene, which proceeds to an approximate equilibrium ratio (1-/2-) of 0.4, rapidly at this temperature. In the initial stages of the reaction, isomerization predominates. As the heating proceeds, the isomer mixture is converted into naphthalene and di- and trimethylnaphthalenes via transmethylation (a non-reductive reaction), and to methyltetralins via hydrogenation of either of the rings of the methylnaphthalene substrates. The tetralin is formed either from the hydrogenation of naphthalene or from the

demethylation of methyltetralin initially formed. Hydrocracking of the tetralins resulted in a mixture of alkylbenzenes. Small amounts of cyclohexane, methylcyclohexane, decalin and indans were formed in addition to the above products. The major reaction sequences involving the methylnaphthalenes are presented in Figure 3.

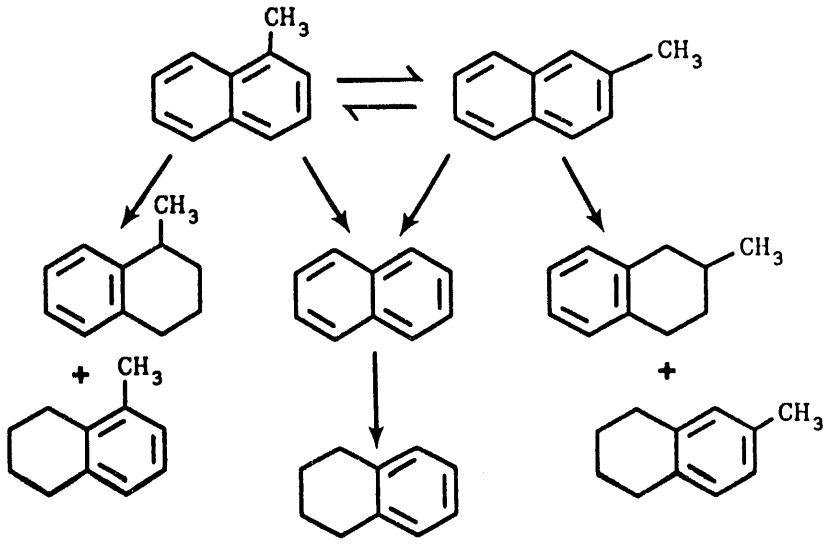

Figure 3. Hydrogenation/hydrocracking/isomerization of 1-methylnaphthalene.

3.3.2 Pillared clay-supported Ni-Mo Catalysts

3.3.2.1 Characterization

3.3.2.1.1 Infrared method

Infrared spectroscopy of the pyridine complex was used to determine the relative proportion of Lewis and Bronsted acid sites in chromia pillared clay and chromia pillared clay-supported sulfided Ni-Mo catalysts. In the infrared spectrum of the pyridine absorbed chromia pillared clay catalyst, the bands at 1444 and 1541 cm-1 are assigned to the pyridine-Lewis acid coordination bond, and the pyridine-Bronsted acid bond respectively. Similarly in Ni-Mo loaded and chromia pillared clay, the bands at 146 and 1530 cm were assigned to the pyridine-Lewis acid coordination bond, and the pyridine-Bronsted acid bond respectively. The relative intensities of these bands were converted to the concentration ratio by using the respective extinction coefficients. The ratios of the corrected concentrations of Lewis sites to Bronsted sites were 1.84 for chromia pillared clay and 2.27 for chromia pillared clay supported Ni-Mo catalysts (Tables 3 and 4).

TABLE 2

REACTIONS OF 1-METHYLNAPHTHALENE

REACTION TEMP. =400°C, REACTION TIME = 3 HRS,
CATALYST/SUBSTRATE=0.5, 1-METHYLNAPHTHALENE = 7.04 MMOLS.

Reductant (g)	Conversion (%)	1-/2-Menaph.	Major Products (mmoles)
None	74.6	0.41	Naph. (0.6)
Isopentane (0.2)	88	0.40	Naph. (0.4)

3.3.2.1.2 Thermogravimetric analysis

Thermogravimetric techniques were used to determine the total acid sites and stability of the catalyst. In the TGA experiment, the weight of the catalyst increased by 5.86 wt% for chromia pillared clay and 4.69 wt% for sulfided Ni-Mo loaded chromia pillared clay catalysts. The weight increase is due to the chemical adsorption of the pyridine at both Lewis and Bronsted acid sites, and is a measure of the total acidity of the catalyst. The total acidity for chromia pillared clay is 0.75 meq/g and Ni-Mo loaded chromia pillared clay catalysts is 0.60 meq/g. Upon slowly heating the catalyst (2°C/min.) to 300°C, all of the chemically adsorbed pyridine could be removed. The majority of the pyridine (4.16 wt% for chromia pillard clay and 3.31 wt% for Ni-Mo loaded chromia pillared clay) was absorbed between 105 and 140°C, while the remainder was absorbed between 140 and 202°C. The inflection points at 105 and 140°C are believed to represent the onset of pyridine loss from Lewis acid and Bronsted acid sites, respectively. Heating the catalyst beyond 300°C resulted in a small weight loss which could be due to the decomposition of the catalysts. Thus, the relative amount of Lewis and Bronsted sites are 2.42 for chromia pillared clay and 1.79 for Ni-Mo loaded chromia pillared clay catalysts (Tables 3 and 4).

3.3.2.2 Catalytic Hydrodesulfurization of Diphenylsulfide

The catalytic activities of solid acid catalyst (SZC-5) and Ni-Mo supported on high chromium chromia pillared clay for hydrodesulfurization of diphenylsulfide were investigated. The reactions of diphenylsulfide with these catalysts were carried out at 300°C for 3 hours in the presence of molecular hydrogen at 1000 psig. The microreactor conditions and conversion data are given in Table 5.

TABLE 3

ACID SITES OF CHROMIA PILLARED CLAY
INFRARED ABSORBANCE OF PYRIDINE COMPLEX

	A	E
1441 cm^{-1} (Lewis-Pyridine Band)	0.61	0.084
1541 cm^{-1} (Bronsted-Pyridine Band)	0.23	0.058

Ratio of Lewis/Bronsted Acid Sites = 1.84

Total Acid Sites From TGA-Pyridine Absorption/Desorption:

	Total Acid Sites (mmol/g. Cat.)	Ratio of Lewis/Bronsted Acid Sites
Chromia Pillared Clay	0.75	2.42

TABLE 4

ACID SITES OF NI-MO LOADED CHROMIA PILLARED CLAY
INFRARED ABSORBANCE OF PYRIDINE COMPLEX

	A	E
1446 cm^{-1} (Lewis-Pyridine Band)	1.26	0.084
1530 cm^{-1} (Bronsted-Pyridine Band)	0.38	0.058

Ratio of Lewis/Bronsted Acid Sites = 2.27

Total Acid Sites From TGA/Pyridine Absorption/Desorption:

	Total Acid Sites (mmole/g. Cat.)	Ratio of Lewis/Bronsted Acid Sites
Ni-Mo Loaded Chromia Pillared Clay	0.60	1.79

The reaction of diphenyl sulfide with Ni-Mo loaded chromia pillared clay catalyst resulted in almost complete conversion of diphenyl sulfide into benzene. Small amounts of cyclohexane and hexane were also formed. The absence of benzenethiol, dibenzodithiin, or phenyldisulfide suggests that both aryl-sulfur bonds are cleaved by this catalyst. Furthermore, side reactions leading to the formation of coke and oligomeric material were prevented by dispersion of sulfided Ni-Mo in chromia pillared-clay. The reaction of diphenyl sulfide with SZC-5 (5% zinc chloride supported on silica gel) resulted in only 51.5% conversion into products. The major products were benzene and benzenethiol. The catalytic activity of SZC-5 is much less than the that of SZC (50% zinc chloride on silica gel).

3.3.3 Catalytic Hydrotreating of Model Compounds with Hydrotalcite Catalysts

The reactions of model compounds such as bibenzyl, diphenysulfide, benzothiophene, dibenzothiophene, diphenylether, and quinoline were carried out with pillared catalysts such as phthalate-pillared hydrotalcite and molybdenum-loaded hydrotalcite. The reactions were carried out at 300-350°C for 3 hours both with and without hydrogen. The mass balance of the methylene chloride-insoluble product indicated this product to be essentially the recovered catalyst.

TABLE 5

CATALYTIC HYDRODESULFURIZATION OF DIPHENYL SULFIDE

REACTION TEMP. = 300°C, TIME = 3 HRS,
CATALYST/SUBSTRATE = 0.5, HYDROGEN = 1000 PSIG

Catalyst (g)	DPS (mmol)	Conversion (%)	Major Products (mmol)
NiMoHCPC (0.25)	2.75	98	Benzene (4.75)
SZC-5 (0.25)	2.68	15.5	Benzene (0.44) Benzenethiol (0.1)

Reactions of diphenylsulfide with phthalate-pillared hydrotalcite in the absence of hydrogen gas indicated very small conversion of diphenylsulfide into products. A trace of benzene was the only product from this reaction. However, when the same reaction was carried out in the presence of 1000 psig molecular hydrogen, 86.4% of the diphenylsulfide was converted into products. The major product from this reaction was benzene along with a small amount of thiophenol. Unlike silica gel-zinc chloride catalyst the hydrotalcite gave no oligomeric

product or dithiin. The mass balance of the methylene chloride-insoluble fractions indicated no change in the weight of the catalyst after the reaction, which may suggest that condensation reactions leading to the formation of coke or polymeric material do not occur with this catalyst. The catalyst was not extensively decomposed.

The reaction of diphenylsulfide with molybdenum-loaded hydrotalcite gave slightly higher conversion (88.9%) of diphenylsulfide. The major product from this reaction was benzene. Small amounts of cyclohexane, thiophenol, and cyclohexylthiol were also formed. The reaction with molybdenum supported hydrotalcite was also carried out with benzothiophene at 350°C for 3 hours in the presence of 1000 psig molecular hydrogen. This reaction gave 94% conversion of benzothiophene into products. The major product from this reaction was ethylbenzene, while other products included benzene, toluene, ethylcyclohexane, and hydrogenated benzothiophene. No coke or oligomers were produced in this reaction. However, under the same conditions the conversion of dibenzothiophene was only 8%. The product distribution was complex and due to lack of calibration and GC/MS data, the products have not been determined.

The possible loss of catalytic activity of the molybdenum supported catalyst during reaction was also investigated by reacting the catalyst recovered from the reaction of benzothiophene with diphenylsulfide at 300°C for 3 hours in the presence of 1000 psig molecular hydrogen. This reaction with recovered catalyst gave almost complete conversion of diphenylsulfide. Benzene was the major product along with a small amount of hexane. The enhanced catalytic activity
of the recovered catalyst may be due to the activation of the catalyst during the first run.

The catalytic activity of molybdenum supported hydrotalcite for hydrodeoxygenation and denitrogenation was investigated by hydrotreating diphenylether and quinoline with this catalyst at 350°C for 3 hours in the presence of 1000 psig molecular hydrogen. The diphenylether gave 66% conversion into products. The major products from this reaction were benzene, cyclohexane, hexane, and phenol. Interestingly, a large amount of cyclohexane was formed in this reaction. Cyclohexane may formed from the hydrogenation of benzene formed in the initial stages of the reaction. The percent conversion of quinoline into products was 75%. This reaction gave a highly complex product distribution. The products identified so far are benzene, cyclohexane, toluene, ethylbenzene, propylbenzene, propylaniline, and tetra hydroquinoline.

The hydrocracking activity of hydrotalcite and molybdenum-loaded hydrotalcite was investigated by reacting bibenzyl with these catalysts. The reaction of bibenzyl was carried out at 350°C for 3 hours in the presence 1000 psig hydrogen with hydrotalcite. This reaction, unlike the reaction with diphenylsulfide, resulted in a small conversion of bibenzyl into products. Benzene, toluene, and ethylbenzene were major products of this reaction. The reaction of bibenzyl with molybdenum supported hydrotalcite at 300°C for 3 hours and in the presence of 1000 psig hydrogen gave a small percent conversion. Traces of toluene were the only products.

TABLE 6

CATALYTIC HYDROTREATING OF MODEL COMPOUNDS
REACTION TIME = 3 HRS, CATALYST/SUBSTRATE = 0.5

Catalyst (g)	Substrate (mmol)	H_2 (psi)	Temp. (°C)	Conversion (%)	Major Products (mmol)
HT (0.25)	DPS (2.77)	None	300	3	Benzene (tr.)
HT (0.25)	DPS (2.95)	1000	300	86.4	Benzene(4.43) Benzenethiol (0.12)
Mo-HT (0.25)	DPS (2.79)	1000	300	88.9	Benzene (4.5) Cyclohexane (0.1)
Mo-HT (0.25)	BT (4.0)	1000	350	94	Ethylbenzene (2.67) Ethylcyclohexane (0.4) Benzene (0.2) Toluene (0.2)
Mo-HT (0.25)	DBT (2.72)	1000	350	8	Complex
Recov. MO-HT (0.24)	DPS (2.71)	1000	300	100	Benzene (5.1) Cyclohexane (0.1)
Mo-HT (0.25)	DPE (2.8)	1000	350	66	Benzene (1.6) Cyclohexane (1.2) Phenol (0.3)
Mo-HT (0.25)	Quin. (4.08)	1000	350	75	Complex
Mo-HT (0.25)	BB (2.75)	1000	300	12	Benzene (0.04) Toluene (0.04) Ethylbenzene (0.12)
Mo-HT (0.25)	BB (2.76)	1000	350	25	Benzene (0.04) Toluene (0.1) Ethylbenzene (0.2)
M-HT (0.25)	1-MN (3.67)	1000	350	49	1-MN (0.2) 2-MN (1.7) Decalin (0.2) Naph (0.06) Tetralin (0.12) Methyltetralins(1.1)

TABLE 6 (CONTINUED)

CATALYTIC HYDROTREATING OF MODEL COMPOUNDS
REACTION TIME = 3 HRS, CATALYST/SUBSTRATE = 0.5

HT = Hydrotalcite
Mo-HT = Molybdenum exchanged hydrotalcite
DPS = Diphenylsulfide
BT = Benzothiophene
DBT = Dibenzothiophene
BB = Bibenzyl
DPE = Diphenyl ether
Quin. = Quinoline
MN = Methylnaphthalene

The reaction of 1-methylnaphthalene was also investigated to determine hydrocracking/hydrogenation and isomerization activity of hydrotalcite catalysts. The major products from this reaction are decalin, tetralin, 1- and 5-methyltetralins. Small amounts of benzene, toluene, ethyl and propylbenzenes were also formed. No isomerization to 2-naphthlalene occurred.

4.0 REFERENCES

1. Derbyshire, F., et. al. ACS Fuel Chem. Prepr., 33, 3, 188, 1988.

2. Garg, D.; Givens, E.N. Fuel Proc. Technol., **1984**, 9, 29 ; Kovach, S.M.; Castle, L.J.; Bennett, J.V.; Svrodt, J.T.; Ind. Eng. Chem. Prod. Res. Dev., **1978**, 17, 62 .

3. Mills, G.A.; Beodeker, E.R., Oblad, A.G. J. Amer. Chem. Soc., **1950**, 72, 1554.

4. Reichle, W.T. Chemtech, **1986**, 58, 63.

5. Miyata, S. Clay and Clay Minerals, **1980**, 28, 50-56.

6. Boehm, et al., Angew. Chem. Int. Ed. Eng., **1977**, 16, 265.

7. Reichle, W.T. U.S. Patent 4 458, **1984**.

8. Reichle, W.T., et al., J. of Catalysis, **1985**, 94, 547.

9. Reichle, W.T., et al., J. of Catalysis, **1986**, 101, 353.

10. Rameswaren, et al., ACS Fuel Chem. Prepr., **1988**, 33 4, 942.

11. Kohjiya, et al., Makromol. Chem., Rapid Commun., **1981** 2, 231.

12. Nakatsuka, T., et al., Japan Bull. Chem. Soc., **1979**, 52, 2449.

13. Olson, E.S.; Quarterly Technical Progress Report for the Period July to September 1989, EERC.

14. Drezdon, M.A. U.S. Patent 4 774 212, 1988.

15. Vogel A., Textbook of Quantitative Inorganic Analysis, 4th edn., Longman Sci. and Tech. Group, Essex, Eng., 1978, p. 434.

FORM EIA 459E
(10/80)

U.S. DEPARTMENT OF ENERGY
FEDERAL ASSISTANCE MANAGEMENT SUMMARY REPORT

FORM APPROVED
OMB No. 1900-0127

Page ___ of ___

1. Program/Project Identification No	2. Program/Project Title	3. Reporting Period
DE-FC21-86MC10637	Liquefaction Reactivity of Low-Rank Coals (3.4	7/01/89 through 6/30/90

4. Name and Address

University of North Dakota Energy & Environmental Research Center
Box 8213, University Station, Grand Forks, ND 58202

5. Program/Project Start Date: 4/01/86

6. Completion Date: 6/30/92

7. FY: 89/90

8. Months or Quarters: Quarters

9. Cost Status — a. Dollars Expressed in: Thousands

10. Cost Chart

Fund Source		Quarter 1st	2nd	3rd	4th	Cum. to Date	Tot. Plan
DOE	P	62	62	93	94	311	311
	A	67	51	65	55	238	
	P						
	A						
	P						
	A						
	P						
	A						
Total P		62	62	93	94	311	311
Total A		67	51	65	55	238	
Variance		<5>	11	28	39	73	

P = Planned A = Actual

Total Planned Costs for Program/Project: $311

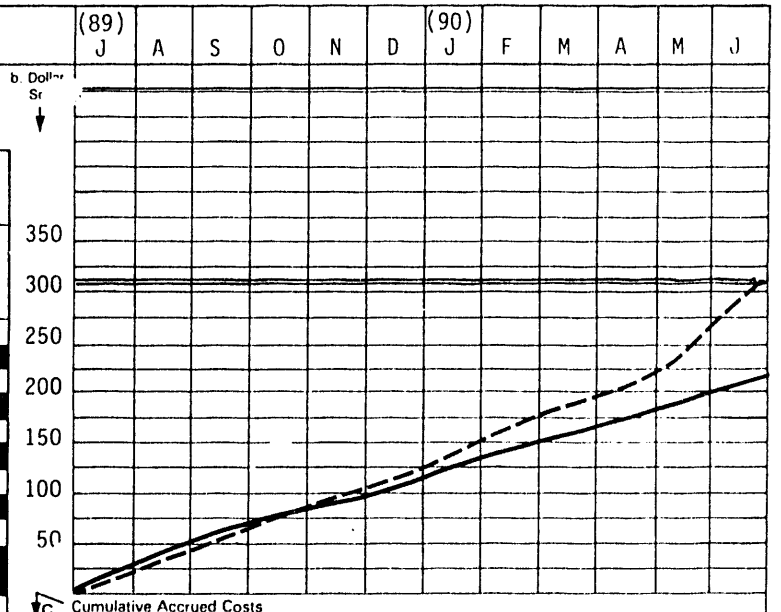

Planned			62			124			217			311
Actual			67			118			183			238
Variance			<5>			6			34			73

11. Major Milestone Status

	Units Planned / Units Complete	Milestones
Task 1: Development and Testing of Pillared Catalysts	P	
	C	
A. Pillared Smectite Catalyst	P	1 ▼ 2 ▼ 3 ▼ 4 △
	C	
	P	
	C	
B. Hydrotalcite Catalyst	P	1 ▼ 2 ▼ 3 △
	C	
	P	
	C	
C. Generation of Pillared Catalysts in situ	P	1 ▽ 2 △
	C	
	P	
	C	
D. Preparation of Low-Severity Feedstock	P	1 ▲
	C	
	P	
	C	
E. Hydrogen Transfer During Hydrotreating	P	1 ▲
	C	
	P	
	C	
Task 2: Solid Acid-Catalyzed Cracking	P	1 ▼ 2 ▼ 3 ▲
	C	
	P	
	C	
Task 3: Effects of Low-Temp. Presolubilization	P	1 ▽ 2 △
	C	
	P	
	C	
	P	
	C	
	P	
	C	

12. Remarks

13. Signature of Recipient and Date

14. Signature of DOE Reviewing Representative and Date

FORM EIA 459E
(10/80)

U.S. DEPARTMENT OF ENERGY
FEDERAL ASSISTANCE MANAGEMENT SUMMARY REPORT

FORM APPROVED
OMB No. 1900 0127

1. Program/Project Identification No.	2. Program/Project Title	3. Reporting Period
DE-FC21-86MC10637	Liquefaction Reactivity of Low-Rank Coals (3.4)	7-01-89 through 6-30-90

4. Name and Address

University of North Dakota Energy and Mineral Research Center
Box 8213, University Station, Grand Forks, ND 58202

5. Program/Project Start Date: 4/01/86

6. Completion Date: 6/30/92

Milestone ID. No.	Description	Planned Completion Date	Actual Completion Date	Comments
Task 1:				
A.	Pillared Smectite Catalyst:			
a.1	Complete preparation	12-89	12-89	
a.2	Complete hydrotreating	02-90	04-90	
a.3	Complete analysis	04-90	04-90	
a.4	Complete report	06-90		
B.	Hydrotalcite Catalyst:			
b.1.	Complete preparation	09-89	09-89	
b.2	Complete test	11-89	11-89	
b.3	Complete analysis and report	01-90		
C.	Complete In Situ Treatment:			
c.1	Complete tests	03-90		
c.2	Complete analysis and report	05-90		
D.	Complete preparation of low-severity feedstocks	02-90	02-90	
E.	Complete hydrogen transfer experiments	05-90	05-90	
Task 2	Solid Acid-Catalyzed Cracking:			
1.	Complete catalyst preparation	08-89	08-89	
2.	Complete tests	10-89	04-90	
3.	Complete analysis and report	11-89	04-90	
Task 3	Low-Temperature Presolubilization:			
1.	Complete tests	09-89		
2.	Complete analysis and report	10-89		

3.5 Gasification Ash and Slag Characterization

GASIFICATION ASH AND SLAG CHARACTERIZATION

Final Technical Progress Report
for the Period July 1, 1989 - June 30, 1990

Including

the Quarterly Technical Progress Report
for the Period April - June 1990

by

Sumitra R. Ness, Research Engineer
Jan W. Nowok, Research Associate
Steven A. Benson, Project Manager

University of North Dakota
Energy and Environmental Research Center
P.O. Box 8213, University Station
Grand Forks, North Dakota 58202

Contracting Officer's Representative: Dr. H. Fred Bauer

for

U.S. Department of Energy
Office of Fossil Energy
Morgantown Energy Technology Center
P.O. Box 880
Morgantown, West Virginia 26507-0880

August 1990

Work Performed Under Cooperative Agreement No. DE-FC21-86MC10637

TABLE OF CONTENTS

TABLE OF CONTENTS (CONTINUED)

LIST OF FIGURES

LIST OF FIGURES (CONTINUED)

LIST OF FIGURES (CONTINUED)

LIST OF FIGURES (CONTINUED)

LIST OF FIGURES (CONTINUED)

LIST OF TABLES

GASIFICATION ASH AND SLAG CHARACTERIZATION

1.0 PROJECT SUMMARY

The purpose of this project is to develop a unified picture of the behavior of inorganic coal constituents in gasification systems. To achieve this goal, the reactions and interactions between inorganic constituents, partitioning of ash components, physical properties, and sintering behavior of ash under gasification conditions must be characterized and interrelated. During the 1989-1990 fiscal year, the Gasification Ash and Slag project Characterization has focused on two main areas. The goals of the first area, characterization of reactions and interactions between inorganic constituents has been accomplished for 5 coals and the chars produced from them, in a 5-10 gram batch pressurized pyrolysis unit under reducing conditions. The second area, slag surface tension measurement, has been studied, resulting in the determination of several physicochemical effects which affect the measurement. Also, strength measurements and sintering studies were performed on various coal ashes and coal ashes with dolomite and limestone additives. The results indicate that interfacial surface tension measurements obtained below the temperature of critical viscosity (T_{cv}) were lower than that determined above T_{cv}. This effect was attributed to a nonequilibrium state of surface tension due to the random distribution of surface active phases in the slag and higher polymerization of silicate structure. The interfacial surface tensions did not vary significantly with temperatures above T_{cv}.

1.1 Project Overview

The Gasification Ash and Slag project was based on research on the characterization of low-rank coal ash and slag systems for gasification which had been conducted at the University of North Dakota Energy Research Center and its predecessor organizations prior to 1985. This work produced the following results: 1) a data base of viscosity-temperature-composition measurements of about twenty slags produced from low-rank coals ashed under gasification conditions, 2) a predictive equation for calculating the Newtonian flow region of the viscosity vs. temperature curve from slag composition which proved to be significantly superior to other available methods for low-rank coals, and 3) explanations derived from the interpretation of laboratory data for virtually every slag-related operational phenomenon observed in fixed-bed slagging gasifiers. The current project extended that work by incorporating 1) high-rank coal slag viscosity studies, 2) viscosity behavior modelling in the non-Newtonian flow regime, 3) new slag surface tension measurements, and 4) ash vaporization experiments coordinated with deposition studies. The original work plan consisted of four tasks for all rank coals: 1) collection and ashing of coals, b) vaporization studies, and c) viscosity and surface tension measurement and d) modelling. The intended outcome of this work was to create generic data bases and models to be used in the design and operation of many types of gasifiers. The current Gasification Ash and Slag Characterization objectives are to 1) determine the

relationship between the structure of molten slag and sintering processes in coal ashes under gasification conditions, 2) establish the effect of sulfer capture sorbents on the variation of molten slag structure and strength development in coal ash deposits, and the mineralogical transformations at temperatures below 1000°C, and 3) study partitioning and reactions of inorganic constituents in the char under simulated gasification conditions.

The data from this project will directly benefit other DOE-sponsored programs by determining the effect of limestone or dolomite reactions on ash agglomeration, slag viscosity, and surface tension. In addition, this data will provide a method to predict the effect of ash volatilization for the evaluation of coals in gasification, turbine, and combined-cycle systems. The volatilization studies will provide information to predict slag flow behavior critical to the operation of a slagging gasifier. Viscosity of coal ash slag and its relationship to temperature are indications of the degree of suitability for coals in slagging gasification units. Inability to properly initiate and maintain slag flow for any coal prohibits its use in a slagging gasifier operation. Flow properties for coal ash slags have been investigated to some extent, but additional investigation covering all ranks of coal and peat is desirable to more accurately characterize the coal ash slags, to refine predictive equations, and to aid in proper coal selection for ultimate use.

1.2 Technical Background

The coal gasification industry presently relies on qualitative empirical methods developed for combustion systems to predict the suitability of a coal and critical operating parameters with respect to ash behavior for a given gasification system. The methods developed for combustion tend to be inaccurate and sometimes produce erroneous predictions of ash behavior for gasification systems. The gasification industry requires better methods to determine the behavior of ash in a gasifier. New methods must be more accurate and rigorous than the methods used at present, in addition to being easily utilized by both operators and engineers.

The successful design and operation of coal gasification processes depends as much on a detailed knowledge of the inorganic matter in coal and the ability to control and mitigate its problems as on the behavior of its carbonaceous portion. Some of the major ash-related problems are slag flow control, slag attack on the refractory, ash deposition on heat transfer surfaces, corrosion and erosion of equipment materials, and emissions control. Such problems are closely tied to the abundance and association of the inorganic components in coal and the system conditions. At the high temperature regimes within a gasifier, the inorganic matter associated with the feed material can change chemically as well as mineralogically. These processes involve volatilization of organically associated inorganic elements, thermal decomposition of minerals, transformation of discrete mineral phases, and interaction of mineral phases. Products include discrete ash particles, gas-entrained species, agglomerates (clinkers), and/or slag. The amount and nature of the products depends on the nature of the inorganic constituents in the coal, on gasification conditions, and on the characteristics of the gasifier, including added material such as catalysts or in situ sulfur-capture

agents. In general, the products formed depend on the temperature within the gasifier. The higher the temperature, the greater the extent of ash melting and ash agglomeration. The extreme case is the formation of a homogeneous molten slag. At this stage, all mineral transformations have occurred, resulting in a slag that is approximately at thermal and, possibly, chemical equilibrium. A key aspect to note is that optimum operation of a gasification system relies on the knowledge of how the ash from a given coal will behave. That is, the ash from coal added to a dry-bottom gasifier must not agglomerate or clinker. Likewise, coal ash in a wet- or slagging-type gasifier must form a molten slag with a viscosity within the desired range. Failure of the ash to behave within the operational guidelines may result in poor gasifier performance, leading to possible premature shutdown of the unit. Therefore, a detailed knowledge of the behavior of coal inorganic species, including the formation of high-temperature products, is necessary in order to evaluate a coal for gasification.

The transformation of inorganic components during gasification consists of a complex series of chemical and physical processes. These transformations are dependent upon the physical and chemical properties of the coal and gasification conditions. The behavior of the inorganic components largely depends upon the initial partitioning of ash components. This partitioning influences the distribution of the ash species in slags, entrained ash, and deposits. Partitioning can be responsible for concentrating low-melting species in the entrained ash and on the surfaces of ash particles. These low-melting point phases aid in deposit initiation, growth, and sintering. The low-melting point species also contribute to ash agglomeration. Currently, ash-related problems cannot be accurately predicted by examination of the raw coal because the partitioning phenomena changes the distribution of the inorganic components in the ash. Therefore, the characterization and modelling of partitioning phenomena is critical to the development of methods to predict ash behavior. To date, little information exists on the behavior of inorganic components under closely controlled, pressurized conditions.

Ash deposit and agglomerate formation are dependent upon the physical properties of the ash materials, which are dependent on the ability of inorganic components to react, melt, and assimilate during processes under reducing environments. The physical properties are also strongly influenced by temperature, gas composition, and ash composition. Specific physical properties, surface tension and viscosity, directly affect ash agglomerate, slag, and deposit formation. Other ash properties of interest are compressive strength and wetability. Troublesome coal ash deposits result from the formation of low-viscosity liquid phases and the variability in surface tension of molten coal ashes. These processes are influenced by the structure of the molten slag and directly relate to the chemical composition of coal ashes. For example, the addition of network modifiers such as sodium, calcium, magnesium, and iron (Fe^{2+}) alter the molten slag structure by depolymerization of the silicate network, resulting in significantly lower viscosities. In addition, network modifiers promote crystallization processes. Crystallization of species from the melt phase changes the composition and physical properties of the residual liquid phase. Accordingly, the surface tension and viscosities can be significantly affected by the presence of crystals in the melt. Under the reducing conditions found

in gasifiers and advanced combustion systems, relatively low-melting point phases contain higher levels of iron. The characteristics of these iron-rich phases significantly affect the slagging and sintering behavior of coal ash.

The efforts of the program are focused on the following objectives:

1. To determine the mechanisms of inorganic transformations that lead to inorganic partitioning, ash deposition, and slag formation under gasification conditions;

2. To determine the factors that influence the sintering behavior of coal-derived ashes under gasification conditions; and

3. To develop a better means of predicting the behavior of inorganic components as a function of coal composition and reducing conditions.

The theoretical and experimental approach used in this project is two-fold. The first is to use bench-scale systems to recreate gasification conditions. Char and ash samples from these units are analyzed to characterize the partitioning of the chemical and mineralogical species. This data can then be used in the development of a theoretical model to predict partitioning of ash species in gasification systems. The second approach is to measure and characterize physical properties of coal ashes and slags to elucidate information on the performance of a particular sample in a gasification system.

The study of slag and deposit physical properties will include slag viscosity and surface tension measurements. Most coal ash slags exhibit an area of Newtonian flow characteristics at the high-temperature end of their liquid region, then, as temperature decreases, reach a point referred to as the temperature of critical viscosity, T_{cv}, where the flow character changes to non-Newtonian. These characteristics differ for each coal and are very dependent on the composition of the coal ash. Previous investigations have established that a viscosity value of less than 250 poise is required for adequate slag flow by gravity through a slag tap. For prediction of satisfactory slag flow in any slagging gasification operation, a value of no greater than 100 poise at 1300°C is a better criterion to use. In the past, several attempts have been made to define the Newtonian or linear portion of the log viscosity-temperature curve based on coal ash composition. Most of these were devised from experimental work with bituminous coal ash slags. Attempts to apply these correlations to low-rank coals have been unsuccessful. Of these numerous correlations, two (IRSID and Urbain) appeared to have some degree of applicability and, of the two, the Urbain appeared to have the best potential for modification and refinement to cover low-rank coal ash slags. Through the efforts of Streeter, Diehl, Schobert, Kalmanovitch, and Frank, a revised form of the Urbain equation called the Modified Urbain Equation was developed for use in predicting viscosity of slags from low-rank coal ashes.

Surface tension of a liquid is a measure of the ability of the liquid to "wet" or spread over and attack a surface. Several experimental methods are available for determination of surface tension of liquids at room temperature

or at slightly elevated temperatures. At high temperature the determination of surface tension becomes significantly more difficult, and the choice of methods is limited. In the operation of a slagging gasification unit, the effect of wetting any surface could be quite detrimental. If the surface is a refractory surface, the wetting activity could involve penetration of cracks and pores that could lead to erosion and degradation of the refractory and ultimately, cause failure. In addition, the surface tension and viscosity data are needed to determine the amount of ash in gasification systems. The relationship between surface tension and viscosity must be developed in order to predict ash deposition. Work has focused on determining slag viscosity and surface tension related to the sintering and agglomeration processes. Improvement of models used to predict viscosity (based on temperature and chemical composition of the ashes) has been one of the objectives. Progress is being made on relating slag chemical composition, as expressed by the base/acid ratio, to the surface tension of slag droplets on various substrates. In-depth research has been conducted on the mechanisms of sintering or deposit strength development in ash deposits. In the case where the gasifier is coupled with another unit that directly utilizes the hot product gas stream, such as a turbine, vaporization of slag components could lead to serious operational problems due to alkali attack on the turbine blades. Under certain conditions of sulfate composition and metal temperature, condensed alkali sulfates will melt on the turbine blades, accelerating the oxidation process.

2.0 OBJECTIVES/BACKGROUND

2.1 Task A: Inorganic Reactions

This task involves determining the reactions and interactions that coal inorganic constituents undergo under gasification conditions. Two coals will be studied: a Sufco, Utah, bituminous coal and a Montana subbituminous coal. The reactions will be studied under simulated gasification conditions using a modified version of the pressurized pyrolysis unit (PPU) at the EERC. The coals will be characterized using chemical fractionation and computer-controlled scanning electron microscopy (CCSEM). Chars will be produced in the PPU as a function of time. The chars will be analyzed using CCSEM and scanning electron microscopy point count (SEMPC). These advanced analytical techniques give extensive data on the change in size distribution, mineralogy, and chemistry of inorganic species. In particular, the SEMPC data can be used to determine the viscosity and relative reactivity, as defined by base/acid ratio, of the liquid phases, as well as the bulk chemical composition of the sample. This will allow both the determination of the partitioning of ash species as well as the effect of char formation on the ash species with respect to potential sintering behavior. The pressurized drop-tube furnace at the EERC will also be used to form char under simulated gasification conditions, both under entrained and fluidized conditions. The results will be used to determine the effect of gasifier design on inorganic reactions and ash partitioning.

2.1.1 Task A: Inorganic Reactions - Modifications

Because the SEMPC data from the 1988-1989 studies could be further used for interpretation of inorganic reactions and interactions, characterization of the Sufco bituminous and the Montana subbituminous coals was dropped to allow more data interpretation and manipulation of the PPU data. New approaches to interpretation of the SEMPC data were base/acid distributions calculated on the liquid or amorphous phases detected in the chars, and tracking of the calcium and iron into the aluminosilicate matrix with the use of ternary (elemental) phase diagrams to determine the effects of temperature and pressure on these char properties.

2.2 Task B: Partitioning of Ash Components

This task will involve the detailed comparison of the ash species formed in the PPU or pressurized drop-tube furnace with the parent coal. The gas-entrained species will be determined by difference in the case of the PPU data, and by sampling in the case of the drop-tube furnace. The effect of gasification conditions and residence time on partitioning will be evaluated. Analytical techniques will include CCSEM and SEMPC.

2.2.1 Task B: Partitioning of Ash Components - Modifications

Task B was postponed until the 1990-1991 year due to delays in construction of the pressurized drop-tube furnace. Data interpretation was enhanced in Task A to replace Task B.

2.3 Task C: Ash Sintering Under Gasification Conditions

This task will involve the determination of viscous flow sintering behavior of ash systems under gasification conditions. The strength of ash pellets will be determined under gasification atmospheres as a function of time and temperature. The effect of sorbent additives such as dolomite and limestone in the sintering process will also be evaluated. Selected samples will be analyzed by SEMPC, X-ray diffraction, and X-ray fluorescence.

2.4 Associated Task

As this project involves development of methodologies to predict ash behavior in gasification systems, we plan to enhance our relationship with industrial-scale operators such as Dow and Texaco. This will ensure that our approach to studying ash behavior in gasification systems can be validated and developed.

3.0 RESULTS AND DISCUSSION

3.1 Task A: Inorganic Reactions

Partitioning phenomena was studied using the data generated from the PPU (pressure pyrolysis unit) for previous Ash and Slag tasks. The PPU reactor was loaded with 5 to 10 grams of coal placed in ceramic crucibles. The

reactor was first pressurized under a 10%H_2/90%N_2 atmosphere, then heated over a period averaging 1.5 hours to the desired temperature. Conditions were held for two hours, then cooled under H_2/N_2 atmosphere overnight. The chars were low temperature ashed, then analyzed under SEMPC. Coals used were Indian Head, Velva, Pittsburgh #8, Illinois #6, and Wyodak. The test matrix consisted of runs at 650°C and 850°C, for each coal at the pressures, 15 psi, 200 psi, and 400 psi.

Interpretation of the SEMPC data began with the calculation of the base/acid ratio for each point designated as amorphous by the SEMPC technique. [The SEMPC technique characterizes the chemical composition of each point, analyzing an area of $3(\mu m)^2$. If the composition matches a given crystalline phase, it is categorized accordingly; the rest are designated as amorphous (non-crystalline) or remain unclassified.] The base/acid ratios of all the amorphous points are presented as a distribution for each of the chars. The base/acid ratios distribution provides relative insight into the potential behavior of the ratios amorphous phases and char properties. The quantity and base/acid of amorphous phase shows possible reactions occurring over the pressure and temperature regimes studied. The results for the coals studied are presented in the following sections.

Presented here are the distributions of the base/acid ratios calculated on the SEMPC points designated as amorphous. In addition, the elemental Al-Si-Fe and Al-Si-Ca ternary phase diagrams were plotted to track assimilation of iron and calcium into the aluminosilicate matrix.

3.1.1 Indian Head Coal and Chars

3.1.1.1 Base/Acid Ratio

Indian Head chars (shown in Figures 1-6) produced at 650°C and 850°C at constant pressure show no significant difference in quantity and base/acid ratios of the amorphous phases. However, chars produced at 15 and 200 psi and constant temperature show that the quantity of amorphous phase and the spread of the base/acid ratio (hence the reactivity and possibly agglomeration and deposition potential) are increased. The histograms also show that chars produced at 650°C and 850°C at atmospheric pressure have nearly identical distributions in quantity and spread of amorphous phases as the low temperature ash of the coal. This suggests that the temperature at which the chars are produced does not have a large effect on the reactivity and quantity of amorphous phase reactivity.

3.1.1.2 Al-Si-Ca

The following data (Figures 7-11) show the reactions occurring between calcium and aluminosilicates. At constant pressure, a more homogeneous system is formed with increasing temperature. At 650°C, higher pressure limited interaction, while no effect was discernable at 850°C.

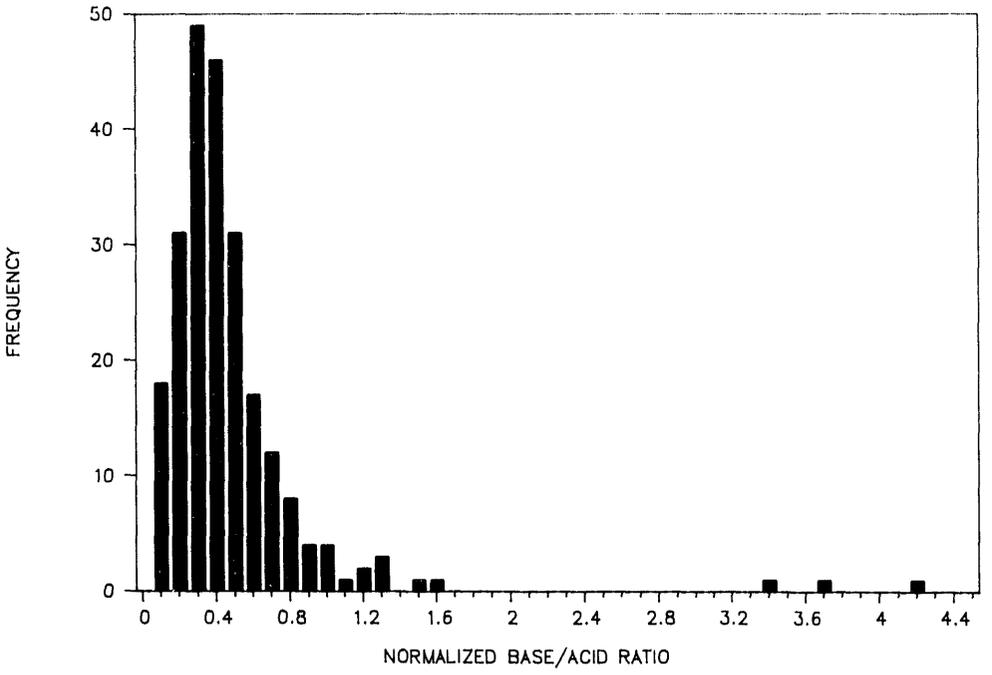

Figure 1. Base/acid ratio distribution of Indian Head coal low temperature ash.

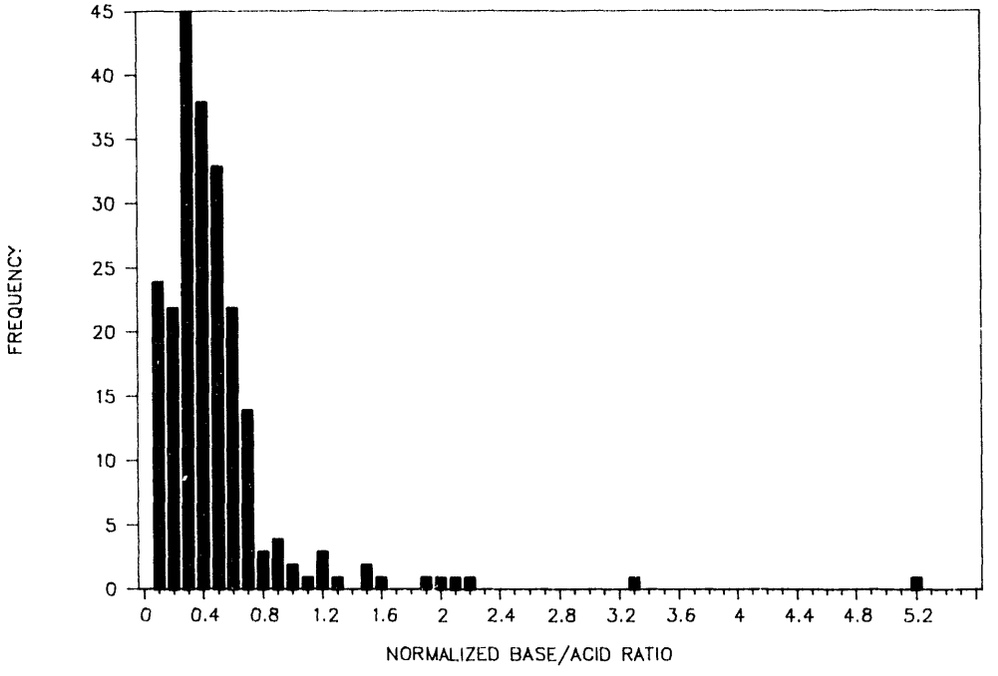

Figure 2. Base/acid ratio distribution of Indian Head char 650°C/15 psi low temperature ash.

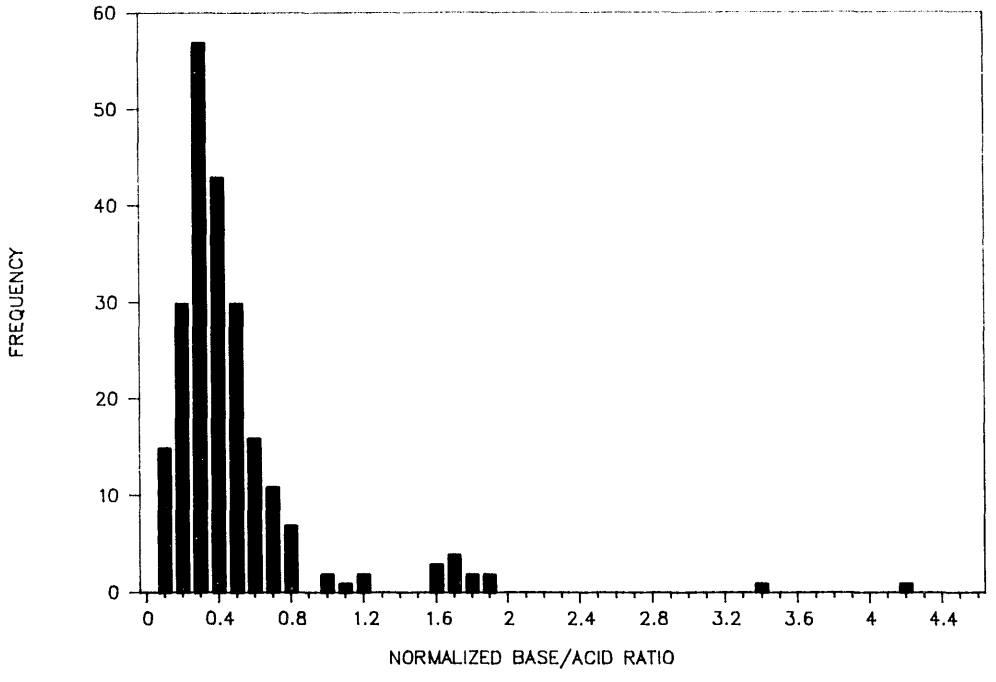

Figure 3. Base/acid ratio distribution of Indian Head char 850°C/15 psi low temperature ash.

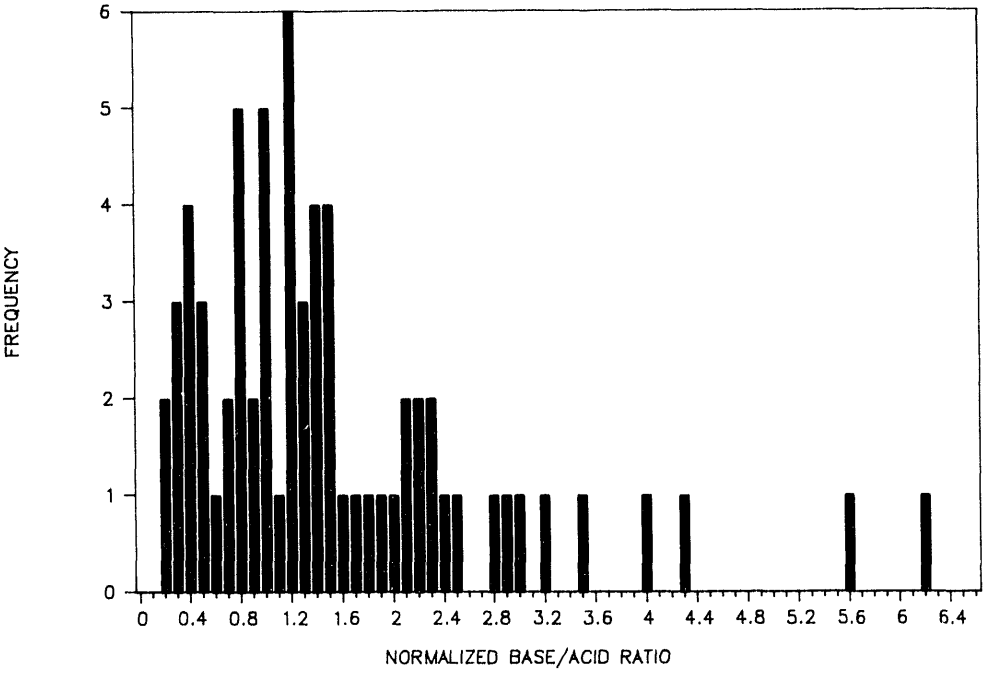

Figure 4. Base/acid ratio distribution of Indian Head char 850°C/200 psi low temperature ash.

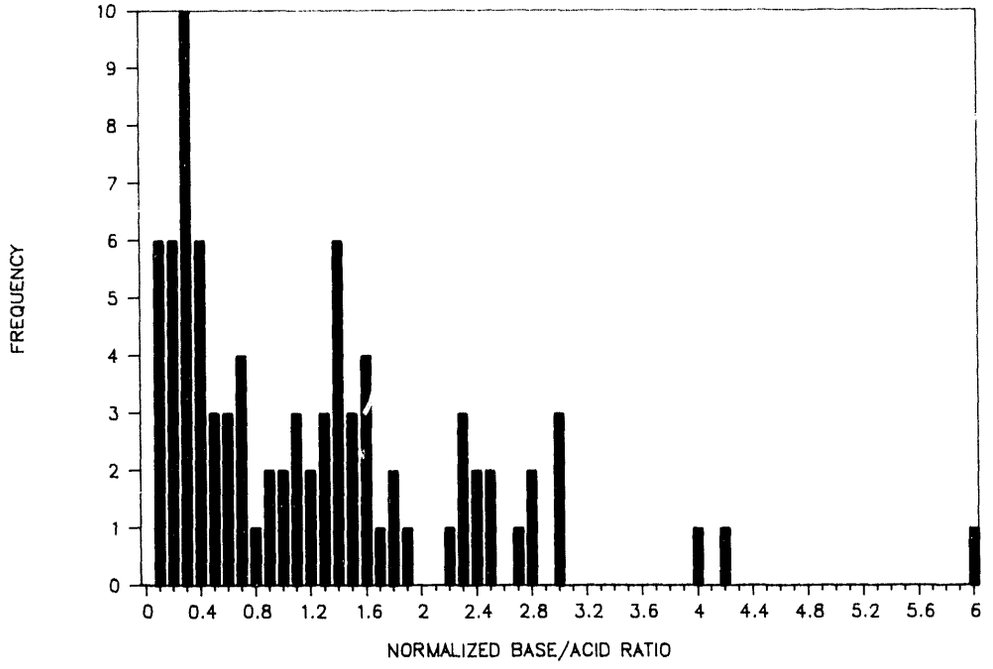

Figure 5. Base/acid ratio distribution of Indian Head char 650°C/200 psi low temperature ash.

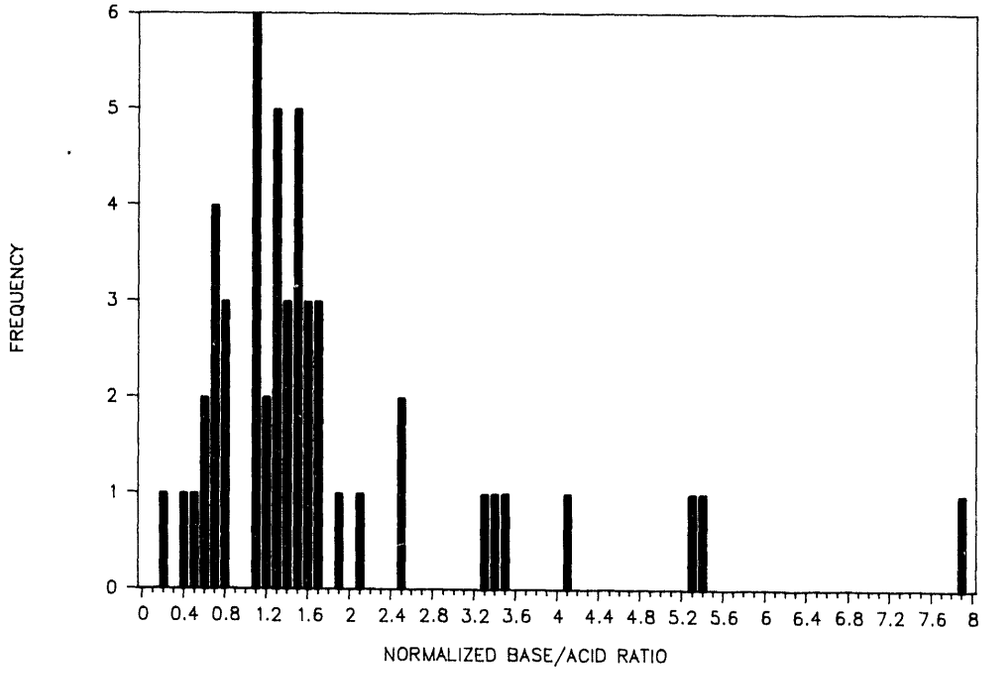

Figure 6. Base/acid ratio distribution of Indian Head char 650°C/400 psi low temperature ash.

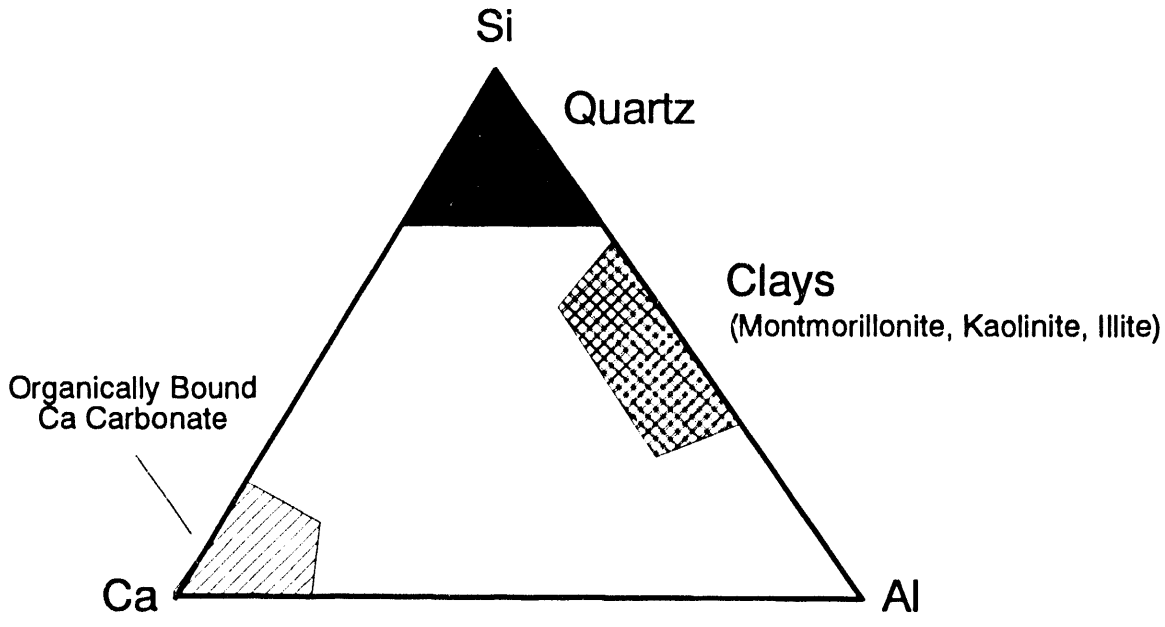

Figure 7. Al-Si-Ca ternary phase diagram depicting relevant coal minerals.

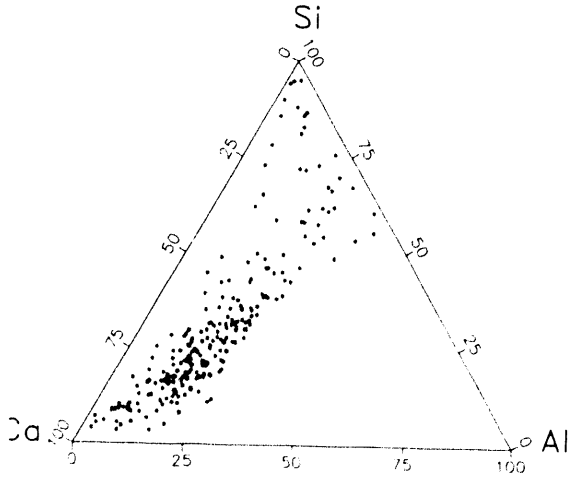

Figure 8. Indian Head Char, 650°C/15 psi.

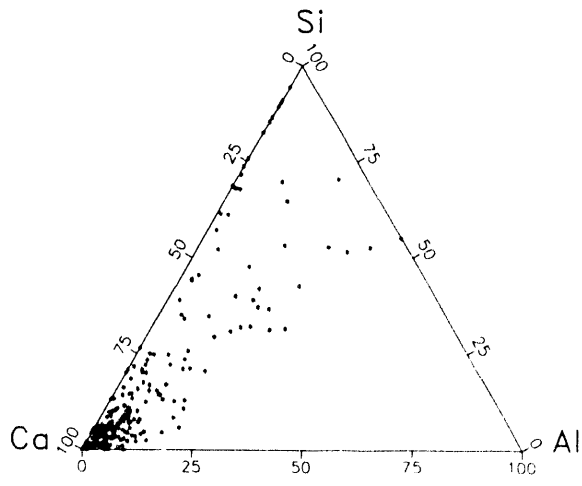

Figure 9. Indian Head Char, 650°C/200 psi.

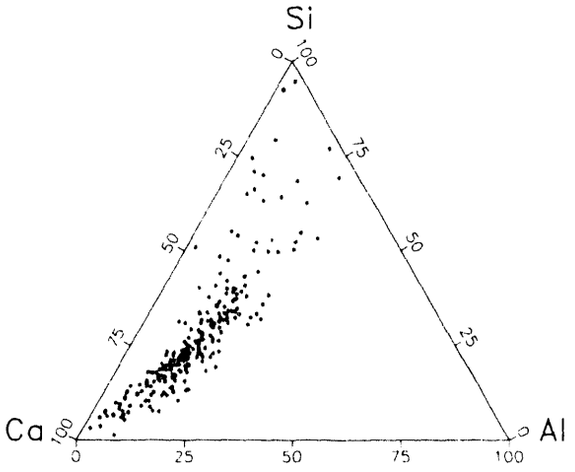

Figure 10. Indian Head Char, 850°C/15 psi

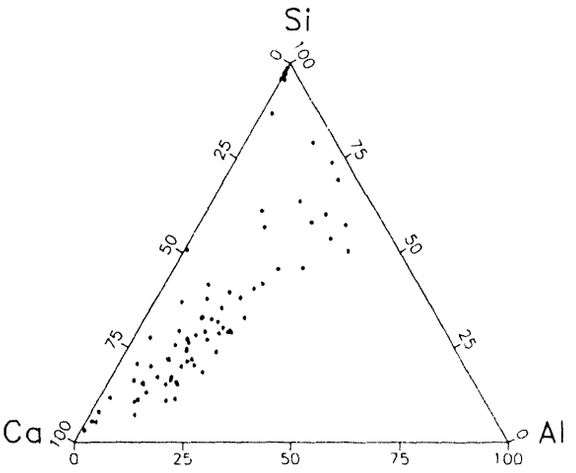

Figure 11. Indian Head Char, 850°C/200 psi

3.1.1.3 Al-Si-Fe

The reactions between iron and aluminosilicates are shown in Figures 12-14. The main conclusion drawn from these diagrams is that higher pressure limits the Fe-Al-Si reactions and interactions. It is speculated that the interaction of iron with crucible or reactor wall is responsible for the lesser amounts of iron seen at lower pressures while at higher pressures, these interactions are inhibited.

3.1.2 Wyodak Coal and Chars

3.1.2.1 Base/Acid Ratio

Wyodak coal and chars (shown in Figures 15-21) showed markedly different trends than the Indian Head coal. The LTA of the Wyodak coal showed almost no amorphous phase. The spread of base/acid ratio decreased at higher pressures from atmospheric at 650°C and increased at higher pressures from atmospheric at 850°C. Increased temperatures at constant pressures increased the spread of base/acid ration. The quantity of the base/acid ratio was shifted lower with increasing temperatures at 15 psi to 200 psi while the reserve was true at 400 psi. At 650°C, the base/acid ratio quantities were shifted lower with increasing pressure while at 850°C they were shifted higher.

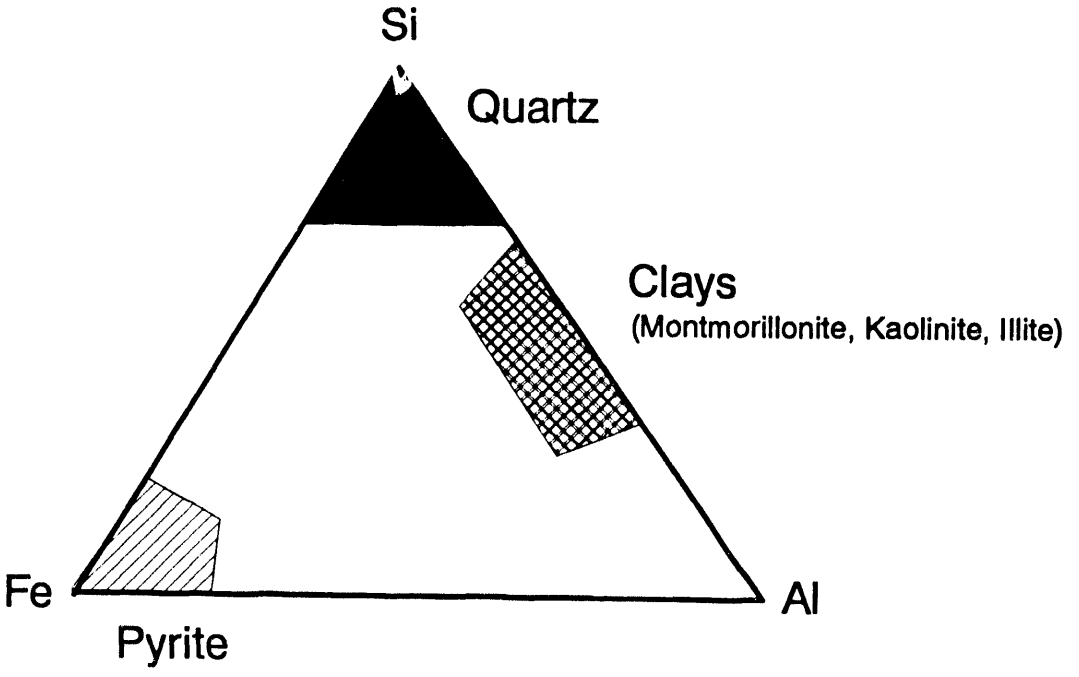

Figure 12. Al-Si-Fe ternary phase diagram depicting relevant coal minerals.

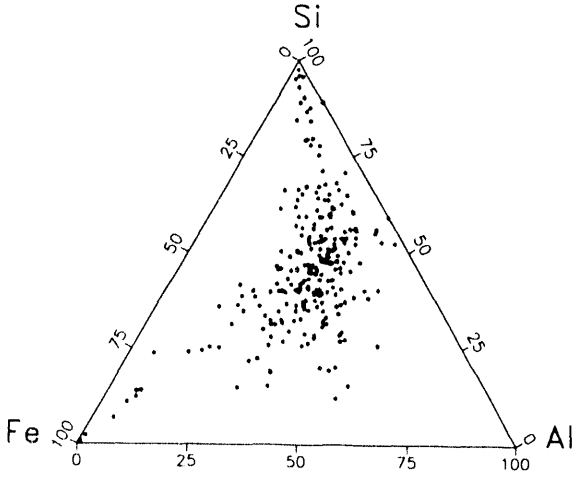

Figure 13. Indian Head Char, 650°C/15 psi.

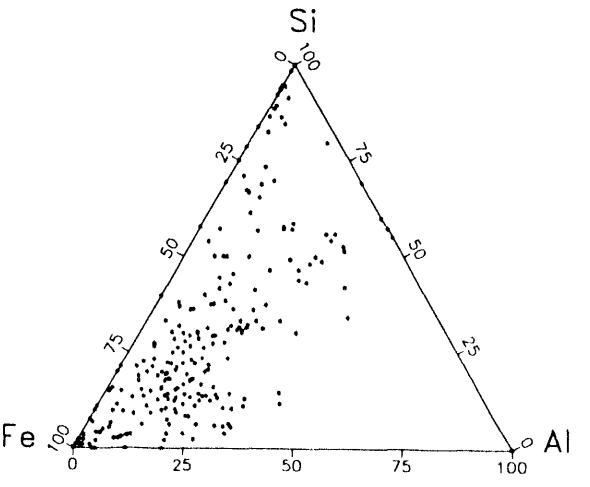

Figure 14. Indian Head Char, 650°C/200 psi.

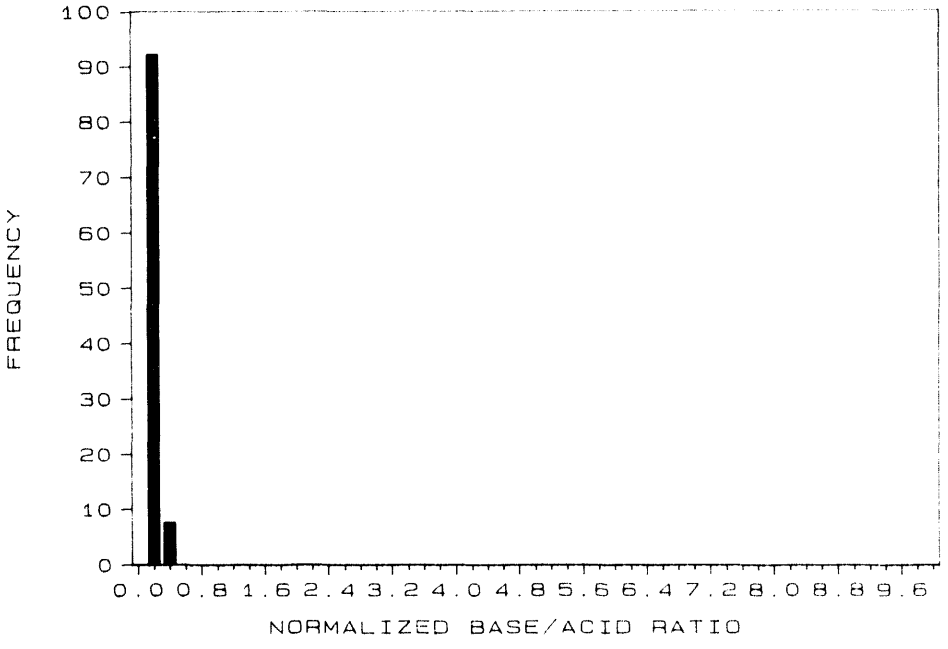

Figure 15. Base/acid ratio distribution of Wyodak coal low temperature ash.

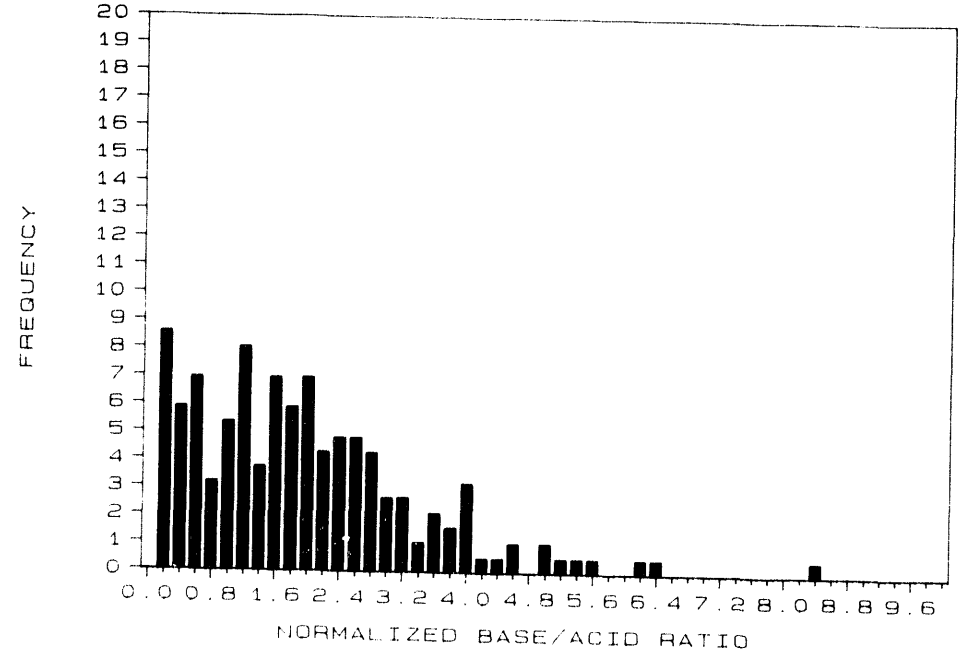

Figure 16. Base/acid ratio distribution of Wyodak char 650°C/15 psi low temperature ash.

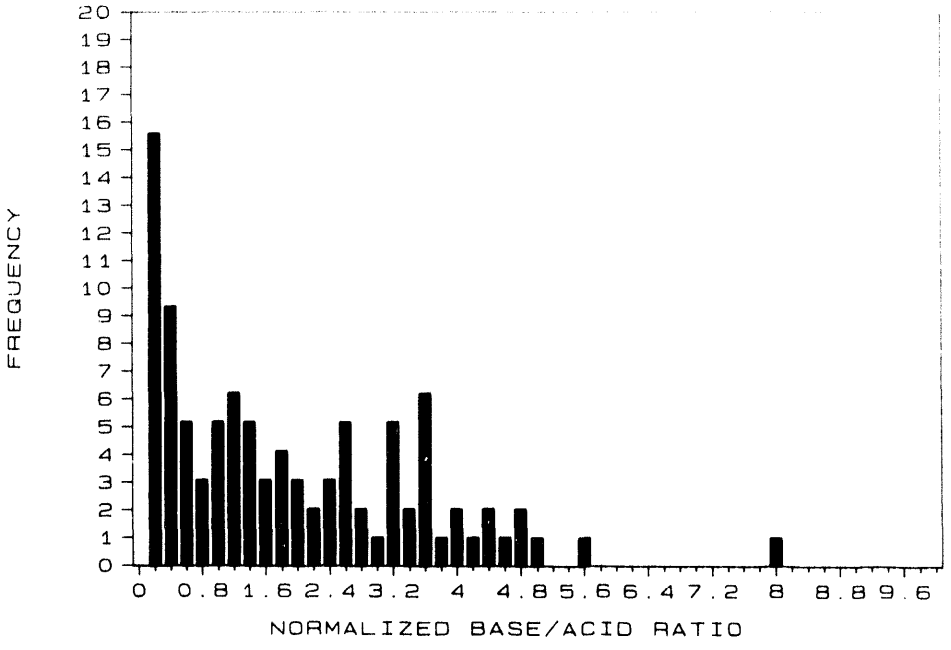

Figure 17. Base/acid ratio distribution of Wyodak char 850°C/15 psi low temperature ash.

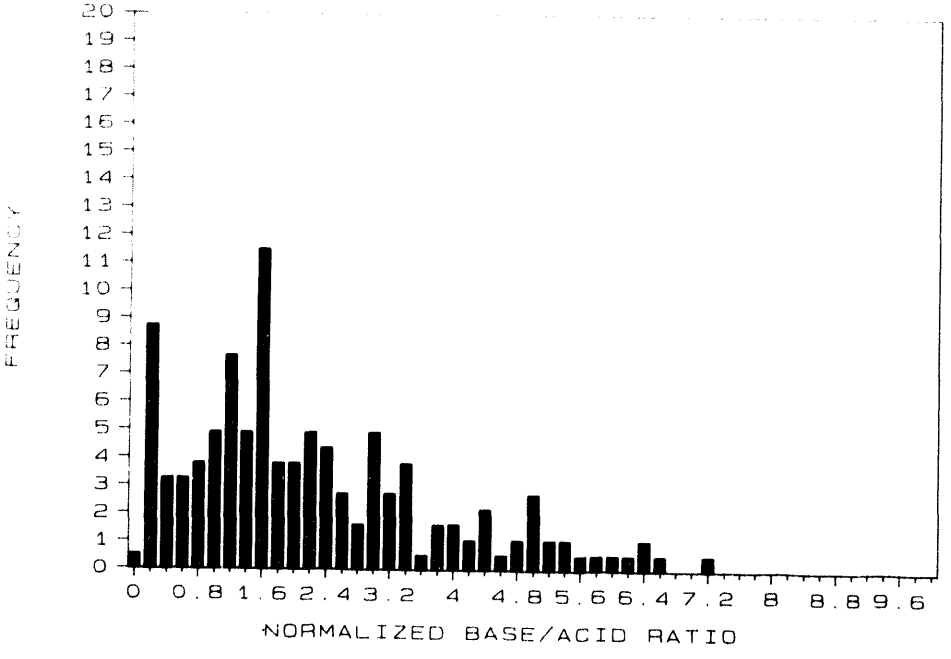

Figure 18. Base/acid ratio distribution of Wyodak char 850°C/200 psi low temperature ash.

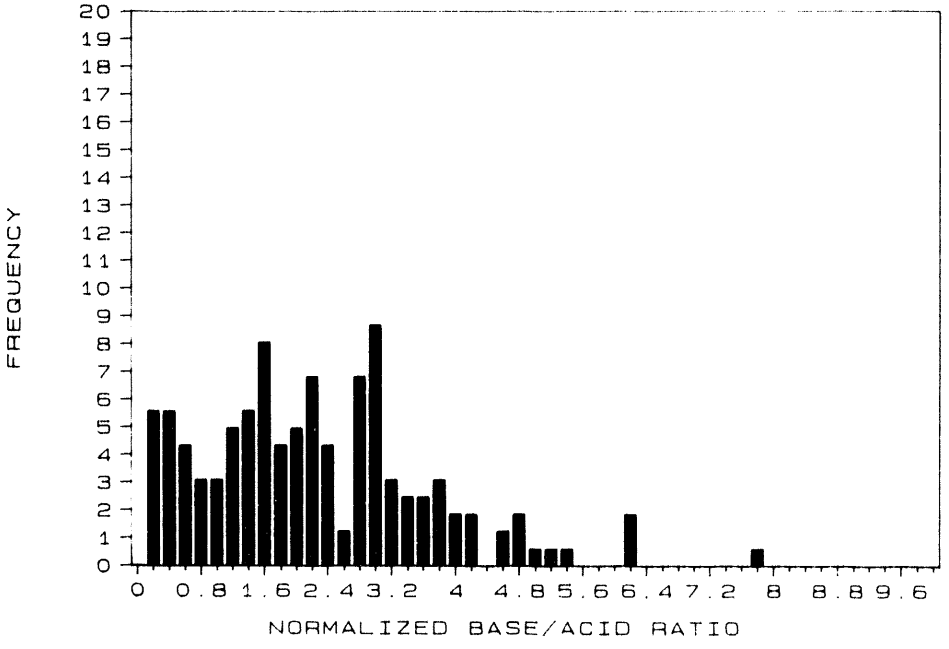

Figure 19. Base/acid ratio distribution of Wyodak char 850°C/400 psi low temperature ash.

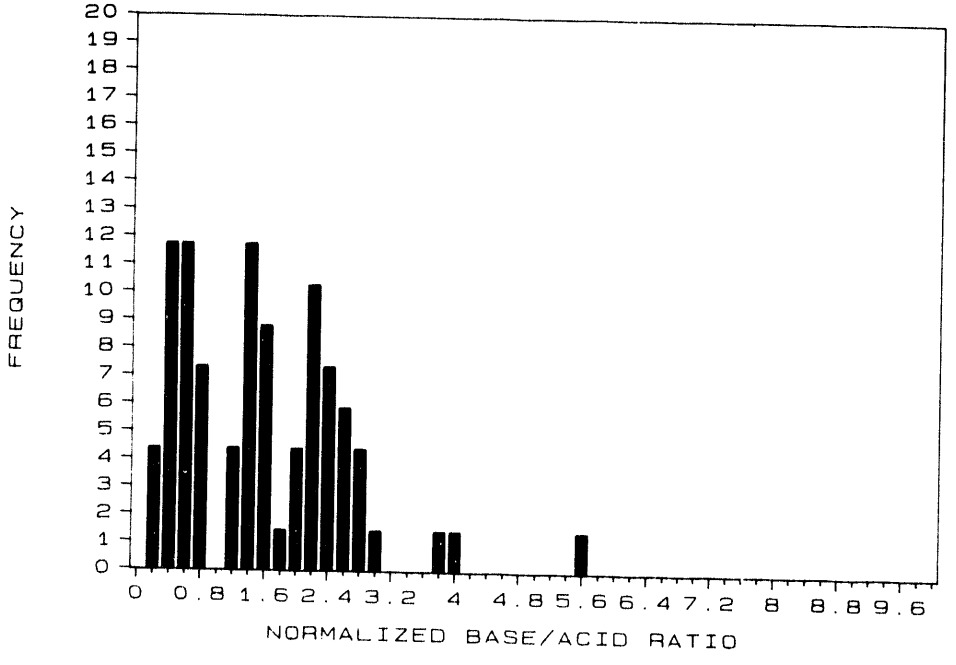

Figure 20. Base/acid ratio distribution of Wyodak char 650°C/200 psi low temperature ash.

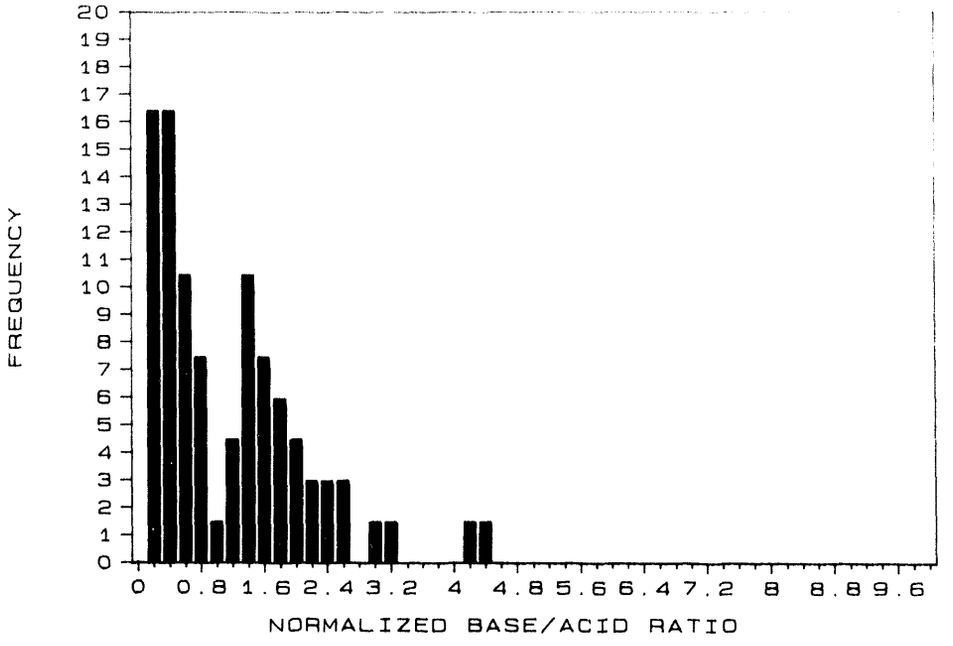

Figure 21. Base/acid ratio distribution of Wyodak char 650°C/400 psi low temperature ash.

3.1.2.2 Al-Si-Ca

The main effect shown in the diagrams (Figure 22-27) is that more calcium reacts at higher temperatures (constant pressure), as expected. Pressure showed no discernable effect. Please refer also to Figure 7.

3.1.2.3 Al-Si-Fe

Figures 28-32 show the reactions of iron and aluminosilicates. Pure iron phases were dominant at higher pressures. Again, this could be due to reaction of iron with the crucible and reactor causing less interaction between iron and the aluminosilicates. Please refer also to Figure 12.

3.1.3 Velva Coal and Chars

3.1.3.1 Base/Acid

The Velva coal shown in Figures 33-37 showed only one amorphous point in the SEMPC analysis, so a base/acid ratio distribution was not calculated. The char produced at 650°C and 850°C and 15 psi showed no difference in the spread of base/acid ratio but the 850°C char showed, as expected, an increase in the quantity of amorphous phase. However, at constant pressure of 400 psi, the char at 650°C showed only a small amount of amorphous with a wide spread of

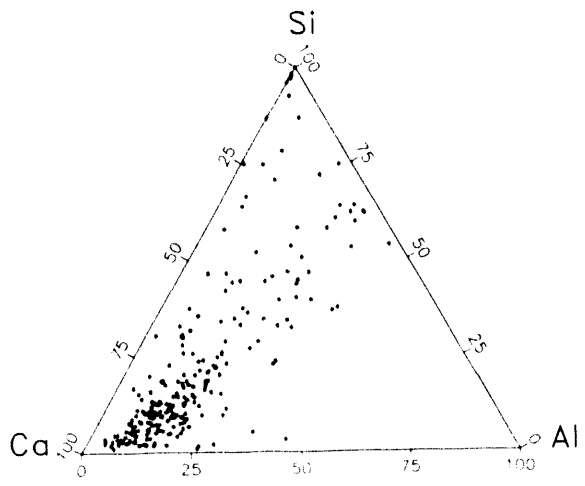

Figure 22. Wyodak Char, 650°C/15 psi.

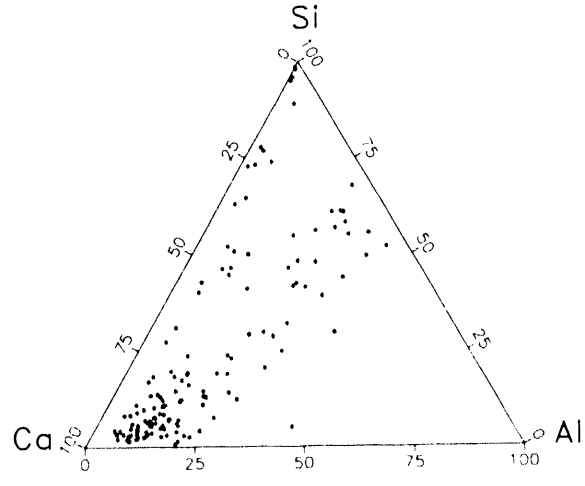

Figure 23. Wyodak Char, 850°C/15 psi.

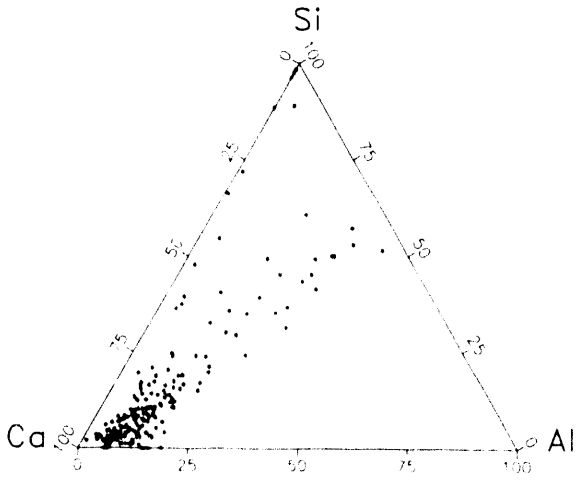

Figure 24. Wyodak Char, 650°C/200 psi.

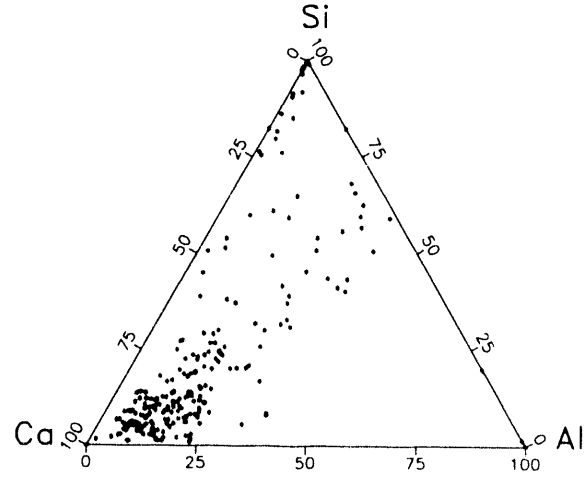

Figure 25. Wyodak Char, 850°C/200 psi.

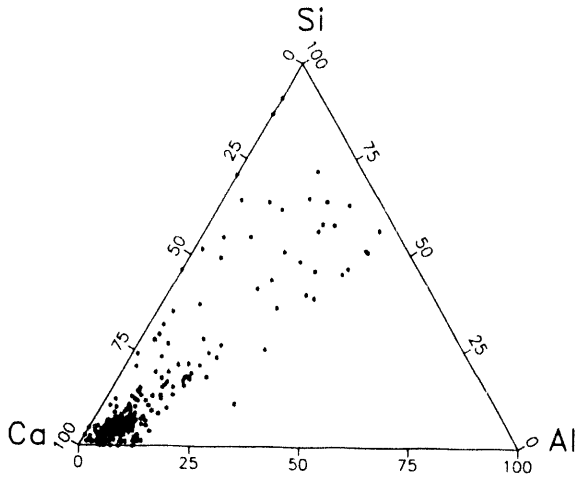

Figure 26. Wyodak Char, 650°C/400 psi.

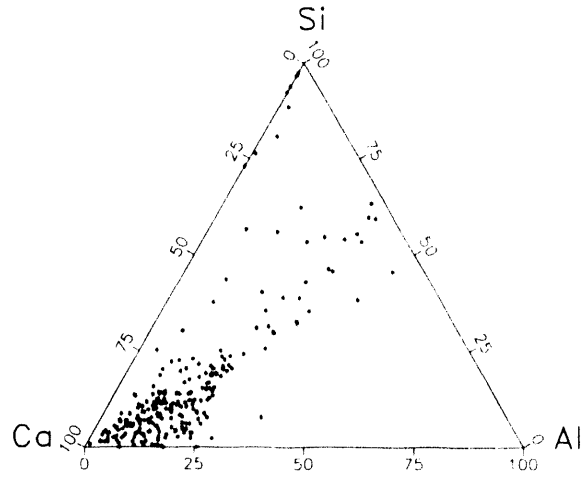

Figure 27. Wyodak Char, 850°C/400 psi.

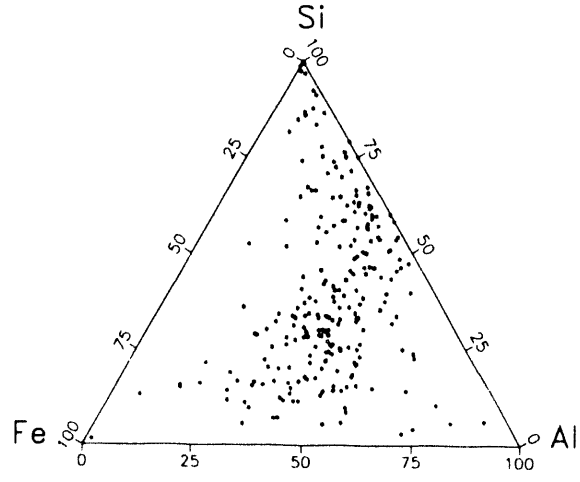

Figure 28. Wyodak Char, 650°C/15 psi.

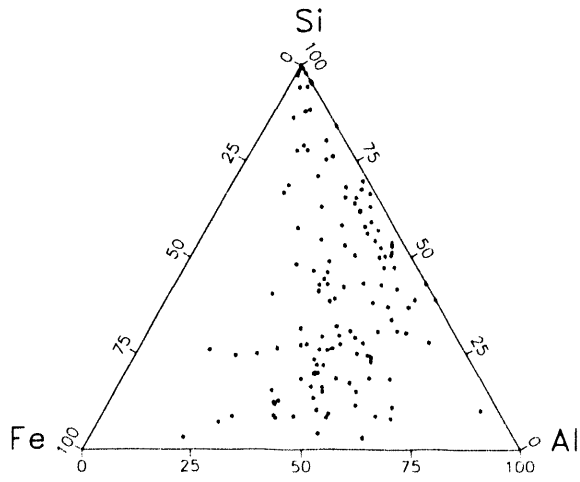

Figure 29. Wyodak char, 850°C/15 psi.

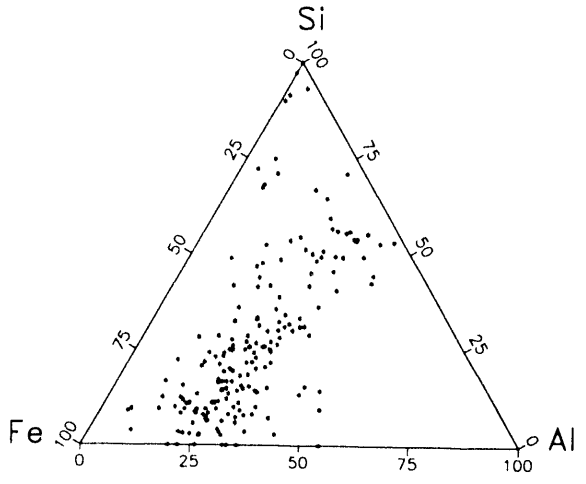

Figure 30. Wyodak Char, 650°C/200 psi.

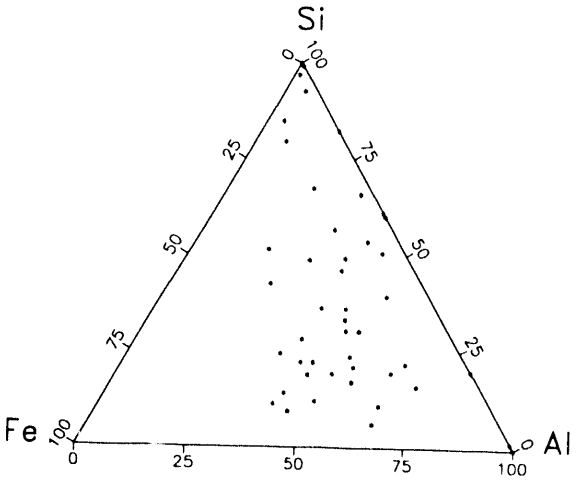

Figure 31. Wyodak char, 850°C/200 psi.

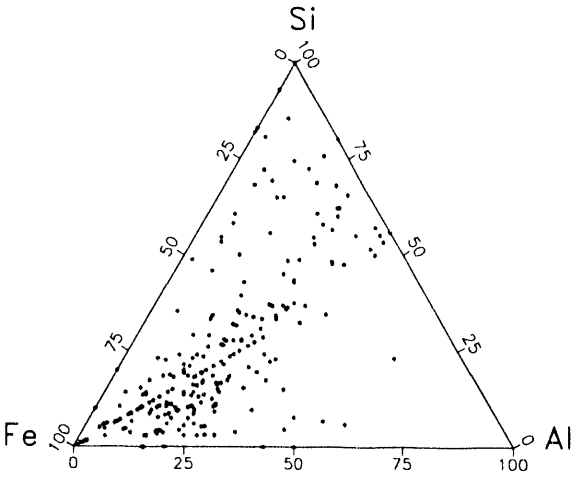

Figure 32. Wyodak Char, 650°C/400 psi.

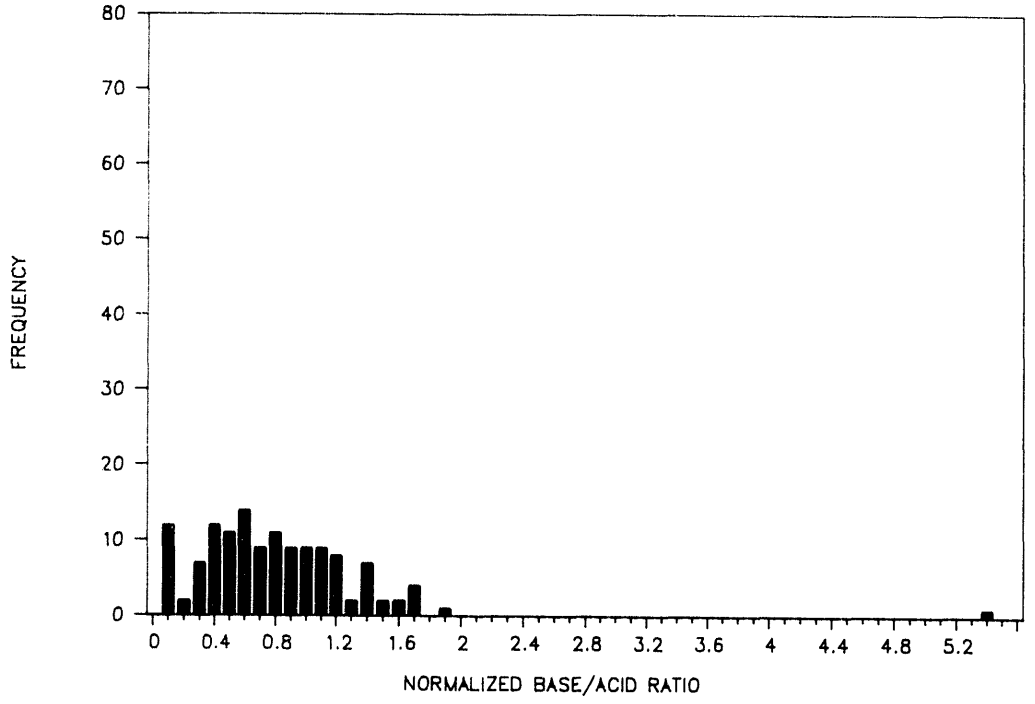

Figure 33. Base/acid ratio distribution of Velva char 650°C/15 psi low temperature ash.

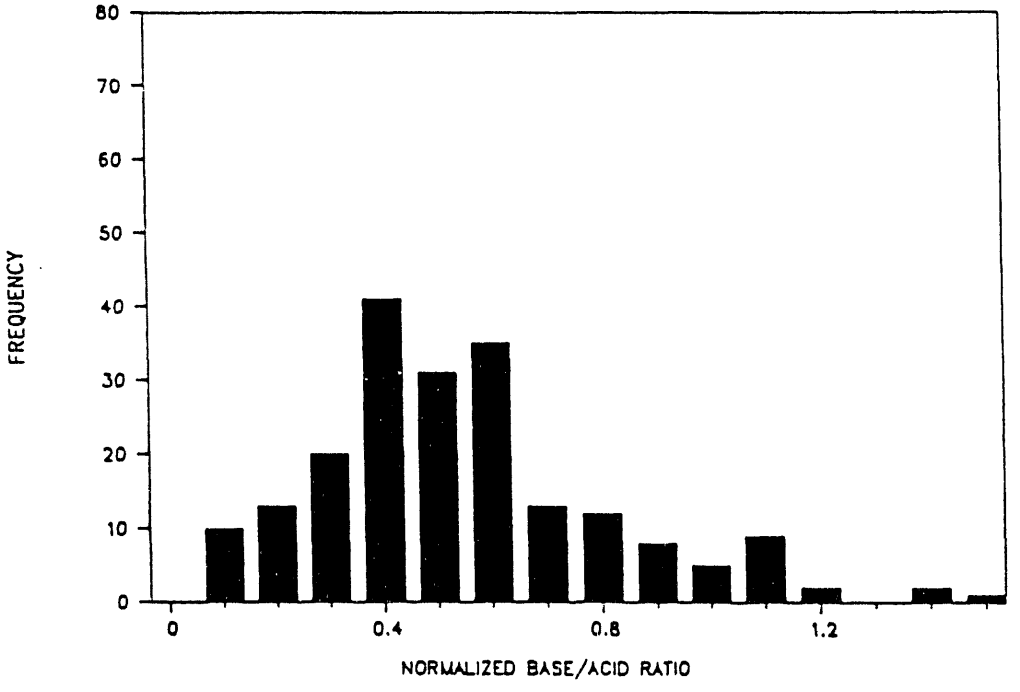

Figure 34. Base/acid ratio distribution of Velva char 850°C/15 psi low temperature ash.

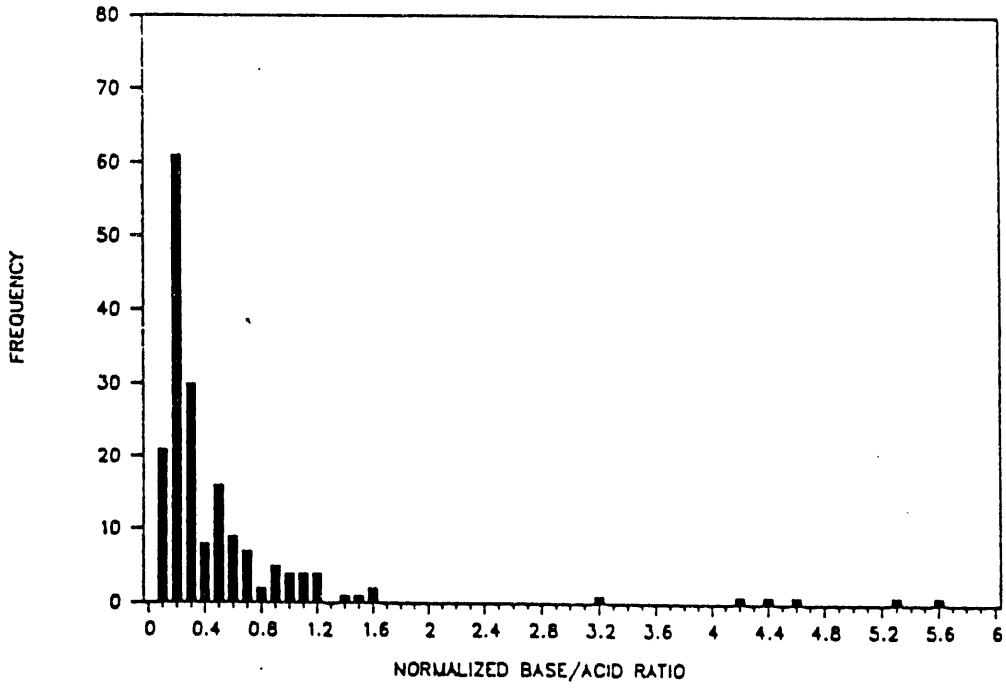

Figure 35. Base/acid ratio distribution of Velva char 850°C/200 psi low temperature ash.

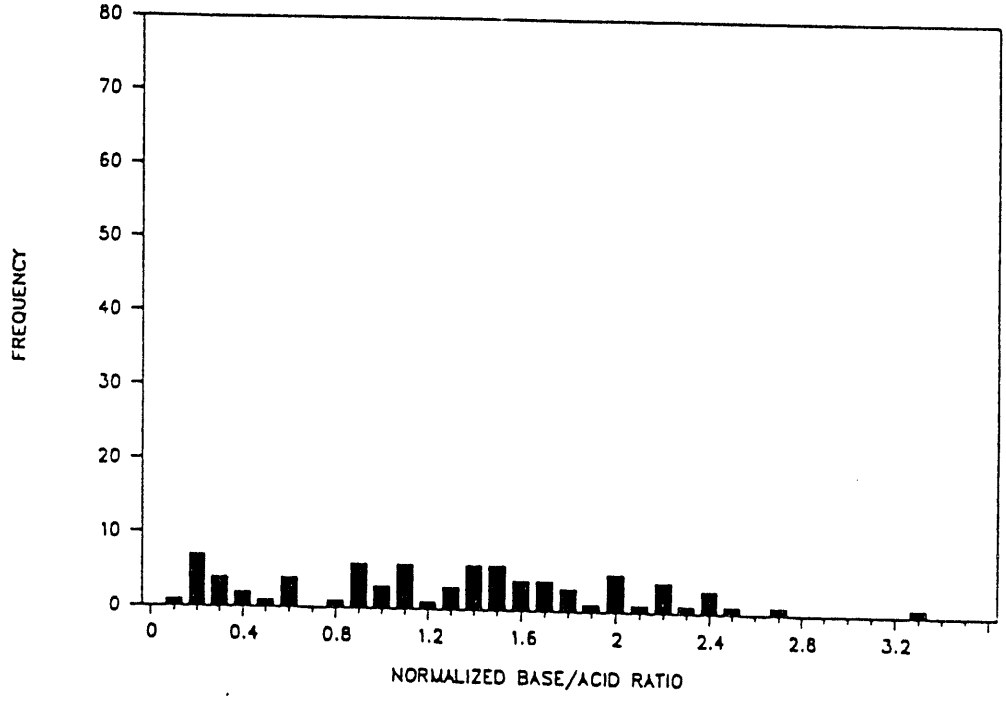

Figure 36. Base/acid ratio distribution of Velva char 650°C/200 psi low temperature ash.

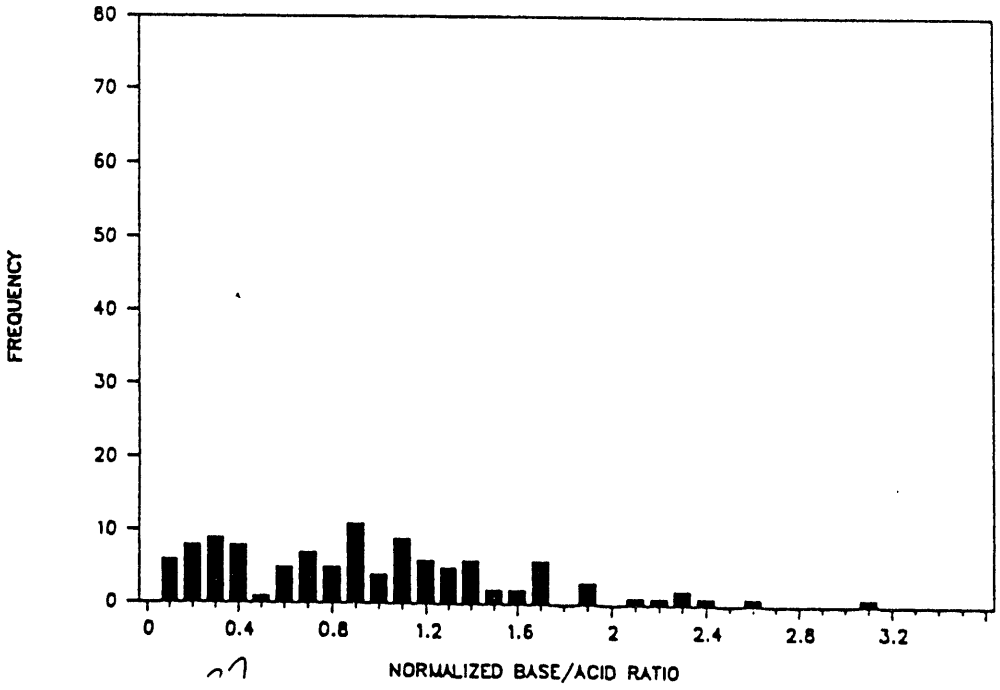

Figure 37. Base/acid ratio distribution of Velva char 650°C/400 psi low temperature ash.

base/acid ratio, whereas the 850°C showed a significant amount of a more homogenous amorphous phase. The chars produced at 15 and 400 psi at constant temperature of 650°C or 850°C showed no significant difference in the amount of base/acid spread in the amorphous phase. Again, this suggests that temperature plays a more important role than pressure in mineralogical or chemical changes in many coals.

3.1.3.2 Al-Si Ca

Velva coal contains such a high quantity of organically bound calcium, that tracing the reactions is difficult. The data is presented in Figures 38-42, but no trends are evaluated. Please refer also to Figure 7.

3.1.3.3 Al-Si-Fe

The iron-aluminosilicate plots of the Velva coal (Figures 43-47) showed an opposing trend to the other coals, which showed more pure iron at higher pressures. The high temperature and high pressure results seem to show an interaction which creates a more homogeneous Fe-Al-Si system. Please also refer to Figure 12.

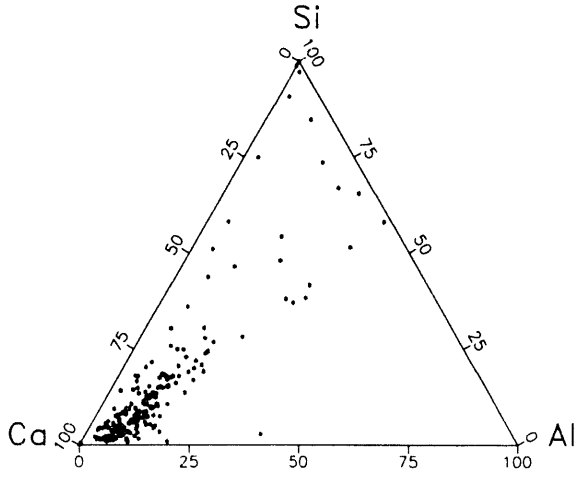

Figure 38. Velva Char, 650°C/15 psi.

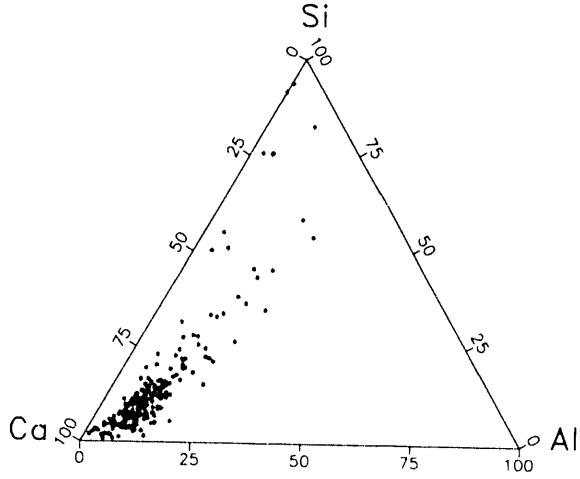

Figure 39. Velva Char, 850°C/15 psi.

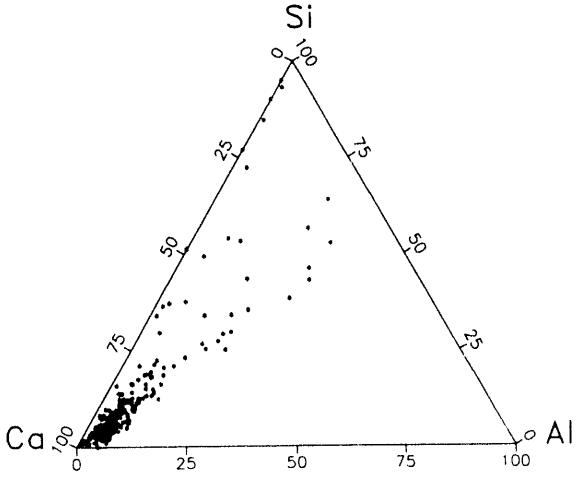

Figure 40. Velva Char, 650°C/200 psi.

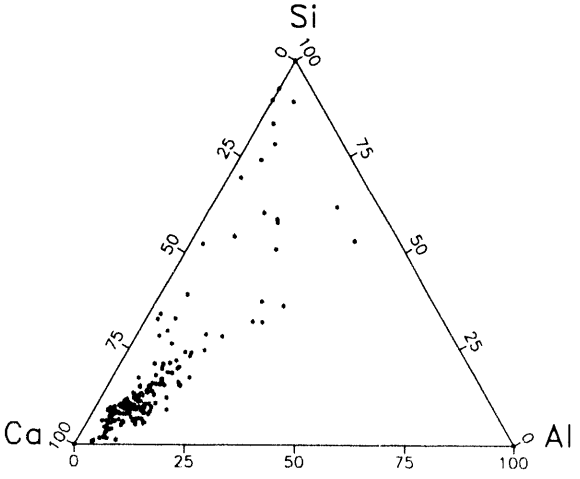

Figure 41. Velva Char, 850°C/200 psi.

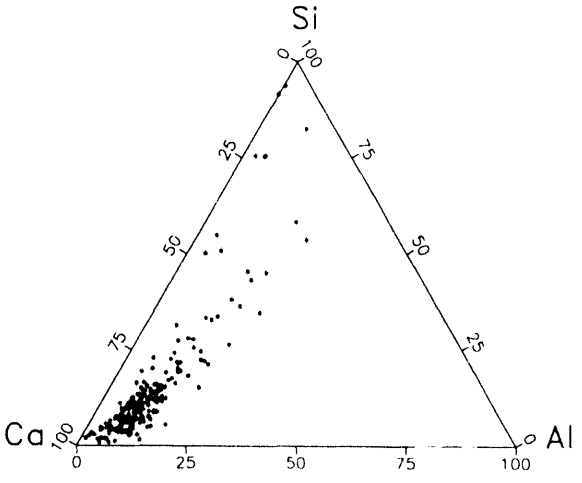

Figure 42. Velva char, 850°C/400 psi.

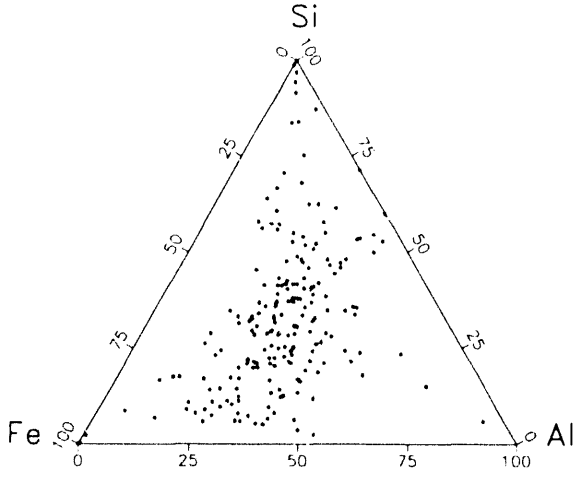

Figure 43. Velva Char, 650°C/15 psi.

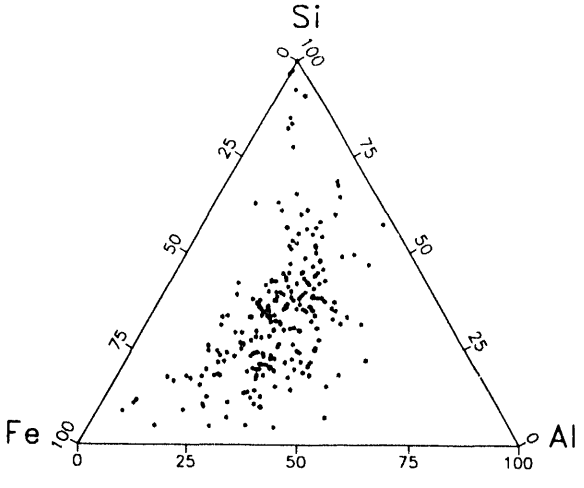

Figure 44. Velva Char, 850°C/15 psi.

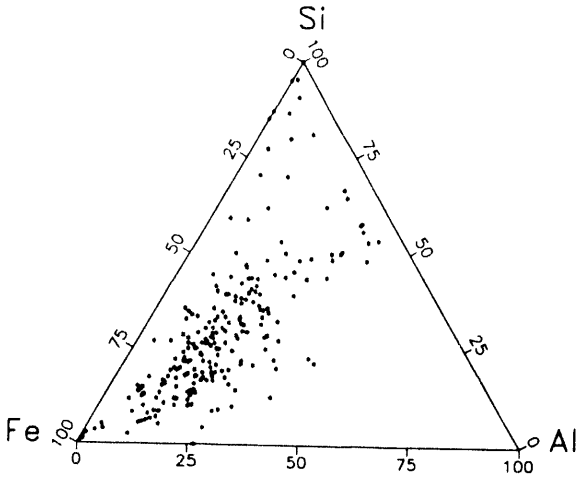

Figure 45. Velva Char, 650°C/200 psi.

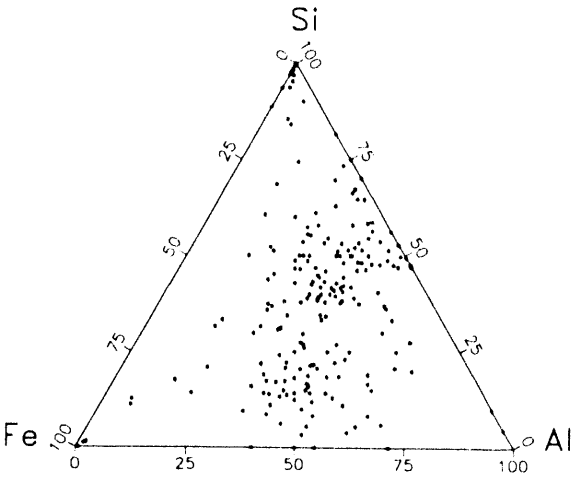

Figure 46. Velva Char, 650°C/400 psi.

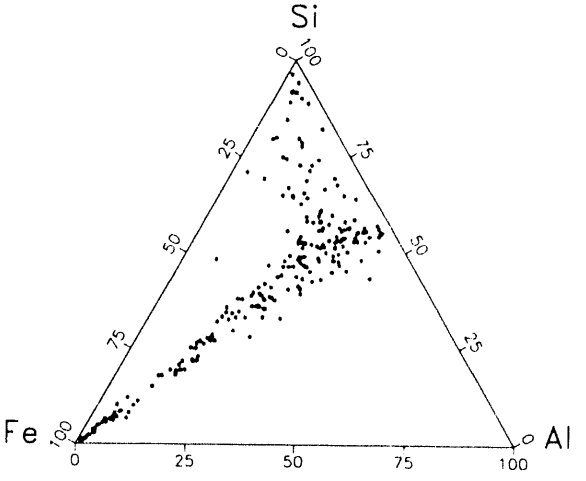

Figure 47. Velva Char, 850°C/400 psi.

3.1.4 Illinois #6 Coal

3.1.4.1 Base/Acid Ratios

The Illinois #6 coal shown in Figures 48-53 showed both pressure and temperature effects on the quantity and spread of the base/acid ratio. The initial LTA ash of the coal showed a significant quantity of a homogeneous amorphous phase. The chars produced at 650°C and 850°C at a constant pressure of 15 psi showed the same spread in base/acid ratio as the coal LTA ash. The 650°C char produced less quantity than the 850°C char as expected. However, both chars produced less amorphous phase than the LTA coal ash. Increasing the pressure of the 650°C and 850°C chars to 200 psi decreased the quantity of amorphous phase produced but did not change the spread of the base/acid ratio. A notable change occurred in the 850°C char at 400 psi. The base/acid spread remained constant but the quantity shifted significantly to lower base/acid ratios.

3.1.4.2 Al-Si-Ca

Illinois #6 coal contains little organically bound calcium so the calcium vaporization potential is lower. The calcium in Illinois #6 exists as carbonate in the calcite phase. Consequently, no reactions or interactions are seen in Figures 54-57. Please also refer to Figure 7.

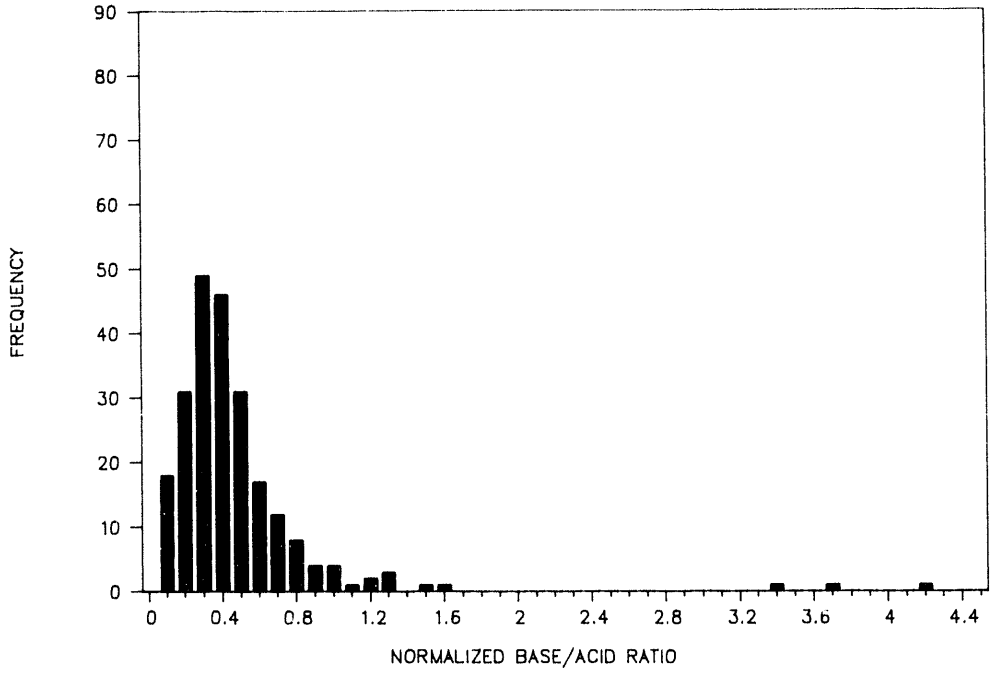

Figure 48. Base/acid ratio distribution of Illinois #6 coal low temperature ash.

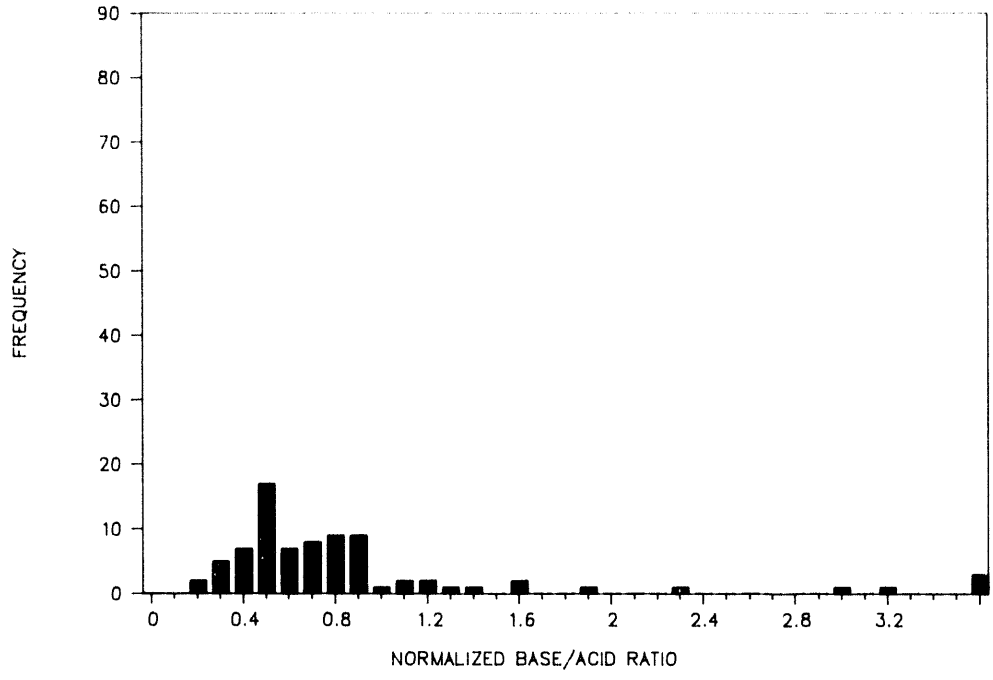

Figure 49. Base/acid ratio distribution of Illinois #6 char 650°C/15 psi low temperature ash.

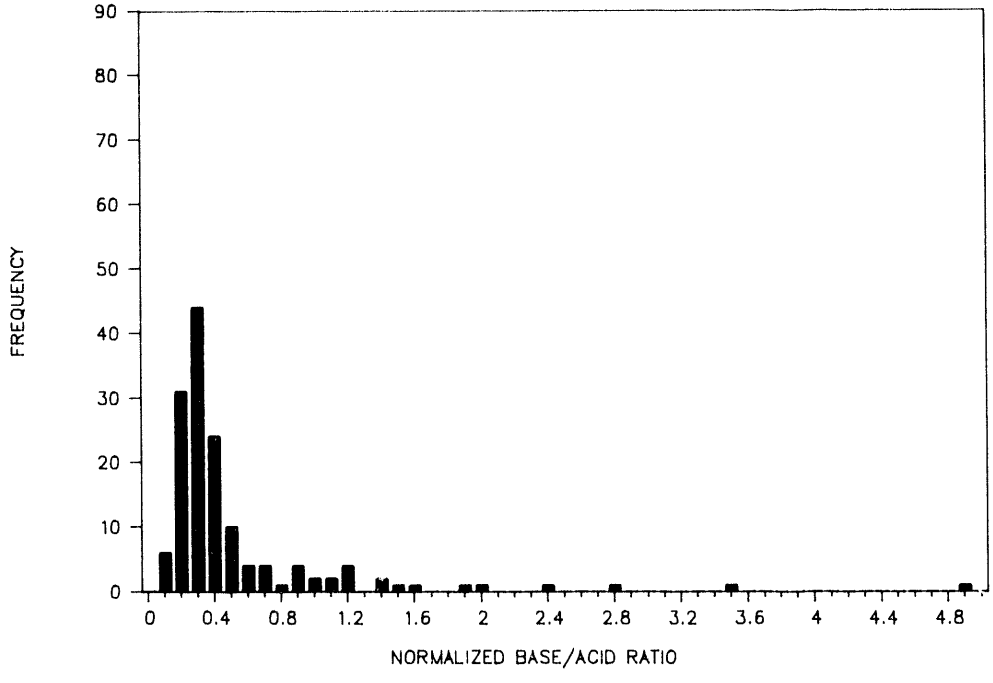

Figure 50. Base/acid ratio distribution of Illinois #6 char 850°C/15 psi low temperature ash.

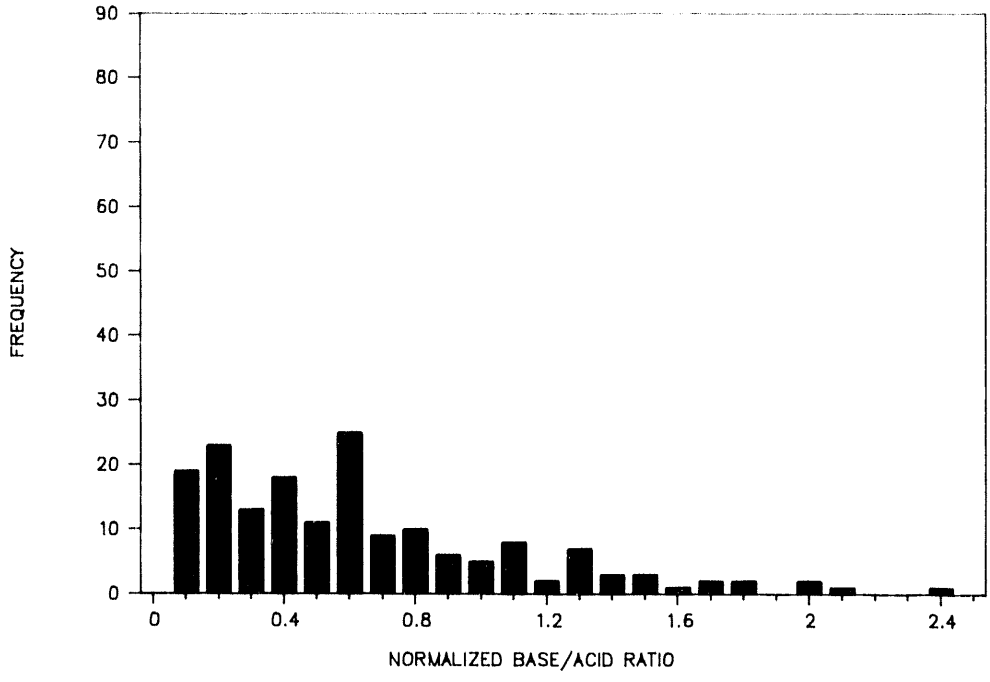

Figure 51. Base/acid ratio distribution of Illinois #6 char 850°C/200 psi low temperature ash.

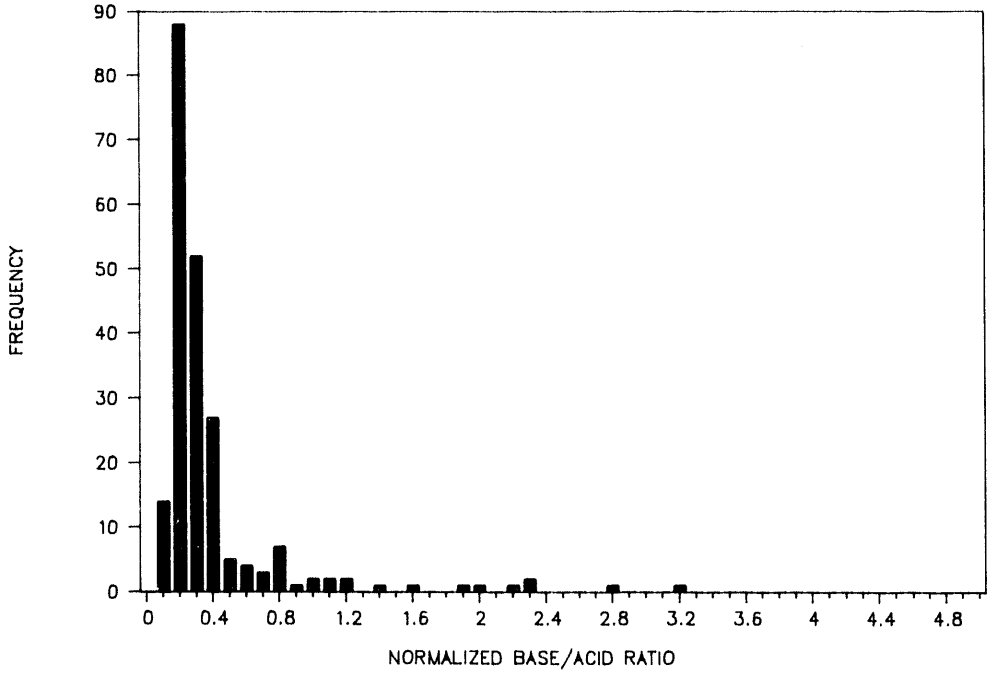

Figure 52. Base/acid ratio distribution of Illinois #6 char 850°C/400 psi low temperature ash.

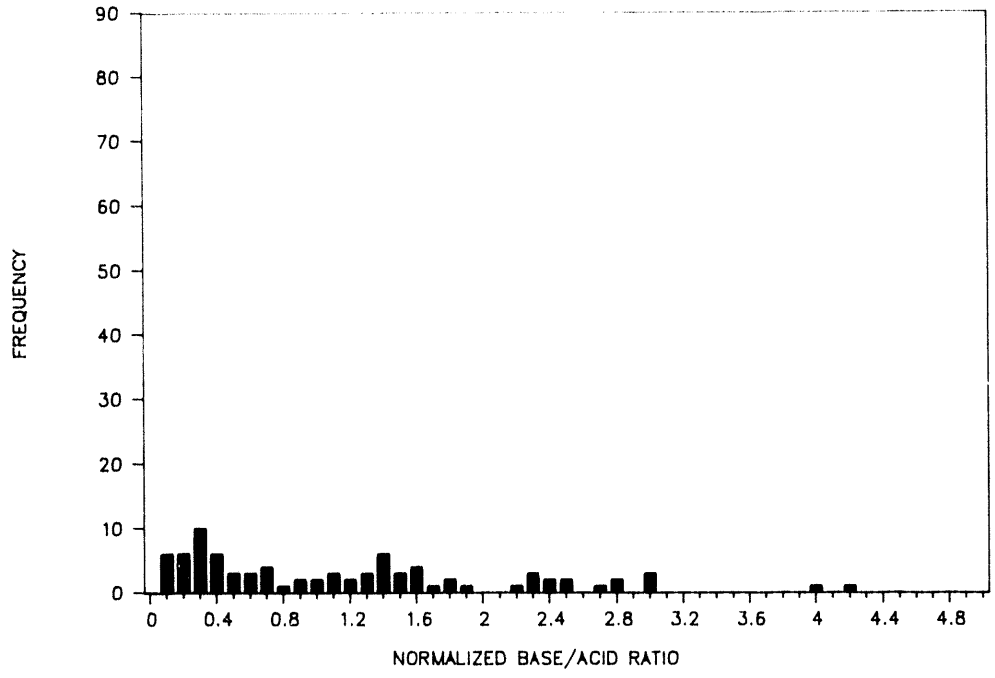

Figure 53. Base/acid ratio distribution of Illinois #6 char 650°C/200 psi low temperature ash.

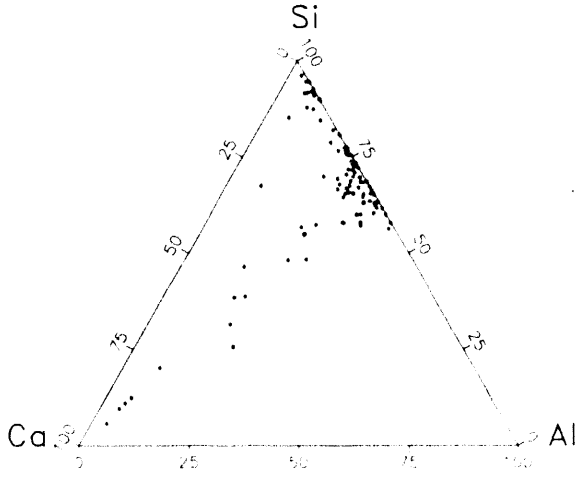

Figure 54. Illinois #6 Char, 650°C/15 psi.

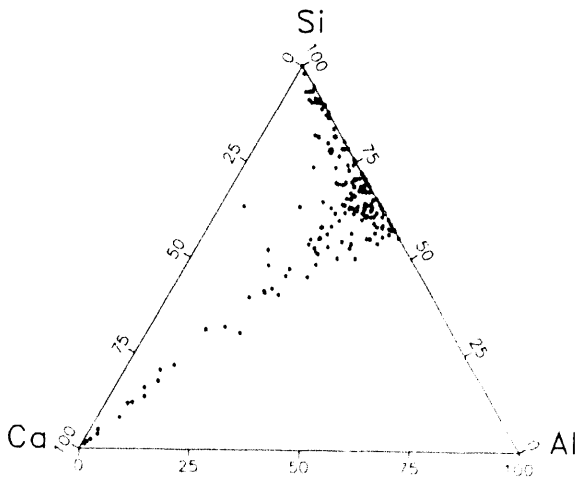

Figure 55. Illinois #6 Char, 850°C/15 psi.

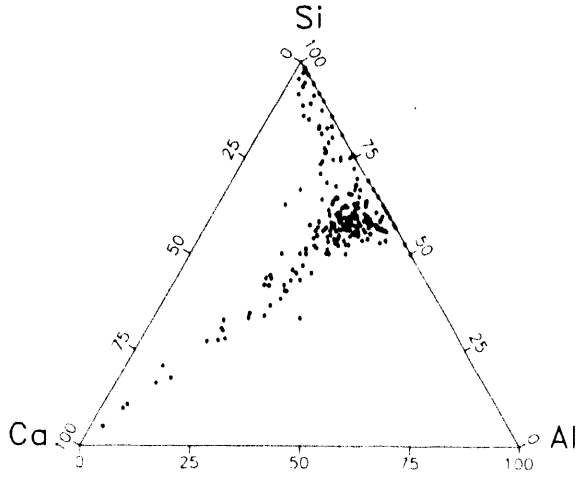

Figure 56. Illinois #6 Char, 650°C/400 psi.

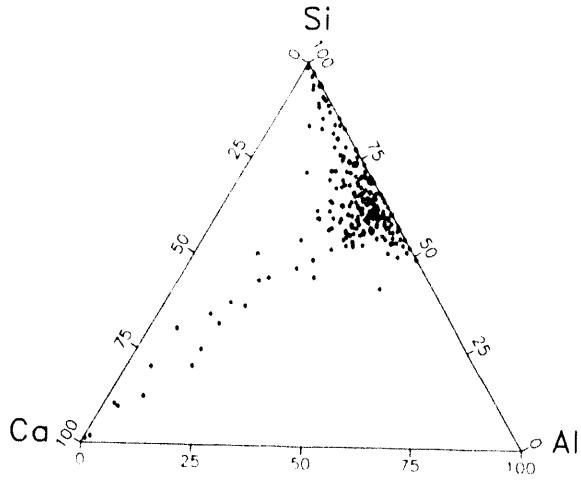

Figure 57. Illinois #6 Char, 850°C/400 psi.

3.1.4.3 Al-Si-Fe

The most important conclusion from this data (Figures 58-59) is the potential high temperature-high pressure interaction producing a greater number of iron particles. Please refer also to Figure 12.

3.1.5 Pittsburgh #8 Coal

3.1.5.1 Base/Acid

The data in Figures 60-63 show that this coal varied the least with temperature or pressure. The SEMPC analysis of the LTA coal ash did not analyze many points, indicating that the ash had almost no amorphous points. For this reason the data has been omitted. The effect of increasing the temperature from 650°C to 850°C at 15 psi slightly, but not significantly, decreased the amount of amorphous phase, but the base/acid ratio spread was nearly identical, as was the shape of the distribution. For chars produced at 850°C, the pressure variation of 15, 200, and 400 psi did not change the spread or the shape of the base/acid ratio. The greatest portion of amorphous phase was detected in the 200 psi char, followed by the 400 psi char, with the smallest amount in the 15 psi char. The reason for the variation in quantity of amorphous phase has not been established.

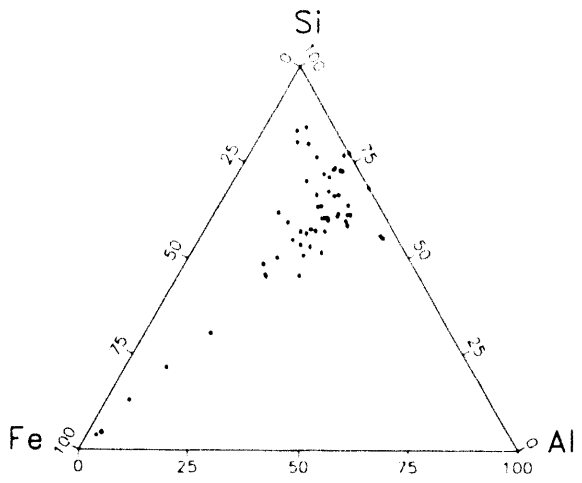

Figure 58. Illinois #6 Char, 650°C/15 psi.

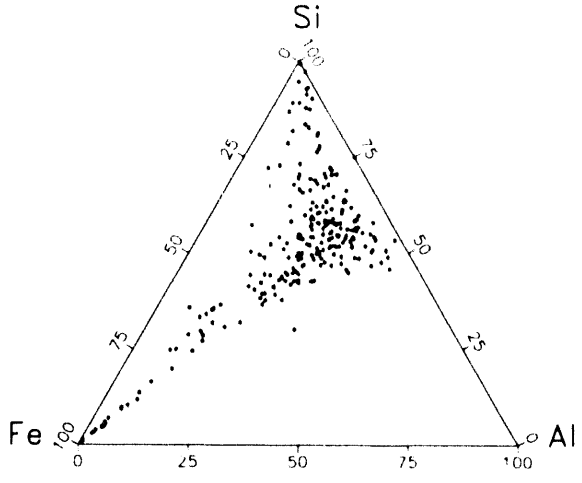

Figure 59. Illinois #6 Char, 850°C/400 psi.

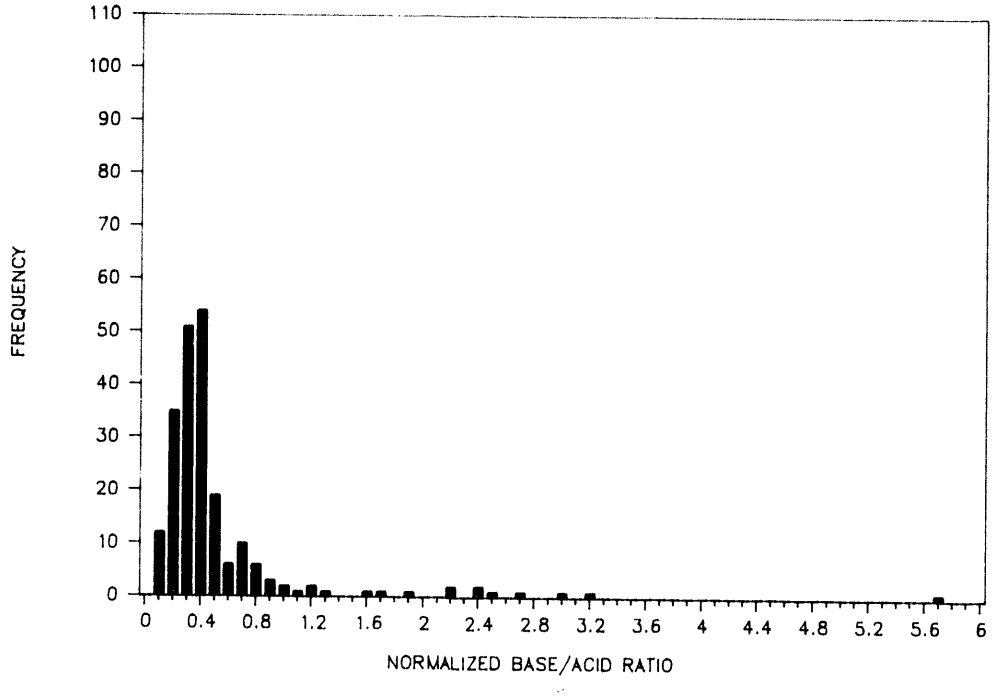

Figure 60. Base/acid ratio distribution of Pittsburgh #8 char 650°C/15 psi low temperature ash.

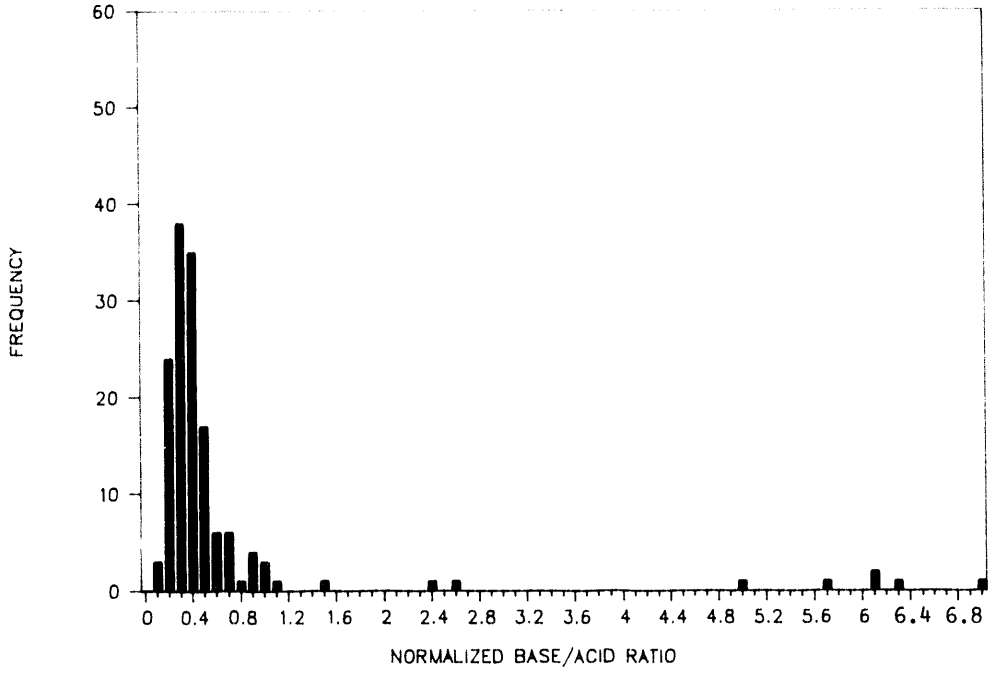

Figure 61. Base/acid ratio distribution of Pittsburgh #8 char 850°C/15 psi low temperature ash.

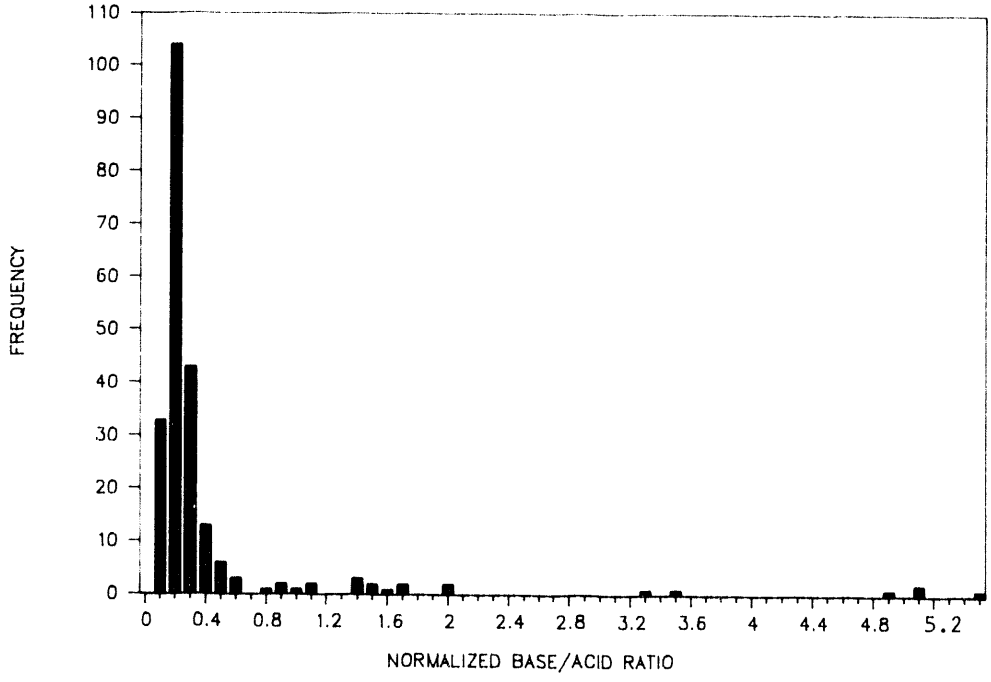

Figure 62. Base/acid ratio distribution of Pittsburgh #8 char 850°C/200 psi low temperature ash.

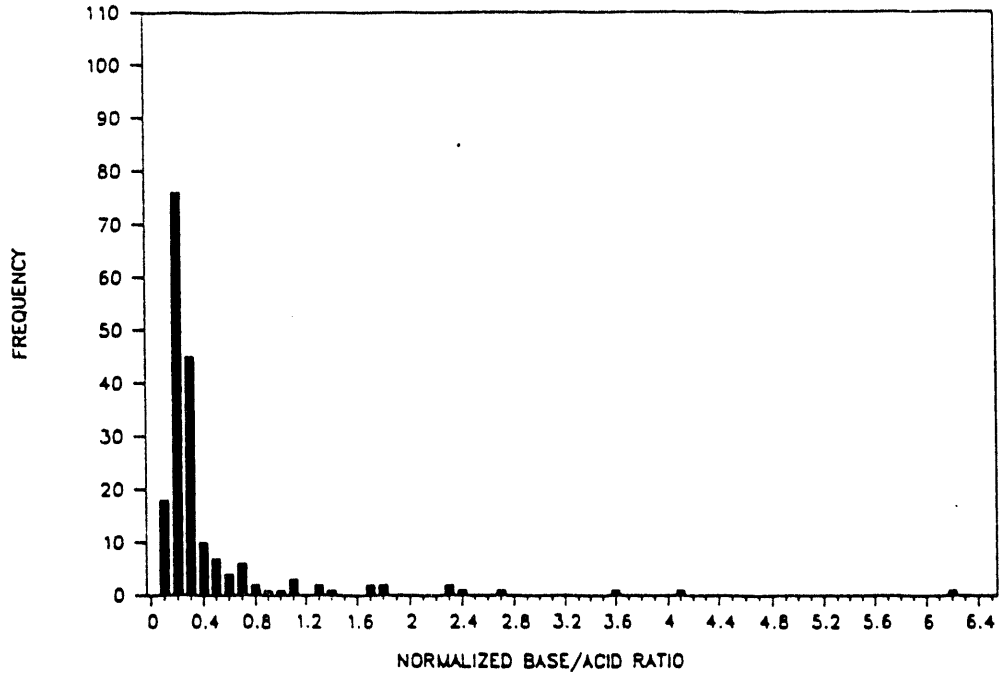

Figure 63. Base/acid ratio distribution of Pittsburgh #8 char 850°C/400 psi low temperature ash.

3.1.5.2 Al-Si-Ca

No discernable effects are seen in the Pittsburgh #8 chars (Figures 64-68), suggesting that the effects of temperature and pressure are generally greater in low rank coals. Again, please refer to Figure 7.

3.1.5.3 Al-Si-Fe

The Pittsburgh #8 chars showed that temperature and pressure do not play a significant role in Fe-Al-Si formation (Figures 69-72). Please also refer to Figure 12.

3.2 Task C: Ash Sintering Under Gasification Conditions

The objective of this task is to define the relationship between sintering parameters described by Frenkel's viscous flow molded as γ/η and base/acid ratio. So far, the surface tension has been measured at the temperature of sessile drop formation, usually, below the temperature of critical viscosity, T_{cv}. However, at this temperature silicates exist in the highly polymerized forms which effect the magnitude of surface tension. Therefore, it was necessary to determine all possible variables which effect the accuracy of the surface tension before γ/η ratio calculations.

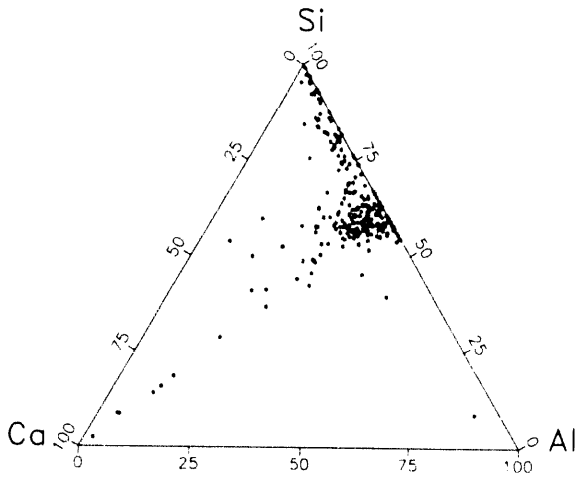

Figure 64. Pittsburgh #8 Char, 650°C/15 psi.

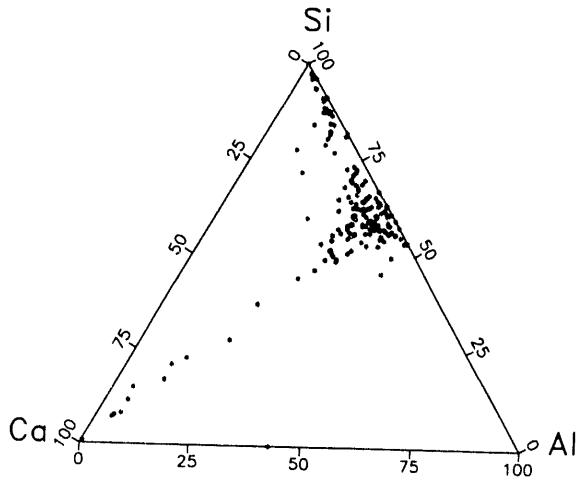

Figure 65. Pittsburgh #8 Char, 850°C/15 psi.

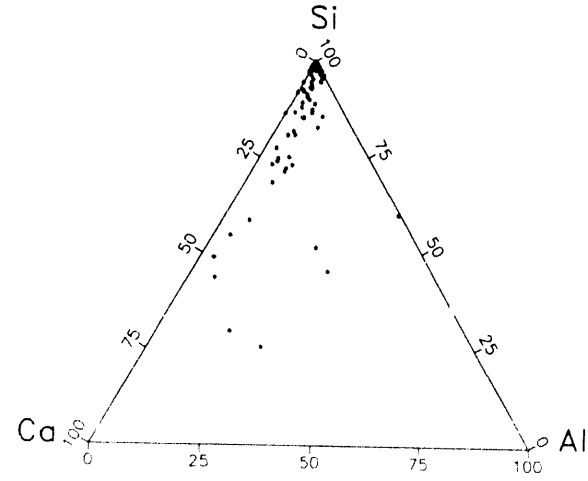

Figure 66. Pittsburgh #8 Char, 650°C/200 psi.

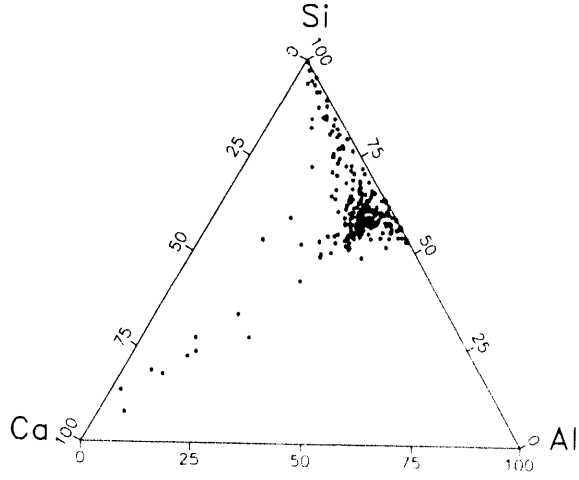

Figure 67. Pittsburgh #8 Char, 850°C/200 psi.

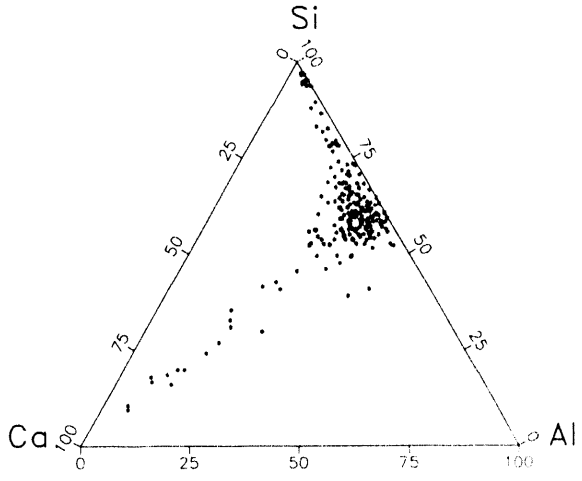

Figure 68. Pittsburgh #8 Char, 850°C/400 psi.

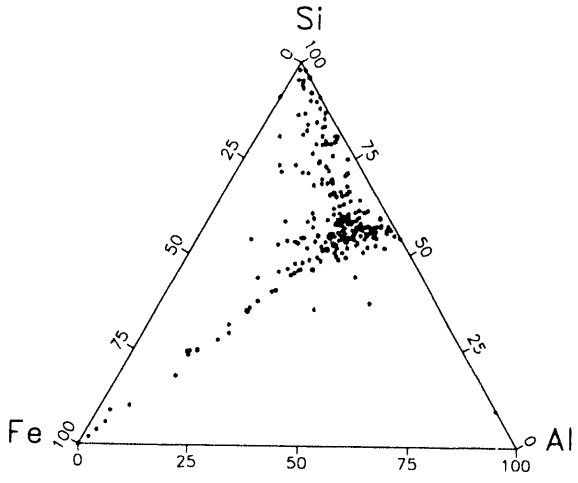

Figure 69. Pittsburgh #8 Char, 650°C/15 psi.

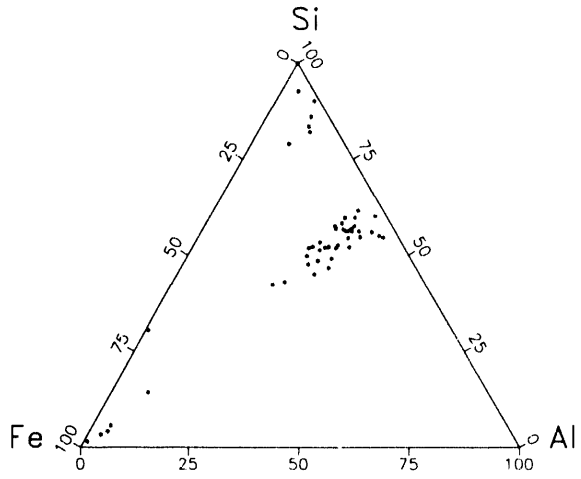

Figure 70. Pittsburgh #8 Char, 850°C/15 psi.

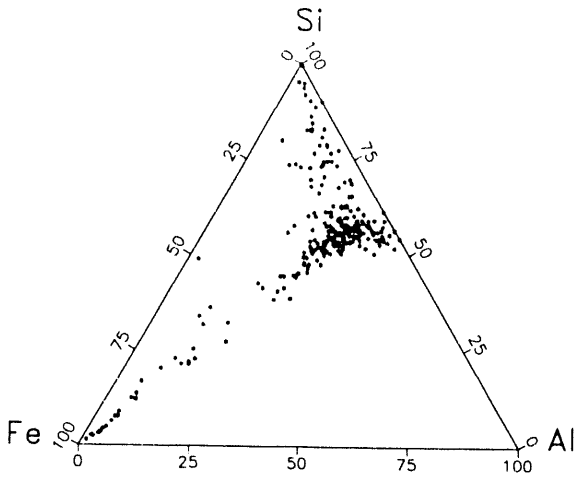

Figure 71. Pittsburgh #8 Char, 850°C/200 psi.

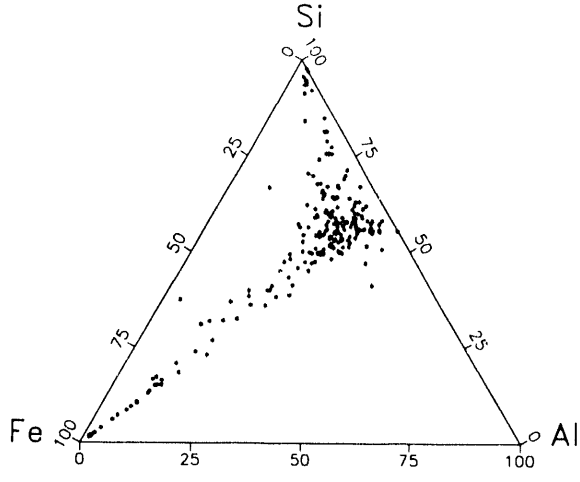

Figure 72. Pittsburgh Char, 850°C/400 psi.

The results of this work are also reported in "Physicochemical Effects Determining the Accuracy of Interfacial Surface Tension of Coal Ashes" by Nowok et.al. in Fuel.

3.2.1 Physicochemical Effects Determining the Accuracy of Interfacial Surface Tension of Coal Ashes

In a slagging type gasifier or in a cyclone combustor, maintaining proper slag behavior is necessary in order to have acceptable operation. The wetting behavior of metal walls, slag layers, and/or refractory surfaces depends on the viscosity and interfacial surface tension of a molten slag. Accurate and reliable surface tension data allow a better understanding of factors that influence spontaneous wetting,[1-8] erosion and degradation of the refractory, sintering properties of fly ash,[9,10] and nucleation of one phase in another.[11] The values of surface tension are expressed by N/m in SI or by dyne/cm in the CGS system.

Ordinarily, surface tension measured at the EERC using the sessile drop technique [12,13] is an intensive thermodynamic property that should be measured on systems that are free from extraneous mechanical, electrical, or chemical interactions. If the surface tension is measured in the presence of an interacting gas, it is called interfacial surface tension.[14] The calculation of surface tension employs procedures which permit the fitting of a measured drop profile to a theoretical profile by varying two parameters, β and b,

using a nonlinear regression program. The shape factor (β) and the radius curvature (b) at the drop apex are related by the equation:

$$\beta = \frac{b^2 g}{\gamma} \quad (d_m - d_{gas}) \qquad (1)$$

where γ is the surface tension, g is the gravitational acceleration, and d_m and d_{gas} are the densities of liquid slag and gas, respectively. Two principal errors based on the measurement of the drop profile and density were discussed elsewhere.[15] The intention of this paper is to discuss possible physical and chemical effects that have an influence on the accuracy of the interfacial surface tension values in molten coal ashes on vitreous carbon.

3.2.1.1 Theoretical Approach

Viscosity-temperature relationships reflect the structure, crystallization phenomena, and phase equilibria of coal ash melts. Magmatic glasses, especially in silica-rich compositions are thought to exist in polymerized forms.[16] The viscosity of the system is mostly dependent on the strongest bond in the system.[17]

The coexistence of different phases in melts will change the measured values of interfacial surface tension. The data plotted in Figure 73 illustrate how the variations in the properties of the slag, as shown by the viscosity measurements, may influence the determination of the interfacial surface tension. At some point during the cooling, the slope of the viscosity versus temperature curve increases more rapidly. The temperature at which this transition occurs is termed the temperature of critical viscosity, T_{cv}. This effect was attributed to a selective separation of solid material from the liquid,[18] likely due to crystallization processes and the increase of the degree of polymerization of a silicate melt. If the interfacial surface tension is determined below the critical temperature of viscosity, it may be affected by the nonhomogenity of the slag (solid and liquid components having different chemical compositions). If the surface tension is determined above T_{cv}, it will provide information on the structural changes of the melt with increasing temperature.

Surface tension measurements made on molten silicates using a modified ring method have shown their increase with temperature.[19] Some other experiments which used drop weight, dipping cylinder, or bubble pressure methods indicated that surface tensions, for silicates, decrease slightly with temperature.[20]

In recent experiments performed at the Energy and Environmental Research Center, the intention was to determine the interfacial surface tensions using the sessile drop technique in a reducing atmosphere that corresponds to the gasification condition, and in air.

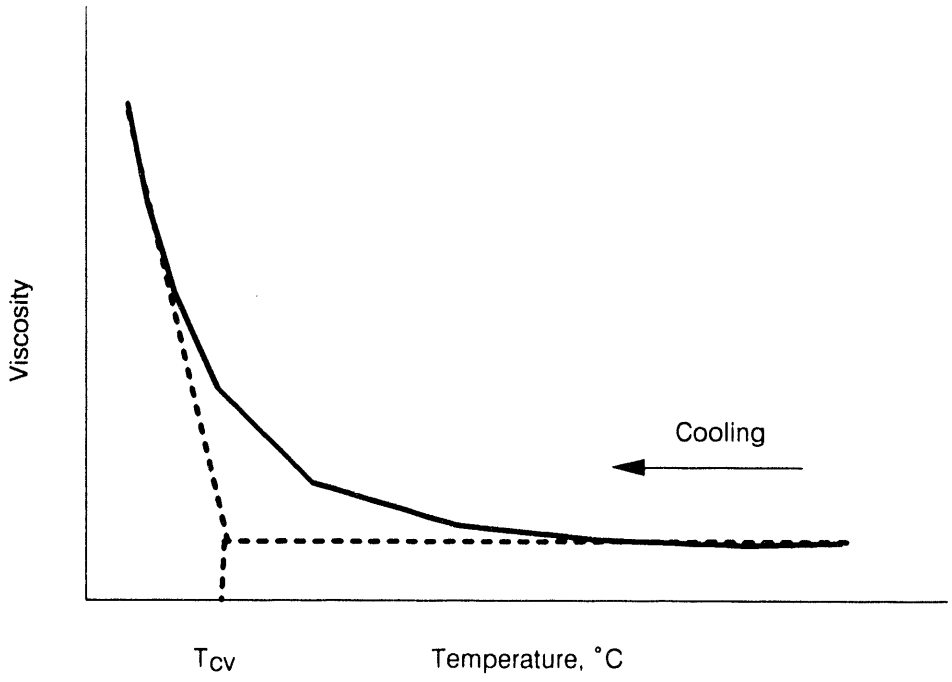

Figure 73. Schematic presentation of viscosity versus temperature.

3.2.1.2 Experimental

Beulah lignite, Pittsburgh #8, and Illinois #6 coals were pulverized to -60 mesh and ashed at 800°C for 24 hours in air. The resulting ashes were melted at 1500°C and homogenized by rotating a platinum bob in the presence of controlled atmospheres; air, H_2/N_2 (8/92), and CO/CO_2 (60/40). The slags were quenched to room temperature and ground to -38 mesh. The homogenation procedure resulted in a more uniform distribution of all coal ash components and, therefore, avoided errors in the determination of interfacial surface tension due to nonequilibrium surface tension values. If the homogenation process is allowed to proceed during surface tension measurements, the determination requires much more time to allow for homogenation of the ash components. Another factor that influences interfacial surface tension measurements is the evaporation of light elements, such as sodium, from the surface of the sessile drop. During evaporation, the chemical potential of surface atoms is varied from those in the bulk. As a consequence, the interfacial surface tension also changes.[21]

Two types of pellets were prepared for surface tension measurements: pulverized glassy slag and small pieces of the crushed slag. The pulverized glassy coal ash slag was pressed by hand into a pellet with a diameter of about 0.7 cm, centered on a plane surface of vitreous carbon, and placed in the horizontal tube furnace preheated to 900°C. It was earlier established that the size of the drop influences the surface tension measurements. A drop with a diameter above 2 cm measured higher surface tension, while for drops with diameters below 1 cm, the surface tension slightly decreased.[22] The

sessile drops were exposed to selected mixtures of flowing gases such as air, H_2/N_2 (8/92), and CO/CO_2 (60/40) throughout the experiment. The drop profile was photographed at selected temperatures and times.

The coordinates of the sessile drop were measured both directly from the film using an optical microscope and from the projected image on graph paper. The calculation of the surface tension was performed by a computerized nonlinear curve fitting procedure. The chemical composition of coal ashes was determined after surface tension measurements by x-ray fluorescence analysis. The compositions of the ashes on a sulfur-free basis are listed in Table 1.

Raask [23] has suggested that iron carbide might be formed at the slag-vitreous carbon interface, and carbon monoxide could be evoluted above 1400°C, mainly in the iron rich slags. The reaction between iron oxide-bearing slags and solid carbon was significant in $FeO-SiO_2$ slags. Lime-rich slags were found to react more slowly with carbon.[24] The interaction of the droplet with the substrate is another uncertainty that influences the experimental results.

The process of gas generation inside the slag droplet causes changes in the sessile drop shape. This effect should be considered when making the calculation of a slag density from the sessile drop coordinates. A number of experiments have shown that a significant change in density occurs when slag droplets are exposed to air at temperatures above 1350°C. Therefore, interfacial surface tensions determined in air were obtained at temperatures below 1350°C. In order to obtain accurate measurements, the droplets were held at each temperature for at least 30 minutes prior to photographing the droplet. The temperature of sessile drop formation is dependent upon the composition of the coal ash; for most coal ashes it occurs below 1350°C. Thus, the temperature of sessile drop formation was selected as a reference temperature. Interfacial surface tension measurements for homogenated slags in a CO/CO_2 atmosphere could be made at temperatures above 1400°C without significant change in slag droplet density. Table 2 gives examples of the density variation as a function of temperature for several slags exposed to CO/CO_2 atmosphere. All results of interfacial surface tension with density error larger than 5% were rejected in further discussions.

The effect of sessile drop annealing on the variation of chemical compositions in the surface layers was performed on model soda and soda-lime silicate glasses as well as on Beulah coal slag. Six silicate glasses were prepared, with the following compositions: $Na_2O-2SiO_2$, $Na_2O-4SiO_2$, $Na_2O-6SiO_2$, $Na_2O-Al_2O_3-SiO_2-0.7Fe_2O_3$, and $Na_2O-CaO-SiO_2$. The interfacial surface tension was measured in air, and the chemical composition was determined by scanning electron microscopy.

For selected coal ashes, viscosity was also measured using a rotating bob viscometer in a CO/CO_2 (60/40) atmosphere to determine the temperature of critical viscosity. Viscosity measurements were started at the highest temperature and then at lower temperatures until the upper limit of the viscometer was approached.

TABLE 1

COMPOSITION OF COAL ASHES (WEIGHT PERCENT EXPRESSED AS EQUIVALENT OXIDE) USED IN THE INTERFACIAL SURFACE MEASUREMENTS

Run No.	Coal Ash	SiO_2	Al_2O_3	Fe_2O_3	TiO_2	CaO	MgO	Na_2O	K_2O
	A. Prepared in air								
1	Beulah	37.5	15.1	11.3	1.6	21.6	6.1	5.7	0.8
2	Pittsburgh #6	50.9	20.2	19.1	1.2	4.7	1.1	0.0	2.6
3	Illinois #6	46.7	20.7	21.2	1.3	6.4	1.1	0.0	2.7
	B. Prepared in H_2/N_2 (8/92)								
4	Beulah	37.9	15.3	11.1	1.6	22.2	5.5	5.7	0.7
5	Pittsburgh #8	51.2	20.7	18.0	1.2	4.8	1.2	0.0	2.6
6	Illinois #6	47.7	19.6	20.7	1.3	6.5	1.2	0.0	2.8
	C. Prepared in CO/CO_2 (60/40)								
7	Beulah	38.0	15.3	10.9	1.6	22.4	5.1	5.8	0.7
8	Beulah/Limestone	33.1	23.0	10.1	1.3	26.1	2.9	2.8	0.7
9	Beulah/Dolomite	34.2	16.2	9.7	1.5	25.8	8.0	4.2	0.5
10	Pittsburgh #8	51.1	20.6	18.2	1.2	4.9	1.2	0.0	2.6
11	Pitt. #8/Limestone	43.1	20.7	16.2	1.1	16.0	0.8	0.0	2.2
12	Pitt. #8/Dolomite	45.9	20.3	16.6	1.1	10.1	3.6	0.0	2.2
13	Illinois #6	47.9	19.5	20.6	1.3	6.7	1.2	0.0	2.8
14	Ill. #6/Limestone	40.9	18.6	1.1	17.5	0.7	0.0	2.3	2.3
15	Ill. #6/Dolomite	42.4	20.2	18.0	1.1	12.4	3.5	0.0	2.3

3.2.1.3 Results and Discussion

The liquid phase exhibits the tendency to contract in order to minimize the surface free energy. At equilibrium, the tensions at the contact between three phases, solid, liquid, and gas, are indicated by the equation:

$$\gamma - \gamma_{sL} = \gamma_{Lv} \cos \theta \qquad (2)$$

TABLE 2

DENSITY OF SLAG DROPLETS CALCULATED FROM THE SESSILE DROP

Temperature (°C)	Density, g/cm³ Beulah Run No. 7	Pittsburgh #8 Run No. 11	Illinois #6 Run No. 13
1300	3.08	2.80	2.51
1325	3.13	NA	2.48
1375	3.07	2.84	2.41
1425	3.12	2.78	2.55
1475	3.07	2.78	2.50
Average	3.09 ± 0.04	2.80 ± 0.04	2.49 ±0.08

Atmosphere: CO/CO_2 (60/40)

where γ_s is the solid surface tension, γ_{Lv} is the interfacial surface tension of molten slag, and γ_{sL} and θ are the interfacial surface tension and contact angle between liquid and solid, respectively. Both the surface tension of the solid and the interfacial surface tension of the molten glass/slag may be changed by absorbed/desorbed molecules and/or products of the chemical reaction.

Table 3 lists values of interfacial surface tension determined for five model glasses and chemical compositions of the bulk and surface layers of the sessile drops. Generally, interfacial surface tension in the sodium oxide-silica system decreases with increasing SiO_2 and the addition of Fe_2O_3.

Structurally, this change is a result of the replacement of weaker

$$-Si-O^- \quad \begin{matrix} M^+ \\ M^+ \end{matrix} \quad {}^-O-Si-$$

bonds by the stronger -Si-O-Si-bonds. In contrast, the viscosity of silicates increases with increasing SiO_2 and Fe_2O_3.[25] There also appears to be significant depletion of sodium content in layers close to the surface of sessile drop. This implies that polymerization of silicates in surface layers may be different than those in the bulk, and this may cause changes in the accuracy of interfacial surface tension.

Thus Equation 2 may be rewritten as:[26,27]

$$\gamma_s - \gamma_{sL} - \pi_s = (\gamma_{Lv} \pm \pi_L) \cos \theta \qquad (3)$$

TABLE 3

INTERFACIAL SURFACE TENSION OF MODEL GLASSES, AND BULK AND SURFACE CHEMICAL COMPOSITION OF SESSILE DROPS

Glass Composition		Interfacial Surface Tension dyne/cm	Temperature (°C)
Bulk	Surface		
Na_2O-$2SiO_2$	Na_2O-$6SiO_2$	572 ± 15	40-1000
Na_2O-$4SiO_2$	Na_2O-$14SiO_2$	445 ± 45	1040-1100
Na_2O-$6SiO_2$	NA	355 ± 13	1320
*SiO_2	--	305 ± 7	1950-2000
Na_2O-$2SiO_2$-$0.7Fe_2O_3$	Na_2O-$6SiO_2$-$2.7Fe_2O_3$	387 ± 35	870
Na_2O-CaO-$2SiO_2$	$0.2Na_2O$-$2CaO$-SiO_2	567	1210

* Reference 20

where π_L and π_s represent the surface pressure of absorbed films on the sessile drop and substrate, respectively. The sign in $\pm\pi_L$ depends on the changes in surface concentration resulting from, or by the formation of, a new thin layer of products (rich in sodium content) or by evaporation of light elements, such as sodium.

Equation 3 also implies that slag interfacial surface tension can be influenced by the formation of thin products on the slag-substrate interface if new liquid products lead to wetting of the substrate.[28]

Figure 74 shows the variation of viscosity and interfacial surface tension with temperature in Na_2O-$0.2Al_2O_3$ model glass, measured in air. Perhaps the most interesting feature of the results is that the γ_{Lv} decreases with increasing temperature above the temperature of critical viscosity, T_{cv} (~1050°C), and that below T_{cv} there is a significant drop in interfacial surface tension.

3.2.1.4 Effect of Time on the Interfacial Surface Tension in Coal Ashes

Table 4 summarizes the interfacial surface tension data for Illinois #6 slags prepared in CO/CO_2 atmosphere (Run Nos. 13-15). The slags were annealed for 0-40 minutes at the temperature at which a completely spherical droplet forms in CO/CO_2. Table 5 shows the variation in interfacial surface tension values for Beulah (Run No. 7) and Pittsburgh #8 (Run No. 11) prepared and measured in CO/CO_2 versus annealing time (0-240 min.). It is evident that there is an increase of interfacial surface tension within 30 minutes, likely due to the stabilization of γ_{Lv}. This seems to be the time required to achieve steady-state conditions in molten slag. Also, there is a great

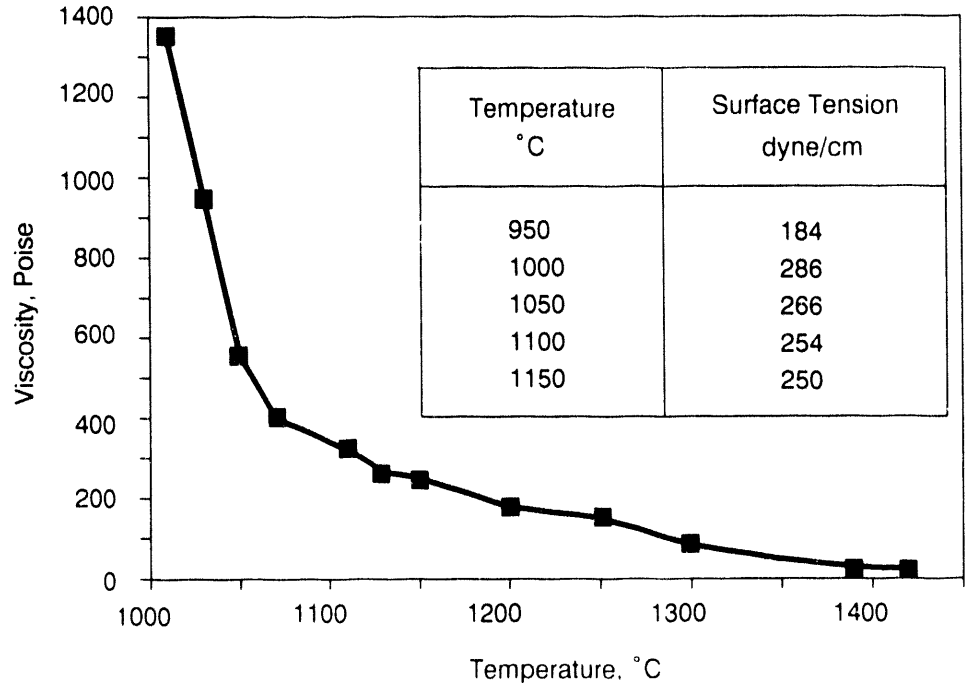

Figure 74. Viscosity-temperature relationship of Na_2O-0.$2Al_2O_3$ model glass and interfacial surface tension values under air atmosphere at selected temperatures.

TABLE 4

INTERFACIAL SURFACE TENSION OF ILLINOIS #6 COAL ASH VERSUS ANNEALING TIME DETERMINED AT THE TEMPERATURE OF SESSILE DROP FORMATION

	Surface Tension, dyne/cm		
Time (min)	Run No. 13 T = 1275°C	Run No. 14 T = 1250°C	Run No. 15 T =1250°C
0-5	205	NA	238
15	244	339	255
30	278	318	259
40	249	329	278

Atmosphere: CO/CO_2 (60/40)

TABLE 5

INTERFACIAL SURFACE TENSION OF BEULAH (RUN NO. 7) AND PITTSBURGH #8 (RUN NO. 11) SLAGS, PREPARED IN CO/CO_2 VERSUS ANNEALING TIME AT THE TEMPERATURE OF SESSILE DROP FORMATION

	Surface Tension, dyne/cm	
Time (min)	Beulah (Run No. 7) TEMP	Pittsburgh #8 (Run No. 12) 1300°C
0-5	420	319
30	460	345
45	472	331
60	468	316
120	423	346
180	369	309
240	211	258

Atmosphere: CO/CO_2 (60/40)

decrease of γ_{Lv} with time above 180 minutes. Chemical composition determined in the Beulah sessile drop (Figure 75) indicates that there is a significant reduction of alkali content in layers close to the surface. This, in turn, decreases the base/acid ratio. As a result, the melt layers close to the surface of sessile drop seem to be more polymerized than a melt in the bulk of the sessile drop.

3.2.1.5 Effect of Atmosphere on the Interfacial Surface Tension in Coal Ashes

It is worth noting that there is a decrease in the interfacial surface tension if coal ash is exposed to reducing atmospheres (Table 6). This may be caused by the increase of reduced iron species available that can modify the glass network or by the multiple structural changes of the melt on the surface layers of the sessile drop due to the reducing of oxygen content in a slag:

$$O_o + CO(H_2) \rightarrow V_o + CO_2(H_2O) \qquad (4)$$

where O_o represents oxygen in a silicate system and V_o is an oxygen deficit. The structural reason for the γ_{Lv} variation is not yet conclusively established. Strictly speaking, the interfacial surface tensions differ depending on the atmosphere in which the coals are heated.

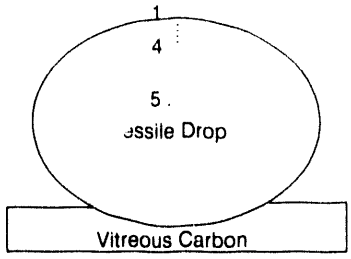

Surface and Bulk Composition of Beulah Sessile Drop

	Analyzed Points, Wt.%				
	1	2	3	4	5
K_2O	0.1	0.2	0.4	0.4	0.5
Na_2O	0.0	0.2	2.1	4.9	5.7
MgO	5.1	6.0	5.8	5.7	5.5
CaO	20.6	21.8	20.1	20.4	21.1
TiO_2	1.5	1.6	1.4	1.3	1.8
Fe_2O_3	12.4	12.7	10.5	11.2	10.5
Al_2O_3	16.2	15.8	18.3	17.8	15.0
SiO_2	42.9	41.2	39.5	38.1	39.6
Base/Acid	0.63	0.69	0.65	0.74	0.76

Figure 75. Surface and bulk composition in Beulah sessile drop annealed at 1300°C for 3 hours.

3.2.1.6 Effect of Temperature on Interfacial Surface Tension in Coal Ashes

The effect of temperature is generally noted by the increase of droplet area. In the multicomponent silicate system nonhomogenity is a very important factor that may change the droplet interfacial surface tension, as mentioned above. Therefore, all experiments were performed on homogenized slags after measuring viscosity. Figures 76-77 show viscosity-temperature relationships and the values of interfacial surface tension. Temperature has a significant effect on the changes of the interfacial surface tension below the temperature of critical viscosity. This effect may be attributed to a non-equilibrium state of γ_{Lv} due to the random distribution of surface active phases in the slag and a higher polymerization of silicate structure. However, there is no significant variation of γ_{Lv} with temperatures above T_{cv}.

3.2.1.7 Effect of Chemical Composition Variation on Interfacial Surface Tension in Coal Ashes

The chemical composition of coal ash slags was varied with the addition of small amounts of limestone or dolomite, usually used as sulfur capture agents in gasification facilities. To obtain a uniform distribution of chemical composition, coal ashes with additives were subjected to the same homogenation procedures as described in the experimental section of this report. Table 7 compares the values of interfacial surface tension decreases with the base/acid ratio. Generally, the interfacial surface tension

TABLE 6

INTERFACIAL SURFACE TENSION OF BEULAH, PITTSBURGH #8, AND ILLINOIS #6 MEASURED IN VARIED ATMOSPHERES DETERMINED AT THE TEMPERATURE OF SESSILE DROP FORMATION

Temperature of Sessile Drop Formation (°C)	Surface Tension, dyne/cm			*Base/ Acid Ratio
	Air	H_2/N_2 (8/92)	CO/CO_2 (60/40)	
Beulah				
1285	802			0.84
1275		615		
1200			408 ± 18	
Pittsburgh #8				
1275	483			0.38
1275		358		
1200			261 ± 5	
Illinois #6				
1200	531			0.45
1175		334		
1275			259	

* $\frac{\text{Base}}{\text{Acid}} = \frac{Na_2O + K_2O + CaO + MgO + Fe_2O_3}{SiO_2 + Al_2O_3 + TiO_2}$

decreases with the base/acid ratio. On the other hand, the base/acid ratio has been demonstrated as a useful measure of slag viscosity.[29] Usually, viscosity decreased with the increase in the base/acid ratio.

3.2.1.8 Conclusions

The accuracy of the interfacial surface tension depends on the degree of polymerization of the melt. The degree of polymerization is dependent upon the variation in the abundance of Si-rich clusters. The variations in the amount of clusters is influenced by the following: annealing temperature, time, ambient atmosphere, and composition of molten slags. The base/acid ratio seems to have a significant effect on the values of γ_{LV}. Generally, interfacial surface tension increases with the base/acid ratio.

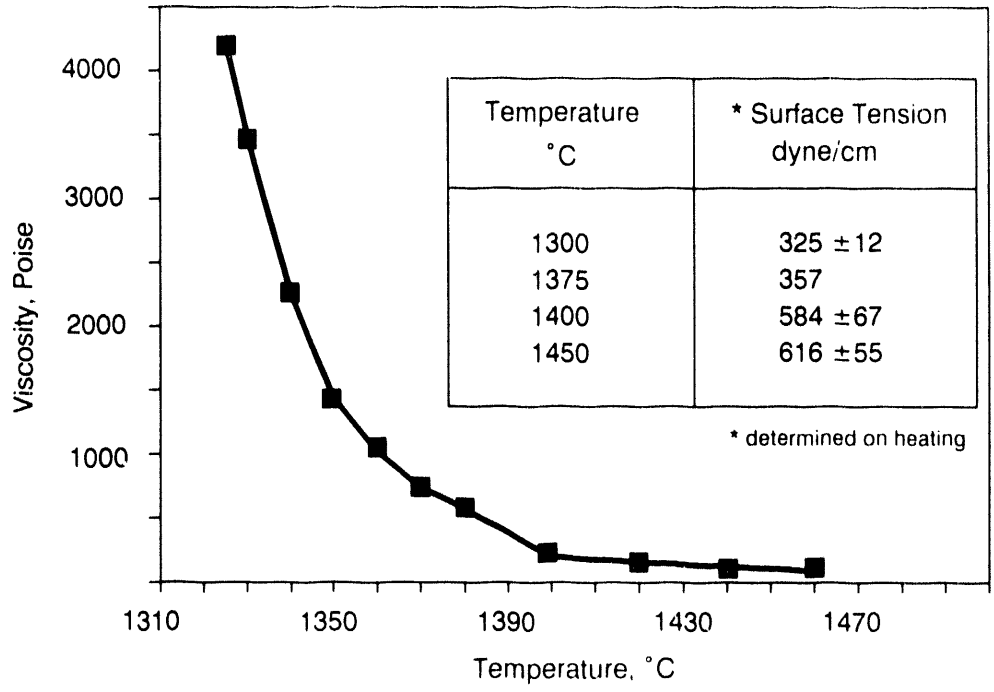

Figure 76. Viscosity-temperature relationship of Pittsburgh #8 slag (run no. 11) and the values of interfacial surface tension determined for selected temperatures. Both experiments were carried out in CO/CO_2 atmosphere.

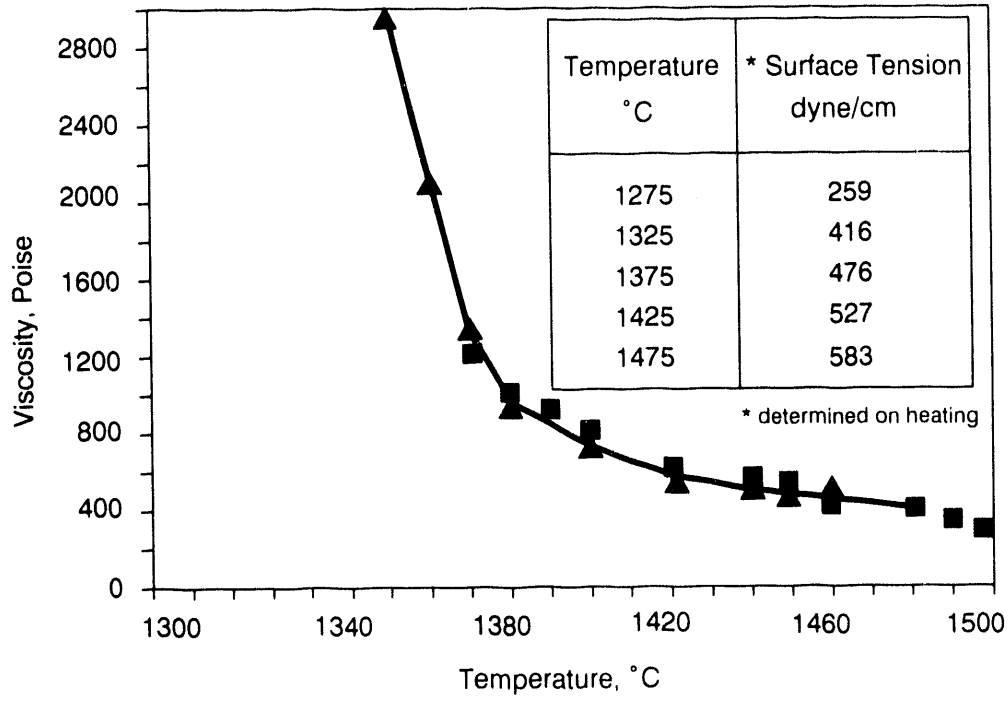

Figure 77. Viscosity-temperature relationship of Illinois #6 slag (run no. 13) and the values of interfacial surface tension determined for selected temperatures. Both experiments were carried out in CO/CO_2 atmosphere.

TABLE 7

INTERFACIAL SURFACE TENSION OF BEULAH, PITTSBURGH #8, AND ILLINOIS #6 COAL ASHES WITH ADDITIVES, DETERMINED AT THE TEMPERATURE OF SESSILE DROP FORMATION

Temperature of Sessile Drop Formation °C)	Interfacial Surface Tension, dyne/cm			*Base/ Acid Ratio
	Coal Ash	Coal Ash + Limestone	Coal Ash + Dolomite	
Beulah				
1200	408 ± 18			0.79
1300		267 ± 4		0.72
1275			419	0.90
Pittsburgh #8				
1200	261 ± 5			0.34
1250		329 ± 20		0.50
1300			389 ± 34	
Illinois #6				
1275	259			0.41
1250		328 ± 10		0.60
1250			269 ± 20	0.52

Atmosphere: CO/CO_2 (60/40)

* $\frac{\text{Base}}{\text{Acid}} = \frac{Na_2O + K_2O + CaO + MgO + 2FeO}{SiO_2 + Al_2O_3 + TiO_2}$

3.2.2 Slag Properties and Ash Deposition

The specific objectives of this work include 1) the correlation of slag properties such as viscosity and surface tension with base/acid ratio, and 2) the determination of the relationships between transport phenomena, sintering processes, and strength development.

3.2.2.1 Background Statement

Base/acid ratio as well as viscosity (η) and interfacial surface tension (γ) have been proposed for use in predicting the fouling and slagging behavior of coal ashes[1,18,25]. The base/acid ratio is used to provide information on the silicate structure related to the polymerization tendency (tendency towards clustering).

Viscosity is a measure of the intermolecular forces of attraction in a fluid, and it provides information on the bulk melt structure. Newtonian flow behavior is expected to occur in coal ash slags above the temperature of critical viscosity, T_{cv}, which can be described in the Arrhenius form:

$$1/\eta = A \exp(-E_1/kT) \qquad (5)$$

where A is a constant, E_1 is an activation energy for viscous flow, T is temperature in K, and k is the Boltzmann constant.

Interfacial surface tension is a measure of the inward forces that must be overcome in order to expand the surface area of a melt, and it provides information on the surface structure of the melt. Ordinarily, surface tension is an intensive thermodynamic property that should be measured on systems that are free from extraneous mechanical or chemical interactions. If the surface tension is measured in the presence of an interacting gas, it is called interfacial surface tension. Both factors, viscosity and interfacial surface tension, depend upon the base/acid ratio.

The sintering behavior of ceramics in the presence of a liquid phase can be described by Frenkel's viscous flow model, which describes the neck formation[26] (Zone A), the shrinkage of the large pores (Zone B), and "surface fluxing" (Zone C)[10], as seen in Figure 78.

The densification of a deposit is proportional to the ratio of γ/η. Thus it is possible that Equation 5 can be rewritten in the following form:

$$\gamma/\eta = B \exp(-E_2/kT) \qquad (6)$$

Equation 6 may furnish information about the sintering process and the strength development of coal ashes which are shown to partially result from the mass transport of the melt. The slope of the curves determined from Equations 5 and 6 can provide useful information about the activation energies for viscous flow. Equation 5 describes the viscous flow of the bulk slag, and Equation 6 represents the viscous flow of a slag in the presence of the surface forces. The force can result from the different tendencies towards clustering (polymerization) of a viscoelastic silicate melt in the surface layers and in the bulk due to the segregation of chemical composition, orientation of structural units, temperature gradient, and/or pressure. In the sintering process, these forces can also result from solid-liquid interfacial interaction γ_{SL}.

A low value for γ/η provides information on the sintering process accomplished by the shrinkage of the large pores, with a low excess liquid phase. A large value for γ/η provides information on the mass transport (e.g. viscosity, diffusivity) in the sintering process assigned to "surface fluxing".[10]

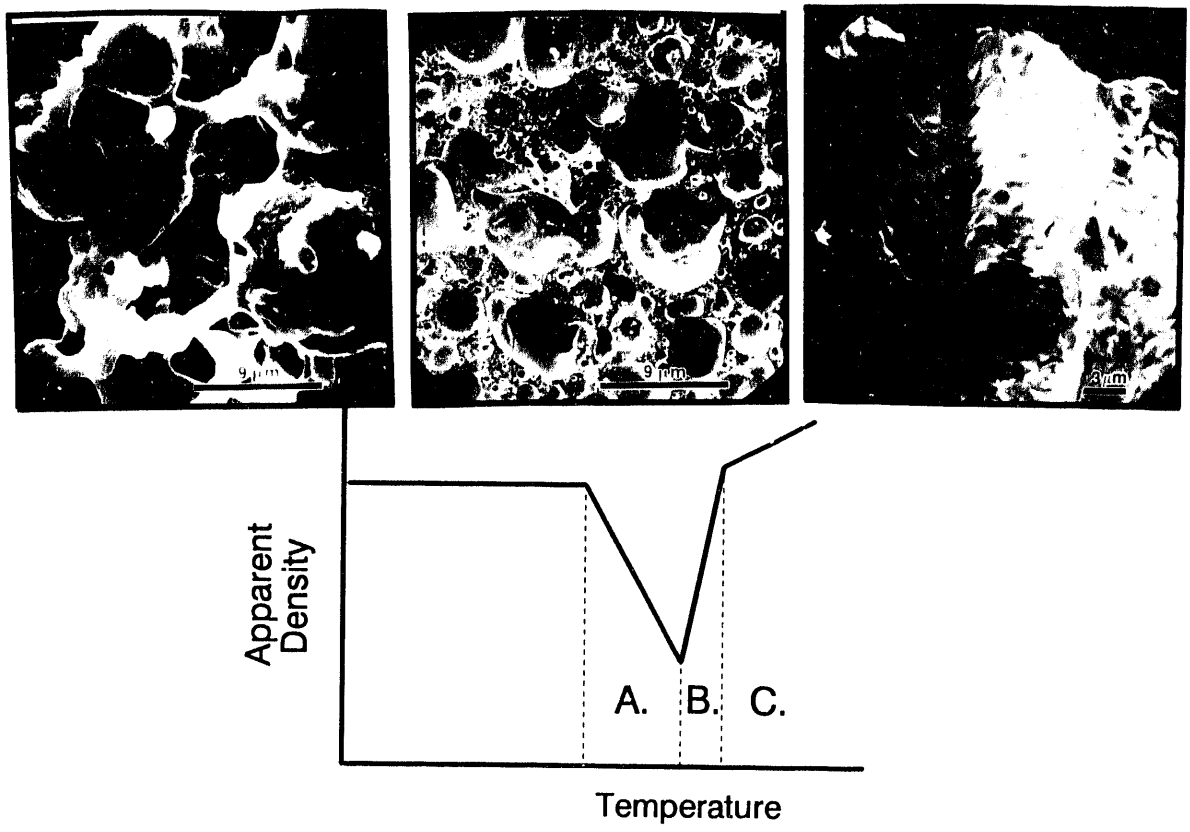

Figure 78. Schematic of the three steps in the sintering of coals ashes[5].

3.2.2.2 Project Description

A major portion of this research involved an investigation of the factors that influence coal ash slag viscosity, surface tension, and compressive strength development under both gasification atmospheres and air. This information indicates that the sintering mechanism of coal ash depends upon the γ/η ratio when determined above the temperature of critical viscosity, T_{cv}.

The viscosity and surface tension are influenced by the structure of the molten slag and are directly related to the chemical composition of the coal ash. For example, the addition of network modifiers such as sodium, calcium, magnesium, and iron (Fe^{2+}) alters the molten slag structure by depolymerization of silicate glass networks. Depolymerization of the silicate network results in significantly lower viscosities. In addition, network modifiers promote crystallization processes. Crystallization of species from the melt phase changes the composition and physical properties of the residual liquid phase. Accordingly, the surface tension and viscosities can be significantly affected by the presence of crystals in the melt. Under the reducing conditions found in gasifiers and advanced combustion systems, relatively low-melting point phases result. This effect is especially profound in slags that contain higher levels of iron. The characteristics of these iron-rich liquid phases significantly affect the slagging and sintering behavior of coal ashes.

3.2.2.3 Results and Accomplishments

3.2.2.3.1 Experimental

Several coal slags having widely varying ash compositions were examined, and their compositions on a sulfur-free basis are listed in Table 8. For some coal ashes, limestone and dolomite were also added. The slag viscosity was measured using a rotating bob viscometer in air and reducing [CO/CO_2 (60/40)] atmospheres.[27,28] Slag surface tension was determined on slags after measuring viscosity by the sessile drop technique both in air and reducing atmospheres.

The sintering tests were conducted on amorphous coal ashes for 15 hours at various selected temperatures. Eight cylindrical specimens (1.52 cm in diameter and 1.90 cm long) were formed in a hand press for each coal ash, sintered at appropriate temperatures, cooled slowly in the furnace, and crushed. Then their average compressive strengths were computed and plotted. The compression took place with a velocity of 1 mm/min. The maximum standard deviation was ±15%. The amorphous coal ashes were prepared by melting appropriate coal ash at 1500°C and quenching at room temperature. The glass was ground to -150 mesh.

3.2.2.3.2 The Surface Tension/Viscosity and Base/Acid Ratio Relationship

One of the principal characteristics of molten coal ashes (slags) is the variation of viscosity and surface tension with temperature, and chemical composition (usually expressed by the base/acid ratio). Figure 79 shows the variation of viscosity and surface tension with temperature determined in CO/CO_2, for Beulah lignite ash.[28] By monitoring changes in the viscosity and surface tension above the temperature of critical viscosity, T_{cv}, a better understanding of the melt structure involved in the sintering process is expected.[10]

The changes of silicate melt structure can be roughly described in terms of the γ/η ratio versus base/acid ratio. In Table 9 and Figure 80, the relationships between γ/η , determined at temperatures above the temperature of critical viscosity, and base/acid ratios are shown. Both properties were measured in air and in CO/CO_2 (60/40) atmospheres.

Generally, there is a prominent increase of interfacial surface tension and viscosity ratios with the base/acid ratio. This is indicated by the systematic increase of the depolymerization silicate network structure. In slags exposed to a CO/CO_2 atmosphere, the iron oxidation state from Fe^{3+} to Fe^{2+} changes the silicate structure. The general trend is that the number of nonbridging oxygens increases with the decrease of $Fe^{3+}/\Sigma Fe$ for highly polymerized melt structures.[29] After measuring the viscosity in a CO/CO_2 atmosphere, the Illinois #6 and Pittsburgh #8 slags were quenched to room temperature. Examination of these samples indicated precipitates of randomly distributed metallic iron were present (Figure 81). These precipitates also had an effect on the activation energy for viscous flow. The relationship between the activation energy of Newtonian viscous flow and the base/acid ratio is shown in Figure 82.

TABLE 8

Composition of Coal Slags[a]

Run No.	Sample[b]	Base/ Acid	SiO_2	Al_2O_3	Fe_2O_3	TiO_2	CaO	MgO	Na_2O	K_2O	P_2O_5
			Determined after viscosity measurements in air								
1	Lignite 2	0.28	45.8	25.7	5.6	6.2	8.9	2.5	4.1	0.5	0.5
2	Montana (Subbituminous)	0.37	47.2	24.0	5.4	1.1	15.5	4.7	0.7	0.7	0.7
3	Lignite 1	0.39	44.3	22.9	12.9	4.7	9.0	1.7	4.0	0.5	0.2
4	Utah (Bituminous)	0.47	47.3	18.9	6.6	1.3	15.7	3.8	4.8	0.6	1.0
5	Sarpy Creek	0.72	38.0	18.1	13.4	1.0	18.5	4.1	5.0	0.3	1.4
6	Gascoyne	1.05	35.2	11.5	8.8	1.5	27.6	7.5	6.7	0.1	1.0
7	Beulah Lignite	1.06	30.1	16.2	12.3	1.7	23.8	7.2	7.4	0.1	1.2
8	Center	1.37	24.4	16.3	12.8	0.8	29.6	9.8	4.7	0.5	1.0
Run No.	Sample[c]	Base/ Acid	SiO_2	Al_2O_3	Fe_2O_3	TiO_2	CaO	MgO	Na_2O	K_2O	P_2O_5
			Determined after viscosity measurements in CO/CO_2 (60/40)								
9	Pittsburgh #8	0.34	51.1	20.6	18.2	1.2	4.9	1.2	0.0	2.6	0.2
10	Illinois #6	0.41	47.3	19.5	20.6	1.3	6.7	1.2	0.0	2.8	0.0
11	Pittsburgh #8 (+Dolomite)	0.44	45.9	20.3	16.6	1.1	10.1	3.6	0.0	2.2	0.1
12	Pittsburgh #8 (+Limestone)	0.50	43.1	20.7	16.2	1.1	16.0	0.8	0.0	2.2	0.0
13	Illinois #6 (+Dolomite)	0.52	42.4	20.2	18.0	1.1	12.4	3.5	0.0	2.3	0.0
14	Illinois #6 (+Limestone)	0.60	40.9	18.6	18.9	1.1	17.5	0.7	0.0	2.3	0.0
15	Indian Head	0.60	36.0	22.1	2.8	1.2	24.0	5.8	1.9	0.9	0.1
16	Beulah (+Limestone)	0.72	33.1	23.0	10.1	1.3	26.1	2.9	2.8	0.7	0.0
17	Beulah	0.79	38.0	15.3	10.9	1.6	22.4	5.1	5.8	0.7	0.0
18	Beulah (+Dolomite)	0.90	34.2	16.2	9.7	1.5	25.8	8.0	4.2	0.5	0.0

[a] Weight percent expressed as equivalent oxide percent
[b] Sample composition from slag viscosity sample determined in air
[c] Sample composition from slag viscosity sample determined in CO/CO_2 (60/40)

3.2.2.3.3 Strength Development

The mechanical properties of the sintered ash pellets were measured in order to understand the mechanisms of ash deposit strength development. The compressive strength of sintered coal ashes depends on temperature, time, and atmosphere (Figure 82, Table 10). Generally, the compressive strength measured on pellets sintered in the reducing atmosphere is greater than that found in pellets sintered in an air atmosphere. Comparison of mechanical properties with γ/η results implies that more liquid phase with a lower viscosity is formed in the reducing atmosphere, probably due to an effect of Fe^{+2}.

TABLE 9

INTERFACIAL SURFACE TENSION AND VISCOSITY DATA
DETERMINED ABOVE THE TEMPERATURE OF CRITICAL VISCOSITY

Run No.	Sample[a]	Base/Acid	Temp(°C)	η(dyne/cm)	γ(Poise)	γ/η
1	Lignite 2	0.28	1350	475	991	0.4
2	Montana (Subbituminous)	0.37	1370	474	405	1.2
3	Lignite 1	0.39	1350	383	360	1.0
4	Utah (Bituminous)	0.47	1370	956	402	2.4
5	Sarpy Creek	0.72	1350	370	68.8	5.4
6	Gascoyne	1.05	1330	379	52.5	7.2
7	Beulah	1.06	1330	225	33.6	6.7
8	Baukol-Noonan	1.37	1350	122	13.8	8.8

Run No.	Sample[b]	Base/Acid	Temp(°C)	η(dyne/cm)	γ(Poise)	γ/η
9	Pittsburgh #8	0.34	1410	492	1290	0.4
10	Illinois #6	0.41	1380	357	878	0.4
11	Pittsburgh (+ Dolomite)	0.44	1330	389	550	0.7
12	Pittsburgh (+ Limestone)	0.50	1360	357	900	0.4
13	Illinois (+ Dolomite)	0.52	1320	269	340	0.8
14	Illinois (+Limestone)	0.60	1330	328	500	0.6
15	Indian Head	0.60	1350	277	132	2.1
16	Beulah (+ Limestone)	0.72	1310	267	80	3.3
17	Beulah	0.79	1240	578	100	5.8
18	Beulah (+ Dolomite)	0.90	1320	419	32	13.0

[a] determined in air
[b] determined in CO/CO_2 (60/40)

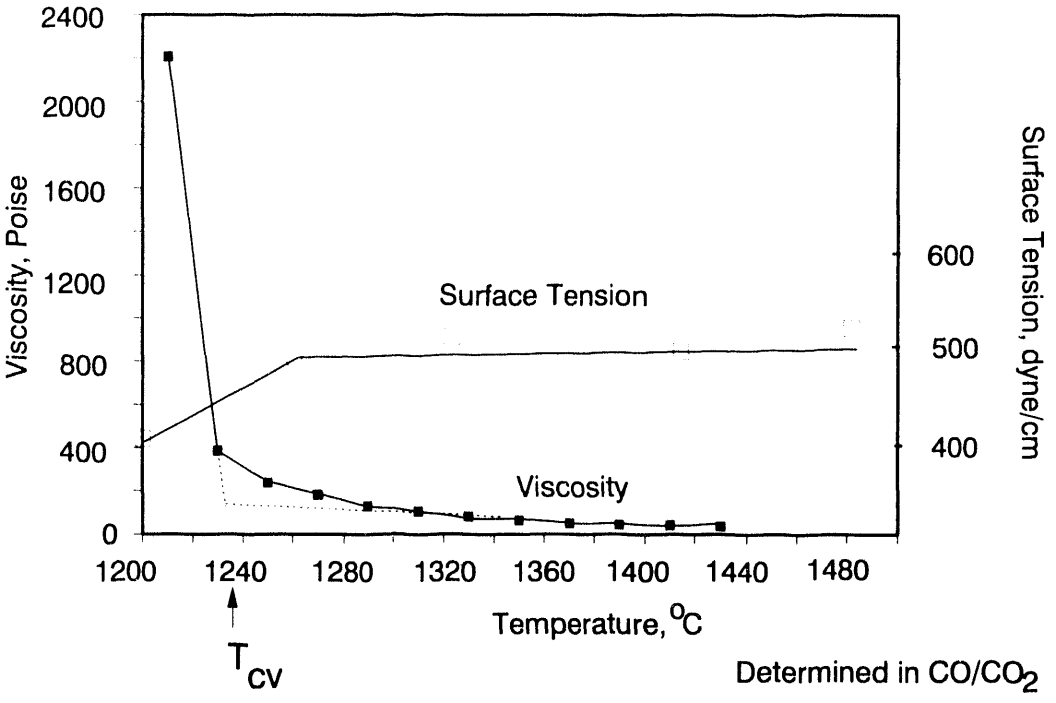

Figure 79. Variations of viscosity and surface tension with temperature.

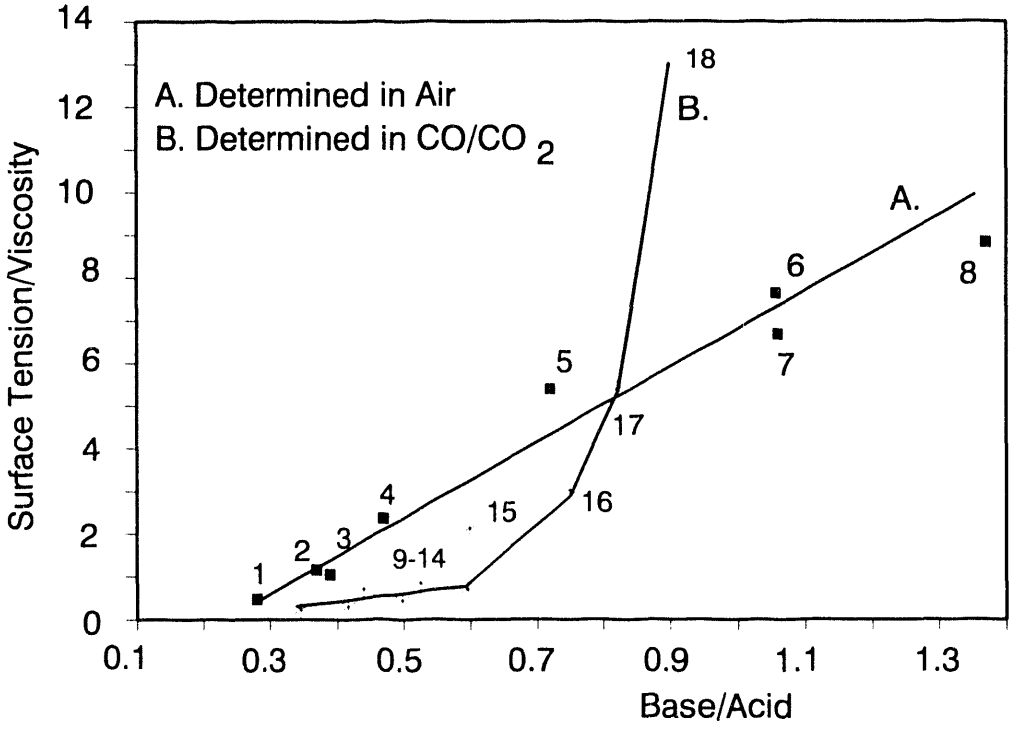

Figure 80. Relations between surface tension/viscosity and base/acid ratio of coal ashes.

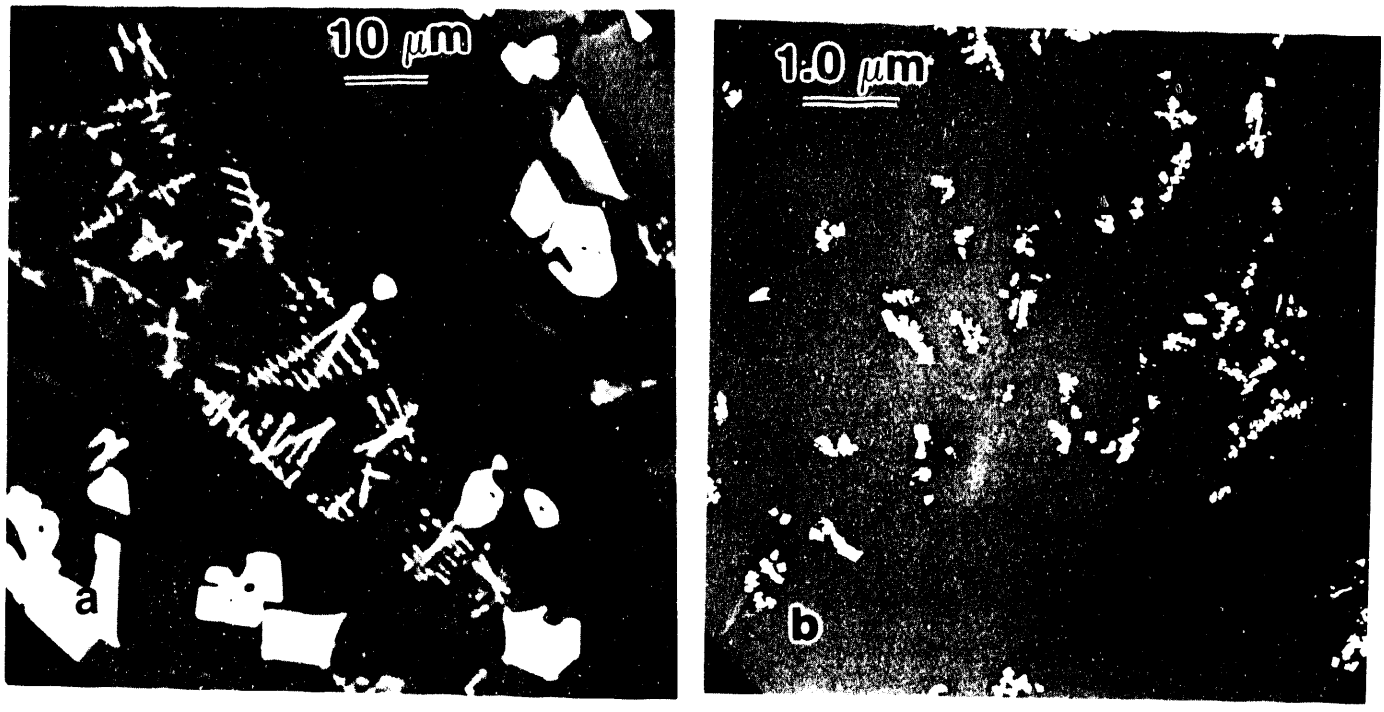

Figure 81. Microstructures of quenched Pittsburgh #8 (a) and Illinois #6 (b) slags after measuring viscosity in a CO/CO_2 atmosphere.

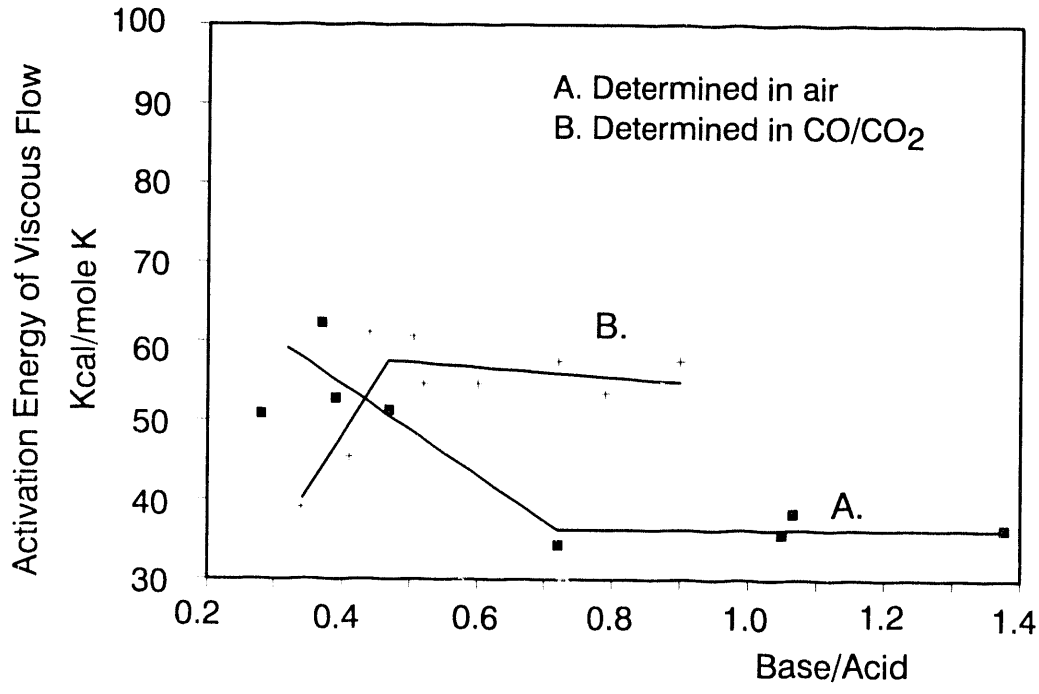

Figure 82. Variation of activation energy of viscous flow as a function of the base/acid ratio.

TABLE 10

COMPRESSIVE STRENGTH DEVELOPMENT IN
SINTERED AMORPHOUS COAL ASHES ($N/m^2 \times 10^8$)

Sample	Atmosphere	900°C	1000oc	1100°C
Illinois #6	Air	0.033	0.36	0.59
Pittsburgh #8	Air	0.01	0.17	0.42
Beulah	Air	0.05	0.09	0.58
Illinois #6	CO/CO_2	0.085	0.41	0.57
Pittsburgh #8	CO/CO_2	0.07	0.57	melt
Beulah	CO/CO_2	0.07	0.08	0.42

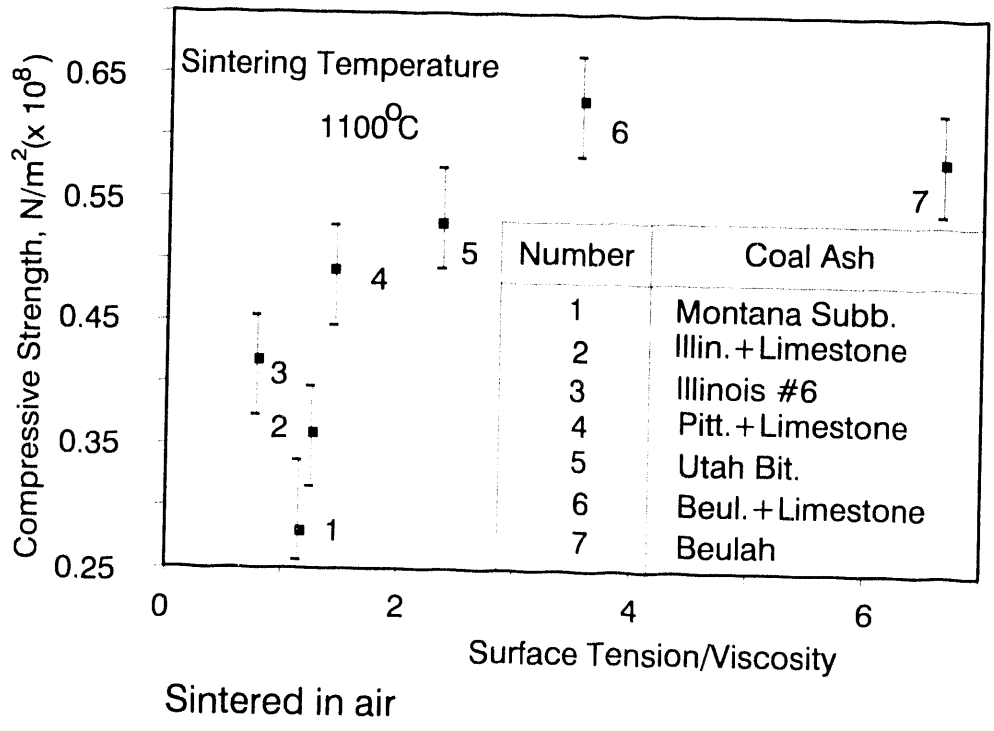

Figure 83. Compressive strength development versus surface tension/viscosity ratio (determined above T_{cv}).

Generally, the quantity and the physical properties of a silicate liquid phase are responsible for the formation of well-sintered coal ash deposits. The slopes of d $\ln(\gamma/\eta)/dT$ determined from appropriate curves seem to provide some information on the reactivity of coal ash during sintering processes. The assumption is that the structure of a melt involved in the sintering process is not significantly varied from that in the bulk ash slag determined from viscosity and surface tension. Table 11 lists slopes of the d $\ln(\gamma/\eta)/dT$ calculated for coal ash in air and CO/CO_2 atmospheres.[10]

There is some correlation between strength and the slope. The low value of the slope corresponds to the high strength development of sintered coal ashes.

3.3 Future Work

During the coming year, work will focus on the inorganic partitioning and physical properties of ash slags. Inorganic partitioning will be initiated using the pressurized drop-tube furnace. Physical properties to be studied include wetability of particles with respect to other particles and deposit strength development at elevated temperatures.

3.4 Associated Task

Contacts with DOW, Texaco, and Shell were developed. A multiclient funded proposal entitled, "Ash Behavior Under Reducing Environments" was written and distributed to several industrial companies. DOW, Texaco, Shell, and EPRI have responded with verbal approval. The targeted start date is Oct. 1, 1990. A copy of the proposal is attached.

TABLE 11

SLOPE OF d $\ln(\gamma/\eta)/dT$ OF
COAL ASH DETERMINED IN AIR AND
CO/CO_2 ATMOSPHERES[5]

	d $\ln(\gamma/\eta)/dT$	
Sample	In Air	In CO/CO_2
Illinois #6	1.0	2.2
Pittsburgh #8	1.4	1.9
Beulah	2.6	6.2

4.0 REFERENCES

1. Raask, E. "Mineral Impurities in Coal Combustion", Springer-Verlag, Berlin, 1985.

2. Moza, A.K. and Austin, L.G. Fuel 1981, 60, 1057.

3. Abbott, M.F., Moza, A.K. and Austin, L.G. Fuel 1981, 60, 1065.

4. Moza, A.K. and Austin, L.G. Fuel 1982, 61, 161.

5. Abbott, M.F. and Austin, L.G. Fuel 1982, 61, 765.

6. Abbott, M.F., Conn, R.E. and Austin, L.G. Fuel 1985, 64, 827.

7. Abbott, M.F., and Austin, L.G. Fuel 1985, 64, 832.

8. Mills, K.C. "Mineral Matter and Ash in Coal," (Editor K.S. Vorres), Am. Chem. Soc., Washington D.C., 1986, p. 195.

9. Nowok, J.W., Benson, S.A. and Kalmanovitch, D.P. Proceedings, Sixth Annual Inter. Pitts. Coal Conf., September 25-29, 1989, vol. 1. p. 90.

10. Nowok, J.W., Benson, S.A., Jones, M.L. and Kalmanovitch, D.P. Fuel 69, 1020, 1028.

11. Doremus, R.H. "Glass Science", John Wiley and Sons, New York, 1973, p. 74.

12. Butler, J.N. and Bloom, B.H. Surface Sci. 1966, 4, 1.

13. Maze, C. and Burnet, G. Surface Sci. 1969, 13, 451.

14. White, D.W.G. Trans. ASM 1962, 55, 757.

15. Sangiorgi, R. Caracciolo, G. and Passerone, A. J. Mater. Sci., 1982, 17, 2895.

16. Hess, P.C. "Physics of Magmatic Process", (Editor, R.B. Horgraves), Princeton University Press, 1980, p. 3.

17. Hochella, M.F., Jr. and Brown, G.E., Jr. Geochim. Cosmochim. Acta 1984, 48, 2631.

18. Sage, W.L. and McIroy, J.B. J. Engin. Power 1960, April, 145.

19. King, T.B. "The Physical Chemistry of Melts", Inst. Mining and Metall., London, 1953, p. 35.

20. Mazurin, O.V. Streltsina, M.V. and Shvaiko-Svaikoskaya. "Handbook of Glass Data', Elsevier, Amsterdam, 1983, part A.

21. Maze, C. and Burnet, G. Surface Sci. 1971, 27, 411.

22. Bonfield, W., J. Mater. Sci. 1972, 7, 148.

23. Raask, E. Trans. ASME J. Eng. Power Ser. A1966, 88, 40 ASME Paper No. 65-WA/FU-1, 1965.

24. Davies, M.W., Hazeldean, G.S.F. and Smith, P.N. "Physical Chemistry of Process Metallurgy: the Richaerdon Conference", (Editors J.H.E. Feffers and R.J. Tait), Inst. Mining and Metall., London, 1973, p. 95.

25. Reid, W.T. 1981. Coal Ash - Its Effect on Combustion Systems. In Chemistry of Coal Utilization, ed. M.A. Elliott, p. 1389-1445. A. Willey-Int. Publ.: New York.

26. Scherer, G.W. 1984. Viscous Sintering of a Bimodal Pore-Size Distribution. J. Am. Ceram. Soc. 67, 709-715.

27. Schobert, H.H., Streeter, R.C. and Diehl, E.K. 1985. Flow Properties of Low-Rank Coal Ash Slags. Fuel 64, 1611-1617.

28. Nowok, J.W., Bieber, J.A., Benson, S.A. and Jones, M.L. 1990. Physicochemical Effects Determining the Accuracy of Interfacial Surface Tension of Coal Ashes. Fuel submitted.

29. Virgo, D., Mysen, B.O. and Seifert, F. 1980. Relationship Between the Oxidation State of Iron and the Structure of Silicate Melts. Carnegie Institute Washington Yearbook, p. 308-311.

COAL ASH BEHAVIOR IN REDUCING ENVIRONMENTS

A Proposal For Multiclient Funding

For Further Information Contact:

Dr. Steven A. Benson
Research Supervisor
(701)777-5177

Dr. Michael L. Jones
Director, CESRI
(701)777-5152

Mr. Edward N. Steadman
Research Associate
(701)777-5157

University of North Dakota Energy and Environmental Research Center
Box 8213, University Station
Grand Forks, North Dakota 58202

TABLE OF CONTENTS

LIST OF FIGURES

LIST OF TABLES

COAL ASH BEHAVIOR IN REDUCING ENVIRONMENTS

1.0 INTRODUCTION

A key factor in the successful design and operation of coal gasification and advanced combustion systems is the ability to control and mitigate ash-related problems. Some of the major ash-related problems are slag flow control, slag attack on the refractory, ash deposition on heat transfer surfaces, corrosion and erosion of equipment materials, and emissions control. Such problems are closely tied to the abundance and association of the inorganic components in coal and the system conditions.

In general, the inorganic components are associated in the coal as minerals or organic complexes (salts of carboxylic acid groups or organic coordination complexes). The minerals associated in coal vary widely in size, composition, and juxtaposition. Juxtaposition refers to the association of the mineral grains with other mineral grains and coal particles. These associations directly influence the chemical and physical transformations that occur during the gasification process. Depending upon the type of gasification system, the inorganic components are initially partitioned into intermediate species in the form of inorganic gases, liquids, and solids. The state of these species at any given stage or position in the gasifier directly influences their behavior at that stage. The transformations and partitioning of the inorganic species directly influence slag flow behavior, extent and type of slag attack on the refractory, corrosion and erosion of materials, as well as growth rate, quantity, and type of ash deposition on heat transfer surfaces.

Current conventional analytical methods for coal and coal ash materials do not provide adequate detail regarding their complex chemical and mineralogical properties. Advanced analytical techniques are currently being used to determine the association and forms of inorganic components in coals (1,2) and coal ash-derived materials (3,4). In addition, other laboratory-scale techniques are routinely used to determine viscosity, surface tension, sintering behavior, and deposit strength development (5,6). Reducing environments can be simulated in pressurized drop-tube furnace systems to produce intermediate species which can be used to determine inorganic transformations. Utilization of these advanced analytical techniques, coupled with laboratory methods, can potentially provide significant advances in understanding the behavior of inorganic components during gasification that will ultimately lead to better methods to predict and mitigate ash-related problems.

The University of North Dakota Energy and Environmental Research Center (EERC) is one of the world's major coal research facilities. Since its founding in 1951, the EERC has conducted research, testing, and evaluation of coals and associated combustion and gasification technologies. The Center's transfer from the U.S. Department of Energy to the University of North Dakota in 1983 made it possible for the Center's staff to work directly for industry to provide the needed data and practical solutions required for the specific problems and challenges encountered. The EERC possesses state-of-the-art analytical equipment and extensive laboratory- and pilot-scale facilities, providing unique capabilities for research programs.

Extensive research on the transformations of inorganic and mineral components in coal has been conducted at the EERC. Research has been performed to develop methods to determine the association, size, and composition of ash-forming constituents in coal. Techniques are now available to determine the distribution of phases in fly ashes, deposits, and slags. Fundamental studies of the transformation of inorganic components to form intermediate ash components in the form of vapors, liquids, and solids have been performed using a laboratory-scale combustor combined with advanced analytical techniques. Recently, EERC has developed the ability to perform laboratory-scale studies under pressure.

This prospectus details a proposed three-year, multiclient program to determine the behavior of coal inorganic components in reducing environments using advanced methods of analysis coupled with laboratory experiments. The proposed objectives are as follows:

1. to develop further our advanced ash and deposit characterization techniques in order to quantify the effects of the liquid phase components in terms of strength development in ash deposits,

2. to determine the mechanisms of inorganic transformations that lead to inorganic partitioning, ash deposition, and slag formation under gasification conditions,

3. to determine the factors that influence the sintering behavior of coal-derived ashes under gasification conditions, and

4. to develop a better means of predicting the behavior of inorganic components as a function of coal composition and reducing conditions.

2.0 BACKGROUND

Recent work at the Energy and Environmental Research Center has centered on the development of a more quantitative understanding of the behavior of inorganic components in combustion and gasification systems. Specifically, our work has focused on the following key issues:

1. **Advanced characterization methods.** The development of advanced methods to determine the abundance and association of inorganic phases in coals, fly ashes, ash deposits, and slags (1,2,3,4). The utility of these techniques has been demonstrated on coal, fly ash, and ash deposits produced in both combustion and gasification systems, providing greater insight into the mechanisms of ash formation.

2. **Partitioning of inorganic components in combustion and gasification systems.** Work has focused specifically on the processes taking place which form inorganic vapors, liquids, and solids and the partitioning of inorganic components in various sections of the gasifier (i.e., the slag versus the entrained ash and deposits). In addition, the interaction of these components upon gas cooling, deposition, and sintering have been examined in full-, pilot-, and bench-scale systems. Specifically, the

reactions of alkali and alkaline earth silicate, aluminosilicate, and sulfur-containing systems have been examined in detail (7,8,9).

3. **Physical properties of ashes and slag.** Work has focused on determining slag viscosity and surface tension related to the sintering and agglomeration processes. Improvement of models used to predict viscosity (based on temperature and chemical composition of the ashes) has been one of the objectives. Progress is being made on relating slag chemical composition as expressed by the base/acid ratio to surface tension of slag droplets on various substrates (5). In-depth research has been conducted on the mechanisms of sintering or deposit strength development in ash deposits (5,6).

The transformations of inorganic components during gasification and combustion consist of a complex series of chemical and physical processes. These transformations are dependent upon the physical and chemical properties of the coal and gasification conditions. The behavior of the inorganic components largely depends upon the initial partitioning of ash components. This partitioning influences the distribution of the ash species in slags, entrained ash, and deposits. Partitioning can be responsible for concentrating low-melting species in the entrained ash and on the surfaces of ash particles. These low-melting point phases aid in deposit initiation, growth, and sintering. The low-melting point species also attribute to ash agglomeration. Currently, ash-related problems cannot be accurately predicted by examination of the raw coal because the partitioning phenomena changes the distribution of the inorganic components in the ash. Therefore, the characterization and modelling of partitioning phenomena is critical to the development of methods to predict ash behavior. To date, little information exists on the behavior of inorganic components under closely controlled, pressurized conditions.

Ash deposit and agglomerate formation are dependent upon the physical properties of the ash materials which are dependent on the ability of inorganic components to react, melt, and assimilate during processes involving reducing environments. The physical properties are also strongly influenced by temperature, gas composition, and ash composition. Specific physical properties, surface tension and viscosity, directly affect ash agglomerate, slag, and deposit formation. Other ash properties of interest are compressive strength and wettability. Troublesome coal ash deposits result from the formation of low-viscosity liquid phases and the variability in surface tension of molten coal ashes. These processes are influenced by the structure of the molten slag and are directly related to the chemical composition of coal ashes. For example, the addition of network modifiers such as sodium, calcium, magnesium, and iron (Fe^{2+}) alters the molten slag structure by depolymerization of silicate glass networks. Depolymerization of the silicate network results in significantly lower viscosities. In addition, network modifiers promote crystallization processes. Crystallization of species from the melt phase changes the composition and physical properties of the residual liquid phase. Accordingly, the surface tension and viscosities can be significantly affected by the presence of crystals in the melt. Under the reducing conditions found in gasifiers and advanced combustion systems, relatively low-melting point phases result. This effect is especially profound in ashes and slags that contain higher levels of iron. The

characteristics of these iron-rich liquid phases significantly affect the slagging and sintering behavior of coal ashes.

In order to meet the objectives of the program, efforts will be focused on: 1) detailed characterization of the coals; 2) carefully controlled laboratory experiments to produce chars, entrained ashes, deposits, and slags; 3) experiments designed to determine physical properties of deposits and slags; and 4) detailed characterization of materials collected from pilot- and larger- scale gasification equipment. This approach requires the development of advanced methods of analyses. This will include the further development of the automated scanning electron microscope/microprobe techniques to characterize coals, chars, entrained ashes, slags, and deposits. Carefully controlled experimentation that simulates the conditions in larger scale systems must be performed to determine the behavior of coal as a function of coal composition and gasification conditions. Subscale testing offers an opportunity to perform tests under very controlled conditions and greatly reduced costs, compared to larger systems. Physical properties, such as surface tension, viscosity, and strength of ashes and slags will be determined. Specific attention will focus on the development of deposit strength as a result of sintering processes and on the wetting ability of slags on metals and other related materials.

Automated scanning electron microscope/microprobe techniques are used to examine coals, fly ashes, deposits, and slags. These techniques provide the information needed to elucidate mechanisms of inorganic transformations which form intermediate ash, deposits and slags. Two techniques used at EERC to examine the inorganic components in coal and coal-derived materials will be briefly described below.

Computer-controlled scanning electron microscopy (CCSEM) is used to characterize unaltered coal samples and inorganic combustion products. A computer program is used to locate, size, and analyze particles. Because the analysis is automated, a large number of particles can be analyzed quickly and consistently. The heart of the CCSEM analysis system is a recently installed annular backscattered electron detector (BES). The BES system is used because the coefficient of backscatter (the fraction of the incoming beam that is backscattered) is proportional to the square root of the atomic number of the scattering atoms. This permits a high degree of resolution between sample components based on their atomic numbers. This means that coal minerals can be easily discerned from the coal matrix, and fly ash particles can be easily discerned from epoxy in polished sections. Brightness and contrast controls are used to optimize threshold levels between the coal matrix and mineral grains or fly ash particles. When a video signal falls between these threshold values, a particle is discerned and the particle center located. A set of eight rotated diameters about the center of the particle are measured, and the particle area, perimeter, and shape are calculated. The beam is then repositioned to the center of the particle, and an x-ray spectrum is obtained. The information is then stored to a Lotus transportable file for data reduction and manipulation. The CCSEM data provides quantitative information concerning not only the mineral types which are present, but their size and shape characteristics as well. Since the same analysis can be performed on the initial coal and resultant fly ash, direct comparisons can be made and inorganic transformations inferred.

The primary method used to characterize deposits is the scanning electron microscope/microprobe (SEM). The SEM is capable of imaging deposits and determining the chemical composition of areas within deposits down to 1 micrometer in size. The use of the SEM is extremely valuable in identifying materials responsible for deposit initiation, growth, and strength development. The SEM technique most commonly used at the EERC to characterize deposits is called the SEM point count routine (SEMPC). This technique was developed to quantitatively determine the relative amount of phases present in ashes and deposits. The method involves microprobe analysis (chemical compositions) of a large number of random points in a polished cross section of a sample. This technique provides information on the degree of melting and interaction of the various deposited ash particles and provides quantitative information on the abundance of phases present in the deposit. By examining the phases present, the material responsible for the formation of the deposit can be identified. In addition, various regions in the deposit can be examined to determine the changes that occurred with time and possibly with changes in coal composition.

The SEMPC technique is supplemented with morphological and chemical analysis of the microstructural features of the deposit. This is performed using the SEM manually to scan across the samples. Imaging and elemental mapping are performed. In addition, x-ray diffraction is used to determine the crystalline phases present in the deposit as a support for the SEMPC analysis. Bulk chemical analysis of the deposit is also performed with x-ray fluorescence.

3.0 RESEARCH PROGRAM OUTLINE

This research program is divided into four tasks. The proposed program will be conducted over three years.

3.1 Three Year Project Plan

3.1.1 Task 1. Analytical Methods Development

This task focuses mainly on the development of analytical techniques that are necessary to characterize coal, entrained ashes, deposits, and slags. The methods developed in this task will be used in the other tasks to identify the partitioning of components and sintering processes during gasification. Scanning electron microscopy and microprobe analysis (SEM) coupled with advanced methods of image analysis are the primary tools used to characterize the inorganic species. The SEM techniques will be supported by other tools such as x-ray diffraction, x-ray fluorescence (bulk methods), x-ray photoelectron spectroscopy, scanning Auger microprobe, and optical microscopy. The software developed as part of this program will be made available to the sponsors for their use, including the SEMPC technique and the data manipulation software associated with the CCSEM technique.

- Year 1. The research during the first year will involve utilizing image analysis in conjunction with the scanning electron microscopy point count routine (SEMPC) technique to allow for the determination of ash physical properties. The currently used technique will incorporate simultaneous digital image acquisition of all points analyzed. This will enable the

examination of the morphology of specific areas of interest, after the SEMPC analysis has been performed. In addition, a method to determine the porosity of deposits and sintered ashes will be developed by performing image analysis of the stored images obtained from the SEMPC analysis. Coals, entrained ashes, and deposits produced in other tasks will be examined using computer-controlled scanning electron microscopy (CCSEM) and SEMPC.

- Year 2. The key process involved in the development of deposit strength is viscous flow sintering of a reactive liquid phase. The primary purpose of the SEMPC technique is to identify and determine the abundance and chemical composition of the liquid phase components. Processes that occur during sintering involve the assimilation of solid particles into the melt phase, interaction of various liquid phases, reactivity of solid particles, and crystallization from the melt. All of these processes influence the abundance of the liquid and the chemical composition. The work during the second year will focus on developing methods to perform automated image analysis of deposits in conjunction with the SEMPC technique to quantify neck growth and type and degree of crystallization.

- Year 3. The strength of deposits will be determined using the measurements quantified during years one and two of the program. The strength of a deposit can be described by the equation derived by Raask (10), where the strength of the deposit varies with respect to time. The physical properties of importance are the surface tension, viscosity, and radius of the particles. Information generated with respect to the composition of the ash materials, the neck growth, and the porosity of the deposit will allow for the determinations. This task will be closely coordinated with the efforts in task 2 and task 3.

3.1.2 Task 2. Inorganic Partitioning and Ash Deposition

- Year 1. The partitioning of inorganic components based on coal composition and reducing environments will be determined. Modification and shakedown testing of the pressurized drop-tube furnace will be completed. Experiments will be initiated using the pressurized drop-tube furnace system. Examination of the intermediate ash species will determine the particle-size distributions and composition. The partitioning will be determined for two sponsor-selected coals during the first year.

- Year 2. A matrix of tests will be performed using the pressurized drop-tube furnace to determine the effects of operating conditions (temperature, gas composition, and pressure) on the coals tested in year 1. Determination of the partitioning of inorganic components on more coals will be performed. These coals will be selected by the sponsors. A smaller matrix of experiments based on results obtained from the initial experiments in years 1 and 2 will be performed on these coals. The feasibility of performing ash deposition experiments in the pressurized drop-tube furnace will be examined. Testing will also be performed on the two initial coals.

- Year 3. Two more coals will be examined to determine the degree of partitioning and ash deposition propensity using the pressurized drop-tube furnace. Detailed analysis, interpretation of the results, and preparation of the final report will be performed.

3.1.3 Ash and Slag Physical Properties

- Year 1. The work will focus on determining the effect of ash composition (on a particle-by-particle basis) in terms of a base-to-acid ratio on the variation of surface tension and viscosity. In addition, the wettability of particles with respect to other particles in a deposit will be examined as a function of ash particle composition, temperature, and gas composition. Work will focus on the factors that influence the formation and characteristics of the liquid phases involved in the sintering processes under reducing conditions. This work will be closely coordinated with tasks 1 and 2.

- Year 2. The effects of ash composition and physical properties on the development of deposit strength will be determined. Compressive strength will be measured at elevated temperatures. The coal ashes produced from coals used in Task 2 will be used in this task. Pellets will be prepared from coal ashes and synthetic materials and subjected to reducing environments and temperatures characteristic of gasification and advanced combustion systems. Detailed analysis of the starting materials and the sintered products will be performed with the SEMPC technique in order to determine the degree of reaction and to verify the ability of the SEMPC technique to determine the degree of interaction.

- Year 3. The effects of various coal ash compositions on strength development during sintering as a function of time, temperature, and atmosphere will be determined. Prior to sintering, the base-to-acid ratios of individual, sized particles will be determined with the CCSEM technique that determines the chemical composition and size of particles. The base-to-acid ratio provides an indication of the viscosity and surface tension and the variability of these properties for inhomogeneous melts. In addition, work will be conducted to determine the potential particle-to-particle wettability and reactivity based on base-to-acid ratios of individual particles. Strengths will be measured on coal ash pellets that have been produced under temperatures and gas compositions that simulate the proper reducing environments. The strengths determined will be compared to the results obtained from the SEMPC analysis by comparing the degree of neck growth determined with the SEMPC automated image analysis system. Key indicators will be the viscosity distribution of the liquid phase, neck growth, and the pore-size distribution. In addition, the base-to-acid ratio distributions of the sintered pellets will be compared to the initial distribution of the unsintered particles to determine the degree of assimilation of ash species and strength development.

3.2 Project Schedule and Deliverables

TABLE 1. PROJECT SCHEDULE AND MILESTONES--YEAR 1

No.	Task Description	Schedule by Project Months 1	2	3	4	5	6	7	8	9	10	11	12
1	Development of Analytical Methods			a					b			c	
2	Partitioning and Ash Deposition					a			b		c		d
3	Ash and Slag Physical Properties				a	b					c		
4	Final Report												
	Planning and Review Meetings	#								#			

Descriptions of milestones in Table 1 are summarized as follows:

Task 1. Development of Analytical Methods

a. Integrate the SEMPC technique to include image analysis capabilities.
b. Write software to perform simultaneous digital image acquisition.
c. Perform automated determination of deposit and slag porosity.

Task 2. Partitioning and Ash Deposition

a. Complete initial shakedown of the pressurized drop-tube furnace system.
b. Complete modifications to incorporate reducing environments.
c. Complete final shakedown.
d. Complete preliminary runs on two coals.

Task 3. Ash and Slag Physical Properties

a. Install strength measurement apparatus.
b. Prepare and analyze ashes--determine variations in chemical composition of ash particles--develop relationships to viscosity, surface tension, and the activation energy of viscous flow.
c. Complete initial particle-to-particle wettability work with model mixtures and selected coal ashes.

TABLE 2. PROJECT SCHEDULE AND MILESTONES--YEAR 2

No.	Task Description	Schedule by Project Months 1	2	3	4	5	6	7	8	9	10	11	12
1	Development of Analytical Methods						a				b		c
2	Partitioning and Ash Deposition					a					b		cd
3	Ash and Slag Physical Properties							a			b		c
4	Final Report												
	Planning and Review Meetings	#								#			

Descriptions of milestones in Table 2 are summarized as follows:

Task 1. Development of Analytical Methods

a. Develop a method to quantify neck growth in ash deposits
b. Automate determination of deposit crystallinity.
c. Determine crystal versus liquid phase chemistry.

Task 2. Partitioning and Ash Deposition

a. Complete detailed matrix runs on first coal.
b. Complete runs on two more coals (reduced matrix) and detailed analyses of the ashes and deposits produced.
c. Complete detailed matrix runs on second coal.
d. Complete analysis and interpretation of the results.

Task 3. Ash and Slag Physical Properties

a. Complete strength measurements at high temperatures for model mixtures and selected coal ashes for pellets subjected to reducing environments.
b. Complete detailed analysis of sintered materials produced in a.
c. Identify the liquid components responsible for the sintering processes. Focus will be on determining interrelationships of ash reactivity, viscosity, surface tension, base-to-acid ratio, and wettability.

TABLE 3. PROJECT SCHEDULE AND MILESTONES--YEAR 3

No.	Task Description	Schedule by Project Months 1	2	3	4	5	6	7	8	9	10	11	12
1	Development of Analytical Methods						a			b			
2	Partitioning and Ash Deposition		a							b			
3	Ash and Slag Physical Properties							a		b			
4	Final Report Planning and Review Meetings	#										a #	b

Descriptions of milestones in Table 3 are summarized as follows:

Task 1. Development of Analytical Methods

a. Identify the reactivity of ashes based on SEMPC analysis.
b. Determine deposit strength development using SEMPC automated digital image analysis.

Task 2. Partitioning and Ash Deposition

a. Complete runs on two more coals (reduced matrix) and produce detailed analyses of the ashes and deposits.
b. Analysis and interpretation of results.

Task 3. Ash and Slag Physical Properties

a. Complete parametric study of the effects of temperature, gas composition, and time on the strength development in coal ash and synthetic mixtures.
b. Complete the coordination with the SEMPC analysis.

Final Report

a. Complete draft of the final report and submit to sponsors.
b. Submit final report with revisions.

The target date for initiation of the program is August 1, 1990. Task reports will be submitted to the project sponsors at the completion of each task. Bimonthly letter reports will provide updates on the overall project status. Project review meetings will be held twice each year of the program. The draft final report will be submitted to the project sponsors for review one month prior to the final review meeting. The reviewed and edited task reports will be major inputs into the final report.

3.3 Costs of the Project

The costs of the program are summarized in Table 4. The cost to each sponsor of the program is $30,000 per year for three years. The number of sponsors to perform the scope of work presented in this prospectus is four. The additional $120,000 per year will be provided by the U.S. Department of Energy through the Jointly Sponsored Research Program. Chances of getting the U.S. DOE funds are excellent.

TABLE 4. PROJECT BUDGET

No.	Task Description	Schedule by Project Quarters 1 2 3 4 5 6 7 8 9 10 11 12	Estimated Cost($000)
1	Development of Analytical Methods	———	$171
2	Partitioning and Ash Deposition	———	$260
3	Ash and Slag Physical Properties	———	$289
4	Final Report	———	
		Total project cost	$720
	Planning and Review Meetings	# # # # # #	

4.0 BENEFITS OF SPONSORSHIP

Sponsorship of the proposed research will be open to private companies and organizations. Each sponsoring company or organization will become a member of the project's Advisory Committee and will have one vote. An Advisory Committee Chairman will be elected from among the members at the first meeting of the committee. The Advisory Committee will review project plans, budgets, and policies. Specific benefits of participating in the program will include:

- Rapid access to state-of-the-art research on the effects and possible control of ash-related problems in coal gasification systems.
- Cost-effective research at a fraction of the cost available to a single company.
- Ability to rapidly effect transfer of information and data through consultation with EERC staff and sponsor personnel.
- Interaction with other sponsors and with personnel interested in convective pass fouling problems.

Each sponsor shall have a nonexclusive, perpetual, royalty-free, worldwide license to practice any invention, discovery, or improvement (whether patentable or not) conceived or made by EERC as a result of this program. EERC assumes no liability for warranting the validity of any patent issued or for prosecuting patent restrictions on third parties.

5.0 PERSONNEL AND FACILITIES

Project Manager -- Dr. Steven A. Benson

Dr. Benson (B.S Chemistry and Ph.D. Fuel Science) joined the Center in 1977 and is involved in research related to coal combustion and gasification, mineral matter transformations, coal ash fouling and slagging, and advanced methods of analytical analysis. He is currently the supervisor of the Combustion Studies Group in the Combustion and Environmental Systems Research Institute and has been actively involved in coal-related combustion and gasification studies using laboratory- and pilot-scale equipment along with analytical methods of coal and ash characterization most of his career. Dr. Benson will be responsible for the overall technical management of the program, including monitoring project schedules and budgets.

Institute Director - Dr. Michael L. Jones

Dr. Jones (Ph.D., M.S., B.S. Physics), Institute Director for the Combustion and Environmental Systems Research Institute, has been involved in coal combustion research for over eight years and has significant experience in analyzing the fate of mineral matter during combustion. As Institute Director, Dr. Jones is responsible for internal oversight and coordination of the project with other work at UNDEERC.

Principal Investigators

Principal Investigator for Task 1. - Mr. Edward N. Steadman

Mr. Steadman (M.S. Geology, B.S. Geology) has seven years of experience in characterizing coal and coal mineralogy using analytical techniques such as quantitative mineralogy using computer-controlled scanning electron microscopy/microprobe analysis, x-ray diffraction, and optical methods. Mr. Steadman will be responsible for Task 1.

Principal Investigator for Task 2. - Ms. Sumitra R. Ness

Ms. Ness (B.S. Ch.E., B.S. Chemistry) is a research engineer in the Combustion Studies group in CESRI. She is involved in laboratory- and bench-scale characterization and production of char, ash, and slag under both combustion and gasification conditions. She has also worked on thermochemical equilibrium calculations for coal ash and slag systems.

Principal Investigator for Task 3. - Dr. Jan W. Nowok

Jan W. Nowok (Ph.D. Solid State Chemistry, M.S. Physical Chemistry, B.S. Chemistry) has extensive experience in solid-state reactions and chemistry and materials surface characterization. Dr. Nowok has been involved in the study of coal ash and slag physical properties, including high-temperature viscometry, interfacial surface tension, sintering, and strengths of materials.

The Center has personnel and specialized equipment that will be drawn from to complete the proposed work. The staff is highly experienced with sampling utility scale boilers and with characterizing the samples collected. The Center has analytical staff and equipment on-site to provide complete routine and specialized analysis. UNDEERC has recently designed and assembled a pressurized drop-tube furnace system in which ash and slag transformations can be studied under more realistic conditions. Because the pressurized drop-tube furnace is a relatively recent addition to EERC's capabilities, a brief description of the system is provided in Appendix A.

6.0 REFERENCES

1. Jones, M.L.; Kalmanovitch, D.P.; Steadman, E.N.; Benson, S.A. "Application of SEM Techniques to the Characterization of Coal and Coal-Ash Products," Advances in Coal Spectroscopy, in press, 1990.

2. Steadman, E.N.; Zygarlicke, C.J.; Benson, S.A.; Jones, M.L. "A Microanalytical Approach to the Characterization of Coal, Ash, and Deposits," Seminar on Fireside Fouling Problems; Brigham Young University, Provo, Utah, April 1990.

3. Kalmanovitch, D.P.; Montgomery, G.G.; Steadman, E.N. ASME Paper Number 87-JPGC-FACT-4, 1987.

4. Steadman, E.N.; Zygarlicke, C.J.; Benson, S.A.; Jones, M.L. "A Microanalytical Approach to the Characterization of Coal, Ash, and Deposits," ASME Seminar on Fireside Fouling Problems; Brigham Young University, Provo, Utah, April 1990.

5. Nowok, J.W.; Benson, S.A.; Jones, M.L.; Kalmanovitch, D.P. "Sintering Behavior and Strength Development in Various Coal Ashes," Accepted for Publication in Fuel.

6. Nowok, J.W.; Bieber, J.A.; Benson, S.A. "Physicochemical Effects Determining the Accuracy of Interfacial Surface Tension of Coal Ashes," submitted for publication in Fuel.

7. Jones, M.L.; Benson, S.A. "An Overview of Fouling and Slagging in Western Coals," Conference on the Effects of Coal Quality on Power Plants; EPRI, Atlanta, Georgia, Oct. 1987.

8. Zygarlicke, C.J.; Steadman, E.N.; Benson, S.A. "Studies of the Transformations of Inorganic Constituents in a Texas Lignite During Combustion," Progress in Energy and Combustion Science: Special Issue on Ash Deposition, Pergamum Press, 1990, in press.

9. Benson, S.A.; Zygarlicke, C.J.; Toman, D.L.; Jones, M.L. "Inorganic Transformations and Ash Deposition during Pulverized Coal Combustion of Two Western U.S. Coals," Seminar on Fireside Fouling Problems; Brigham Young University, Provo, Utah, April 1990.

10. Raask, E. Mineral Impurities in Coal Combustion; Hemisphere Publishing Company: New York, 1985.

APPENDIX A

EQUIPMENT

A drawing of the drop-tube furnace facility is shown in Figure 1. The pressurized drop-tube furnace has these design goals for operating conditions:

temperature:	ambient to 1500°C
pressure:	ambient to 21.4 atm.
oxygen:	0 to 40%
gas flow:	0 to 20 L/min
residence time:	0 to 1 sec

The large pressure vessel contains the furnace section of the drop-tube furnace. The walls of the pressure vessel are water-cooled to dissipate heat from the furnaces. Above the main pressure vessel are the sections containing the injector and sample feeder. Residence time is determined by how far the water-cooled injector is inserted into the furnace section. The injector can be raised completely out of the furnace section and an isolation valve closed. This allows the injector section to be depressurized without depressurizing the main furnace section. The sample feeder may also be isolated from the injector for filling and servicing without depressurizing the injector or main furnace sections.

The section below the main pressure vessel contains the sampling probe and pressure letdown valves. The sample probe is raised into the furnace section to the sampling point, then lowered, and an isolation valve closed to allow removal of samples and servicing of the probe without depressurizing the main furnace section.

Since the residence time is varied by adjusting the position of the injector, the sampling is always at the same point near the bottom of the furnace section. Optical access to the sampling point is provided by two pairs of opposed ports at right angles in the main pressure vessel. The ports allow visual, photographic, and pyrometric observations of the burning sample. Additional optical access is provided by a fiber optics borescope, contained in the water-cooled injection probe, viewing down the furnace axis and a moveable mirror which can be inserted below the furnace section, when the sample probe is retracted, to view up along the furnace axis.

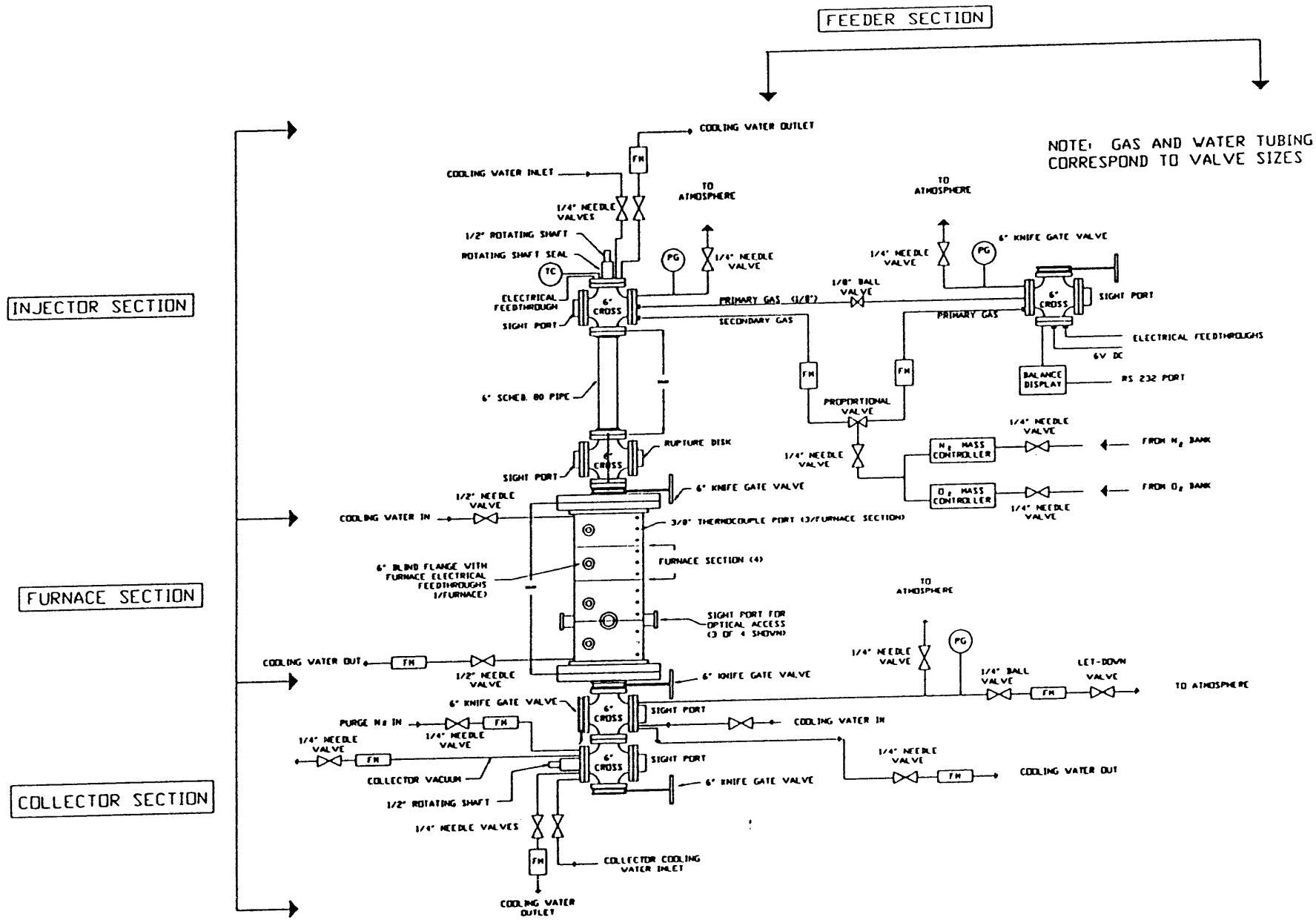

Figure 1. Schematic of pressurized drop-tube furnace process piping.